

**UNIVERSITY OF PRETORIA  
DEPARTMENT OF CIVIL ENGINEERING**

**THE INTERCEPTION CAPABILITIES OF  
SLOTTED DRAINS AS PAVEMENT SURFACE  
DRAINAGE SYSTEMS**

**BERNARD JANSEN VAN VUUREN**

# **THE INTERCEPTION CAPABILITIES OF SLOTTED DRAINS AS PAVEMENT SURFACE DRAINAGE SYSTEMS**

**BERNARD JANSEN VAN VUUREN**

A dissertation submitted in partial fulfilment of the requirements for the degree of

MASTER OF ENGINEERING (TRANSPORTATION ENGINEERING)

In the

FACULTY OF ENGINEERING, BUILD-ENVIRONMENT AND INFORMATION TECHNOLOGY

UNIVERSITY OF PRETORIA

November 2018

## DISSERTATION SUMMARY

### THE INTERCEPTION DRAINAGE CAPABILITIES OF SLOTTED DRAINS AS PAVEMENT SURFACE DRAINAGE SYSTEMS

**BERNARD JANSEN VAN VUUREN**

<b>Supervisor</b>	:	Mr Marco vanDijk
<b>Co-Supervisor</b>	:	Prof Wynand JvdM Steyn
<b>Department</b>	:	Civil Engineering
<b>University</b>	:	University of Pretoria
<b>Degree</b>	:	Master of Engineering (Transportation Engineering)
<b>Key words</b>	:	Slotted drains, interception efficiencies, hydroplaning, water film depth, surface drainage

One of the most common hydraulic risks on a pavement surface is the accumulation of surface runoff caused by insufficient surface drainage. As the water depth on roadway surface increases, the risk for hydroplaning and splash and spray to initiate also increases. Several pavement design considerations can be implemented to minimise the flow depth on a pavement surface such as the geometry design, the variation of pavement surface textures and the focus of this study, the implementation of drainage systems to enhance surface drainage.

After reviewing the various literature of surface drainage on pavement structures, it is evident that minimum research is available for the interception capabilities of the slotted inlets in South Africa. A research study was thus performed at the University of Pretoria (UP) to estimate the interception capabilities of proprietary slotted drains operating under safe driving conditions. The slotted drains evaluated in the study are manufactured and distributed by the company registered as Salberg Concrete Products (Pty), and the drains are not tested for sufficient verification on the hydraulic interception capabilities of the slotted drains.

During the research, a model study was conducted on different drainage systems installed within a pavement structure to simulate the slotted drains operating under various field conditions. This was completed by building pavement models with replica slotted inlets from the actual slotted drains, with adjustable features such as pavement slopes, slotted drain inlet widths and different volumes of sheet flows.

The slotted inlets were tested for operating individually and with a median barrier installed adjacent to its length. All parameters and conditions tested during the experiment are in accordance with a South African National Road Agency Limited (SANRAL) project case study.

A total number of 120 tests were performed during the experiment where slotted inlets were tested performing under the following conditions for maximum sheet flows of approximately 3l/s: pavement cross slopes and longitudinal slopes up to six percent, slotted inlet widths of 20mm, 40mm and 60mm, and slotted drains operating with or without a median barrier. For all parameters tested, nearly all (98-100%) of the sheet flows were intercepted by the slot inlets of the pavement models tested while operating without the median barrier. An additional test was completed on the pavement model operating with a median barrier. It was found that the barrier did not affect the drainage capability of the tested inlet for all the conditions tested, as all the sheet flow was nearly 100% intercepted before the barrier could function.

Calculations were done on the sheet flow test parameter to determine the flow depths and rainfall intensities simulated during the experiment that will typically occur on different pavement widths in practice. Rainfall intensities up to 3000mm/hr can occur on different pavement widths of 3.6m, 7.2m, 10.8m and 14.4m in practice that were simulated during the experiment. By utilising various flow depth prediction models, calculations have shown that sheet flows with water depths higher than 6mm were simulated during the experiment, which can occur on the respective pavement widths in practice. SANRAL (2013) recommended a maximum flow depth of 6mm on pavement surfaces in a 1:5 year storm to prevent any hydroplaning risks. This means that the tested slotted inlets will intercept almost 100% of these sheet flows with the predicted flow depths and rainfall intensities, as calculated per meter flow width, occurring on pavement surfaces during wet pavement conditions.

It is, therefore, safe to conclude that slotted drainage systems operating in practice with the same pavement geometric design, drainage design and pavement texture as tested during the experiment, will have the capability to sufficiently remove almost all the surface water and promote safe driving conditions. For further studies on this topic, actual field observations during rainstorms in practice can be conducted to analyse the effect of splash and spray caused by vehicles travelling during wet pavement conditions which were not considered during the experiment of this study. The investigation to determine the minimum slotted width to intercept 100% sheet flow is also a topic to consider for future research. Additional experimenting on slotted drains can be useful to confirm the results and findings obtained during this study and to develop comprehensive mathematical formulae by describing the interception drainage capabilities of slotted drains as pavement surface drainage systems.

## ACKNOWLEDGEMENTS

I wish to express appreciation to the following organisations and persons who made this dissertation possible:

1. Some information in this dissertation is based on a project by South African National Road Agency Limited (SANRAL). Permission to use their materials, designs and information is gratefully acknowledged. The opinions are those of the author and not necessarily the policy of the company.
2. South African National Road Agency Limited (SANRAL), the Sponsor of the author's studies, and the University of Pretoria for their financial support during the study.
3. The University of Pretoria for the use of the hydraulic laboratory and other facilities during the studies.
4. Mr Marco van Dijk, my supervisor for his guidance and continuous support through the course of my research study.
5. Prof Wynand Steyn, my co-supervisor and the head of the Civil Department at the University of Pretoria, for his guidance and support.
6. The following persons are also gratefully acknowledged for their assistance during the study:
  - a) Mr Hennie Kotze from South African National Road Agency Limited,
  - b) Mr Martin Boonstra from KBK Engineers,
  - c) Ms Cora Bezuidenhout from the library services of the University of Pretoria,
  - d) Mr Marcel Brauns Sales Manager of Salberg Concrete Products (Pty) Ltd,
  - e) Ms Rachel Mahlangu from International Interlending services of the University of Pretoria.
  - f) Ms Adele Labuscagne for proofreading, editing and final formatting of the thesis.
7. Our Heavenly Father, for giving me the knowledge, strength and encouragement to complete my studies.
8. My family and friends for their patience, encouragement and support during the study.

**UNIVERSITY OF PRETORIA**  
**FACULTY OF ENGINEERING, BUILT ENVIRONMENT AND INFORMATION TECHNOLOGY**  
**DEPARTMENT OF CIVIL ENGINEERING**

The Department of Civil Engineering places great emphasis upon integrity and ethical conduct in the preparation of all written work submitted for academic evaluation.

While academic staff teaches you about systems of referring and how to avoid plagiarism, you too have a responsibility in this regard. If you are at any stage uncertain as to what is required, you should speak to your lecturer before any written work is submitted.

You are guilty of plagiarism if you copy something from a book, article or website without acknowledging the source and pass it off as your own. In effect, you are stealing something that belongs to someone else. This is not only the case when you copy work word-by-word (verbatim), but also when you submit someone else's work in a slightly altered form (paraphrase) or use a line of argument without acknowledging it. You are not allowed to use another student's past written work. You are also not allowed to let anybody copy your work with the intention of passing it as his/her work.

Students who commit plagiarism will lose all credits obtained in the plagiarised work. The matter may also be referred to the Disciplinary Committee (Students) for a ruling. Plagiarism is regarded as a serious contravention of the University's rules and can lead to expulsion from the University.

The declaration which follows must be appended to all written work submitted while you are a student of the Department of Civil Engineering. No written work will be accepted unless the declaration has been completed and attached.

**DECLARATION:**

1. I understand what plagiarism is and am aware of the University's policy in this regard.
2. I declare that this submission is my own original work. Where other people's work has been used (either from a printed source, internet or any other source) this has been properly acknowledged and referenced in accordance with departmental requirements.
3. I have not used another student's current or past written work to hand in as my own.
4. I have not allowed, and will not allow, anyone to copy my work with the intention of passing it off as his or her own work

**DISCLAIMER:**

The work presented in this report is that of the student alone. Students were encouraged to take ownership of their projects and to develop and execute their experiments with limited guidance and assistance. The content of the research does not necessarily represent the views of the supervisor or any staff member of the University of Pretoria, Department of Civil Engineering. The supervisor is not responsible for any technical inaccuracies, statements or errors. The conclusions and recommendations given in the report are also not necessarily that of the supervisor, sponsors or companies involved in the research.

**I (full names)** : Bernard Jansen van Vuuren

**Student number** : 11019892

**Subject of work** : The interception capabilities of slotted drains as pavement surface drainage systems

**Date** : 30-11-2018

**Signature** : 

## TABLE OF CONTENTS

	PAGE
<b>1. INTRODUCTION.....</b>	<b>1-1</b>
1.1 BACKGROUND OF PAVEMENT SURFACE DRAINAGE.....	1-1
1.2 PROBLEM STATEMENT (A CASE STUDY).....	1-3
1.3 RESEARCH OBJECTIVES .....	1-4
1.4 SCOPE OF THE STUDY .....	1-5
1.5 METHODOLOGY .....	1-6
1.6 ORGANISATION OF THE REPORT .....	1-6
<b>2. LITERATURE REVIEW .....</b>	<b>2-1</b>
2.1 INTRODUCTION TO PAVEMENT DRAINAGE .....	2-1
2.2 HYDROPLANING.....	2-1
2.2.1 CONTRIBUTING FACTORS TO HYDROPLANING.....	2-2
2.3 SPLASH AND SPRAY .....	2-5
2.4 WATER FILM THICKNESS.....	2-5
2.4.1 PREDICTION METHODS (MODELS).....	2-6
2.4.2 CONTROLLING WATER FILM THICKNESS.....	2-10
2.5 SLOTTED DRAINS.....	2-13
2.5.1 THE FUNCTIONALITY OF SLOTTED DRAINS .....	2-13
2.5.2 THE HYDRAULICS OF SURFACE FLOW .....	2-17
2.5.3 THE INTERCEPTION CAPACITY AND EFFICIENCY OF SLOTTED DRAINS .....	2-20
2.5.4 DISADVANTAGES OF SLOTTED DRAINS .....	2-21
2.6 RELEVANT STUDIES ON SURFACE DRAINAGE .....	2-23
2.6.1 HYDRAULIC CAPACITY AND EFFICIENCY OF SLOTTED DRAINS .....	2-24
2.6.2 SLOTTED DRAINS IN SAG (SUMP) LOCATIONS.....	2-30
2.7 SCALING OF PHYSICAL HYDRAULIC MODELS.....	2-32
<b>3. EXPERIMENT METHODOLOGY .....</b>	<b>3-1</b>
3.1 INTRODUCTION .....	3-1
3.2 PROPRIETARY SLOTTED DRAIN SPECIFICATIONS .....	3-1
3.3 TEST PARAMETERS.....	3-3
3.3.1 PAVEMENT AND PRECAST CONCRETE SURFACE TEXTURES .....	3-4
3.3.2 LONGITUDINAL SLOPE .....	3-4



3.3.3	CROSS SLOPE.....	3-4
3.3.4	MEDIAN BARRIER .....	3-4
3.3.5	RAINFALL INTENSITY .....	3-5
3.3.6	WIDTH OF THE SLOTTED INLET .....	3-5
3.4	MODEL DESCRIPTIONS AND CONSTRUCTION.....	3-5
3.5	EXPERIMENTAL SET UP AND MODEL OPERATIONS .....	3-12
3.5.1	WATER SUPPLY SYSTEM (i) .....	3-12
3.5.2	WATER CATCHMENT AREA (ii).....	3-14
3.5.3	WATER DRAINAGE SYSTEM (iv) .....	3-16
3.6	FLOW MEASURING DEVICES.....	3-17
3.6.1	DEVICE SET UP.....	3-18
3.6.2	VERIFICATION OF MEASUREMENTS .....	3-18
3.7	TEST PROCEDURES .....	3-20
3.7.1	SAND PATCH TEST PROCEDURE .....	3-20
3.7.2	EXPERIMENTAL TEST PROCEDURES.....	3-22
<b>4.</b>	<b>DATA COLLECTION AND ANALYSIS OF RESULTS.....</b>	<b>4-1</b>
4.1	INTRODUCTION .....	4-1
4.2	TEST LIMITATIONS .....	4-1
4.3	SAND PATCH TEST RESULTS.....	4-2
4.4	INTERCEPTION EFFICIENCY TEST RESULTS .....	4-3
4.5	WATER DEPTH MEASUREMENT RESULTS.....	4-13
4.6	GENERAL OBSERVATIONS .....	4-15
4.7	COMPARISON WITH PREVIOUS STUDIES .....	4-16
<b>5.</b>	<b>CONCLUSIONS AND RECOMMENDATIONS.....</b>	<b>5-1</b>
5.1	CONCLUSIONS .....	5-1
5.2	RECOMMENDATIONS .....	5-3
<b>6.</b>	<b>REFERENCES.....</b>	<b>6-1</b>
<b>A.</b>	<b>APPENDIX A .....</b>	<b>A-1</b>
<b>B.</b>	<b>APPENDIX B .....</b>	<b>B-1</b>

## LIST OF FIGURES

	PAGE
Figure 1-1: Detailed cross section of the slotted drain installed adjacent to the median barrier.....	1-4
Figure 2-1: Hydroplaning factors (Chaithoo and Allopi, 2012) .....	2-3
Figure 2-2: Sheet flow on the pavement surface (privately captured) .....	2-4
Figure 2-3: Definition of water film thickness (Anderson et al., 1998).....	2-6
Figure 2-4: Slotted drain inlet (Brown et al., 2009).....	2-13
Figure 2-5: Slotted drain installations on N1 highway near Centurion (privately captured).....	2-14
Figure 2-6: Cross section of the installation scenarios of slotted drains: (A) - with median barrier; (B) - without median barrier.....	2-15
Figure 2-7: Clogging of slotted inlets (privately captured).....	2-22
Figure 2-8: Slotted inlet cover failure and settlement.....	2-23
Figure 2-9: Damaged slotted inlets .....	2-23
Figure 2-10: Assumed water and energy profile for sub-critical flow (Gouws, 1993).....	2-29
Figure 3-1: Cross section design of the propriety slotted drain .....	3-2
Figure 3-2: Type I Model design .....	3-6
Figure 3-3: Type II Model design.....	3-7
Figure 3-4: Pavement surface treatment .....	3-10
Figure 3-5: Visible uneven sand patches .....	3-10
Figure 3-6: Constructed Type I model.....	3-11
Figure 3-7: Constructed Type II model.....	3-11
Figure 3-8: Principle features of test set up (schematic).....	3-13
Figure 3-9: Principle features of the water catchment area, Section A-A.....	3-14
Figure 3-10: Water catchment features (A) .....	3-15
Figure 3-11: Water catchment features (B).....	3-15
Figure 3-12: Principle features of the water drainage system, section B-B.....	3-16
Figure 3-13: Test set up for the Type I models.....	3-17
Figure 3-14: Test set up for the Type II model.....	3-17
Figure 3-15: The principle of magnetic-inductive flow measurements (Sensus, 2018) .....	3-18
Figure 3-16: Bucket test.....	3-19
Figure 3-17: Area marked with chalk .....	3-21
Figure 3-18: Sand spread in a zig zag pattern.....	3-21
Figure 3-19: Sand patch length measurement.....	3-21
Figure 3-20: Sheet flow on the pavement model surface.....	3-22

Figure 3-21: Flow depth measurements .....	3-23
Figure 3-22: Model height measurements for specific slope configuration.....	3-23
Figure 3-23: Water catchment area lifted with model slope adjustments .....	3-23
Figure 3-24: Pavement model elevated at a specific slope configuration.....	3-24
Figure 3-25: Blue dye applied to indicate water flow path slope .....	3-24
Figure 4-1: Results of rainfall intensities and water flow path lengths - all applied test flows .....	4-9
Figure 4-2: Rainfall intensities and flow depth results - 0.5l/s applied test flow.....	4-10
Figure 4-3: Rainfall intensities and flow depth results - 1.0l/s applied test flow.....	4-10
Figure 4-4: Rainfall intensities and flow depth results - 1.5l/s applied test flow.....	4-11
Figure 4-5: Rainfall intensities and flow depth results - 2.0l/s applied test flow.....	4-11
Figure 4-6: Rainfall intensities and flow depth results - 2.5l/s applied test flow.....	4-12
Figure 4-7: Rainfall intensities and flow depth results - 3.0l/s applied test flow.....	4-12
Figure 4-8: Almost 100% sheet flow interception observed for all applied sheet flow .....	4-15
Figure 4-9: Intercepted sheet flow captured in drainage system.....	4-16

## LIST OF TABLES

	PAGE
Table 2-1: Maximum gradients (Committee of State Road Authorities, 1988).....	2-11
Table 2-2: Slotted drain case studies.....	2-15
Table 2-3: Model characteristics and test conditions (Pugh, 1980).....	2-26
Table 3-1: Slotted drain dimensions and specifications.....	3-3
Table 3-2: Type I Model dimensions.....	3-8
Table 3-3: Type II Model dimensions.....	3-8
Table 3-4: Principle features of experimental set up. ....	3-12
Table 3-5: Pump specifications.....	3-14
Table 3-6: Summary of average flow rates.....	3-20
Table 3-7: Test conditions.....	3-25
Table 4-1: Mean texture depth (MTD) results.....	4-2
Table 4-2: Interception efficiency test results, Type I model with a 20mm slotted inlet width.....	4-4
Table 4-3: Interception efficiency test results, Type I model with a 40mm slotted inlet width.....	4-5
Table 4-4: Interception efficiency test results, Type I model with a 60mm slotted inlet width.....	4-6
Table 4-5: Interception efficiency test results, Type II model with a 20mm slotted inlet width.....	4-7
Table 4-6: Maximum estimated flow depths.....	4-13
Table 4-7: Flow depth measurement results - Type I model with 20mm slot inlet width.....	4-14
Table B-1: Flow measurement verification data.....	B-1
Table B-2: Test Data-Type I model, 20mm slot width, 0% longitudinal slope & 2% cross slope.....	B-2
Table B-3: Test Data-Type I model, 20mm slot width, 0% longitudinal slope & 4% cross slope.....	B-3
Table B-4: Test Data-Type I model, 20mm slot width, 0% longitudinal slope & 6% cross slope.....	B-4
Table B-5: Test Data-Type I model, 20mm slot width, 2% longitudinal slope & 6% cross slope.....	B-5
Table B-6: Test Data-Type I model, 20mm slot width, 4% longitudinal slope & 6% cross slope.....	B-6
Table B-7: Test Data-Type I model, 20mm slot width, 6% longitudinal slope & 6% cross slope.....	B-7
Table B-8: Test Data-Type I model, 40mm slot width, 0% longitudinal slope & 2% cross slope.....	B-8
Table B-9: Test Data-Type I model, 40mm slot width, 0% longitudinal slope & 4% cross slope.....	B-9
Table B-10: Test Data-Type I model, 40mm slot width, 0% longitudinal slope & 6% cross slope.....	B-10
Table B-11: Test Data-Type I model, 40mm slot width, 2% longitudinal slope & 6% cross slope.....	B-11
Table B-12: Test Data-Type I model, 40mm slot width, 4% longitudinal slope & 6% cross slope.....	B-12
Table B-13: Test Data-Type I model, 40mm slot width, 6% longitudinal slope & 6% cross slope.....	B-13
Table B-14: Test Data-Type I model, 60mm slot width, 0% longitudinal slope & 2% cross slope.....	B-14
Table B-15: Test Data-Type I model, 60mm slot width, 0% longitudinal slope & 4% cross slope.....	B-15

Table B-16: Test Data-Type I model, 60mm slot width, 0% longitudinal slope & 6% cross slope ..... B-16

Table B-17: Test Data-Type I model, 60mm slot width, 2% longitudinal slope & 6% cross slope ..... B-17

Table B-18: Test Data-Type I model, 60mm slot width, 4% longitudinal slope & 6% cross slope ..... B-18

Table B-19: Test Data-Type I model, 60mm slot width, 6% longitudinal slope & 6% cross slope ..... B-19

Table B-20: Test Data-Type II model, 20mm slot width, 0% longitudinal slope & 2% cross slope ..... B-20

Table B-21: Test Data-Type II model, 20mm slot width, 0% longitudinal slope & 4% cross slope ..... B-21

Table B-22: Test Data-Type II model, 20mm slot width, 0% longitudinal slope & 6% cross slope ..... B-22

Table B-23: Test Data-Type II model, 20mm slot width, 2% longitudinal slope & 6% cross slope ..... B-23

Table B-24: Test Data-Type II model, 20mm slot width, 4% longitudinal slope & 6% cross slope ..... B-24

Table B-25: Test Data-Type II model, 20mm slot width, 6% longitudinal slope & 6% cross slope ..... B-25

Table B-26: Rainfall intensity and flow depth data-0.5l/s applied test sheet flow ..... B-26

Table B-27: Rainfall intensity and flow depth data-1.0l/s applied test sheet flow ..... B-27

Table B-28: Rainfall intensity and flow depth data-1.5l/s applied test sheet flow ..... B-28

Table B-29: Rainfall intensity and flow depth data-2.0l/s applied test sheet flow ..... B-29

Table B-30: Rainfall intensity and flow depth data-2.5l/s applied test sheet flow ..... B-30

Table B-31: Rainfall intensity and flow depth data-3.0l/s applied test sheet flow ..... B-31

## LIST OF ABBREVIATIONS, SYMBOLS AND UNIT OF MEASURE

### ABBREVIATIONS

AASHTO	:	American Association of State Highway and Transportation Officials
AC	:	Asphalt concrete
FHWA	:	Federal Highway Administration
Fr	:	Froude number
GFIP	:	Gauteng Freeway Improvement Projects
MTD	:	Mean Texture Depth
N2	:	National Road 2
NAASRA	:	National Association of Australian State Road Authorities
PVC	:	Polyvinyl chloride
RRL	:	Road Research Laboratory
RTMC	:	Road Traffic Management Corporation
SABS	:	South African Bureau of Standards
Salberg	:	Salberg Concrete Products (Pty) Ltd
SANRAL	:	South African Road Agency Limited
SAPEM	:	South African Pavement Engineering Manual
SBCE	:	Sigma Beta Consulting Engineers
TxDOT	:	Texas Department of Transportation
UP	:	University of Pretoria
USBR	:	United States Bureau of Reclamation
UTFC	:	Ultra-Thin Friction Course
WFD	:	Water Film Depth
WTF	:	Water Film Thickness
Y	:	Water Flow Layer

## SYMBOLS

A	=	area of slot opening (m <sup>2</sup> )
A	=	cross sectional area (m <sup>2</sup> )
A	=	cross sectional area of the catchment/water film (km <sup>2</sup> )
A	=	effective cross sectional plan area of the opening (m <sup>2</sup> )
A	=	volume of sand (ml)
B	=	flow width (m)
B	=	area covered by sand (m <sup>2</sup> )
b	=	total width of flow (m)
C	=	inlet coefficient
C	=	run-off coefficient
C <sub>a</sub>	=	inlet coefficient
C <sub>b</sub>	=	blockage factor
C <sub>D</sub>	=	discharge coefficient
C <sub>o</sub>	=	orifice coefficient
C <sub>w</sub>	=	weir coefficient
d	=	depth at slot inlet measured from the normal cross slope (m)
D	=	hydraulic depth (m)
d	=	water depth at slotted inlet for d > 0.12m (m)
d	=	water flow depth (mm)
E	=	interception efficiency (%)
E <sub>o</sub>	=	ratio of flow in the depressed section to total gutter flow
F	=	blockage factor
Fr	=	Froude number
Fr	=	Froude number immediately upstream of the first slot
g	=	gravitational acceleration (9.81m/s <sup>2</sup> )
H	=	energy head (flow depth), (m)
H	=	total energy head (water depth) above the grid (m)
I	=	rainfall intensity (mm/h)
I	=	average rainfall intensity over a catchment (mm/hr)
k <sub>s</sub>	=	absolute surface roughness (m)
k <sub>u</sub>	=	constant
L	=	slotted drain inlet length (m)
L	=	length of drainage path (m)

L	=	slot length (m)
$l_f$	=	length of flow path (m)
$L_T$	=	slotted inlet length to intercept 100% of the gutter flow (m)
n	=	Manning's roughness coefficient
$n_1$	=	pavement crossfall (%)
$n_2$	=	pavement gradient (%)
P	=	manifold pressure (kPa)
Q	=	flow through a slot opening ( $m^3/s$ )
Q	=	gutter flow ( $m^3/s$ )
Q	=	flow rate ( $m^3/s$ )
Q	=	peak flow ( $m^3/s$ )
q	=	sheet flow ( $ft^3/sec$ )
Q	=	total flow ( $m^3/s$ )
Q	=	total gutter flow ( $m^3/s$ )
$Q_b$	=	bypass flow ( $m^3/s$ )
$Q_i$	=	intercepted flow ( $m^3/s$ )
$Q_i$	=	interception capacity flow ( $m^3/s$ )
$Q_w$	=	flow in width W ( $m^3/s$ )
R	=	hydraulic radius (m)
r	=	roughness coefficient
S	=	Slope of drainage path (%)
$S_{av}$	=	Slope of catchment
$S'_w$	=	cross slope of gutter measured from the cross slope of pavement (m/m)
$S_e$	=	equivalent cross slope (m/m)
$S_f$	=	energy slope of flow path (%)
$S_f$	=	flow path slope (%)
$S_f$	=	friction slope (energy grade line)
$S_L$	=	longitudinal slope (m/m)
$S_x$	=	cross slope (m/m)
T	=	total spread of water (m)
$T_c$	=	time of concentration (hours)
$T_d$	=	texture depth (mm)
TXD	=	mean pavement texture depth (mm)
US	=	United States



V	=	cross sectional average flow velocity (m/s)
V	=	flow velocity (m/s)
W	=	pavement width (m)
W	=	width of depressed gutter (m)
W	=	width of slot (m)
WFD	=	water film depth above the top of the surface asperities (mm)
y	=	water depth (m)
z	=	constant

## UNITS OF MEASURE

%	:	percentage
ft <sup>3</sup> /sec	:	cubic feet per second
km <sup>2</sup>	:	square kilometer
kPa	:	kilo Pascal
m	:	meter
m/m	:	meter per meter
m/s	;	meter per second
m/s <sup>2</sup>	:	meter per second square
ml	:	milli litres
m <sup>2</sup>	:	square meter
m <sup>3</sup> /s	:	cubic meter per second
mm	:	millimetres
mm/h	:	millimetres per hour
s/m <sup>1/3</sup>	:	second per meter a third

## **1. INTRODUCTION**

### **1.1 BACKGROUND OF PAVEMENT SURFACE DRAINAGE**

Drainage of a pavement structure plays a significant role in the pavement's performance when it is subjected to traffic loads in different environmental conditions. Water is the primary cause of accelerated distress, premature reduction in structural capacity and failure of a pavement structure (SANRAL, 2014). The drainage design of the pavement should thus be completed in detail to ensure adequate surface and subsurface drainage without creating a more significant hazard than the stormwater on the pavement surface it wishes to remove.

Surface drainage is the removal of all ponding water on the pavement surface, including the pavement shoulder or any other surface from which it may sheet flow to the pavement edge. However, the risk of water ponding should not be confused with water sheeting. Water ponding occurs when the sheet flow is restricted on the pavement surface and unable to drain for example due to rutting in vehicle's wheel paths or at poor vertical and horizontal alignment designs. As a pavement age, rutting can occur, and water is more likely to accumulate on the pavement surface. Ponding water penetrates through the surface layer of the pavement and weakens the underlying pavement layers which lead to fatal and expensive consequences.

The Road Traffic Management Corporation (RTMC, 2018) stated in their yearly report that 11 437 fatal crashes have occurred on South African pavements between January and December in 2017. Road and environmental factors contributed five percent to these deadly crashes, and 21% and 11.5% were caused by wet road surfaces and visibility issues, respectively. Consequently, water on pavement surfaces was responsible for about 120 fatal crashes during 2017 and thus is pavement surface drainage crucial to enhance safe driving conditions by minimising the risk of hydroplaning and splash and spray.

Hydroplaning, also known as aquaplaning, is the partial or full separation between the wheels of a vehicle and the pavement surface, caused by the excessive water pressures accumulated between the vehicle's wheels and the pavement surface. The water pressures are equal to the forces exerted by the wheels and as these pressures increases; it reduces skid resistance and steering ability of the vehicle diminishes. Hydroplaning is directly proportional to the depth of the water film on the pavement surface and is highly influenced by fundamental factors such as the driver characteristics, vehicle dynamics, pavement conditions (geometric design, drainage design and maintenance) and several environmental factors. According to

Brown et al. (2009), hydroplaning can occur at travelling speeds from 89km/hr with thin water depths of only 2mm.

The three general techniques to reduce the water film thickness on a pavement surface to minimise the risk for hydroplaning and splash and spray is by regulating the pavement geometry, using different pavement surface textures and implementing efficient surface drainage systems (Anderson et al., 1998). The geometry and the surface texture of the pavement are designed to allow surface water to run downwards on the slope of the pavement in a thin continuous film or sheet to be efficiently drained by a drainage system either a drain, a gutter or a curb inlet. Depending on the geometrical design of the pavement, these drainage systems can be installed in the centre of a roadway for wider pavements or at the edge of the pavement to drain water sheeting down the slope.

The placement of slotted drains between adjacent lanes on wider pavements with three to four carriageways is a recommended drainage technique to enhance surface drainage (Anderson et al., 1998). Slotted drains are pipe segments that are cut along its longitudinal length as an opening and usually with bars spaced perpendicular to the pipe opening to form slots for drainage. These drains are placed between adjacent lanes to reduce the distance the water must flow (water flow path length) before it can be removed from the pavement surface.

The implementation of slotted drains as drainage systems on pavements in South Africa is still a sceptical drainage solution for numerous pavement designers as uncertainty in the pavement design practice can often lead to over design, wasted expenses or unsafe pavement structures. Pugh et al., (1980) have conducted a research study mainly on the interception capacity of slotted drains under various pavement conditions. While Brown et al., (2009) with the cooperation of the United States (US) Department of Transportation's Federal Highway Administration (FHWA), investigated the slotted length required for a 100% flow interception of a specific slotted drain design. Both these studies were based on a particular slotted drain design used in the US.

The need of the study thus arose from the uncertainty of the interception drainage capabilities (hydraulic efficiencies) of specific slotted inlets operating under various pavements and environmental conditions in the South African domain.

## 1.2 PROBLEM STATEMENT (A CASE STUDY)

South African National Road Agency Limited (SANRAL) is investigating the possible improvement of the National Road 2 (N2) between the Kwa-Zulu Natal and Mpumalanga border near Pongola. According to the consulting engineers of the project, the client (SANRAL) requires an upgrade of a two-lane carriageway pavement facility to an undivided four-lane carriageway pavement facility, with a total cross sectional pavement width of 21m in the near future. During the preliminary investigation period, there were concerns that on certain superelevation sections there will be excessive rainwater on the pavement surface if it flows over the full width of the pavement.

SANRAL recommended a possible solution to intercept the rainwater in the centre of the pavement, halfway down the slope of the superelevation in some form of a drain. SANRAL has previously implemented concrete drains with grid inlets, installed adjacent to a median barrier, in Gauteng Freeway Improvement Projects (GFIP). Although it has been tested in a model at the University of Stellenbosch (Gouws, 1993), these drains have some problems functioning effectively in practice.

The consulting engineers proposed to install other proprietary pre-cast slotted drains from a specific manufacturer instead of the concrete drains used in the GFIP projects. It is still not definite whether rainwater, flowing down the pavement's superelevation, will adequately be intercepted by the slotted drains at the median of the road. The client may also request to install median barriers adjacent to the slotted drains if this solution is implemented, based on economic evaluations. The cross section of the suggested concept of the proprietary slotted drain to be installed adjacent to a median barrier can be seen in Figure 1-1.

Uncertainties with this possible implementation of the slotted drainage system in this SANRAL pavement upgrade project include:

- How effective will the surface runoff be removed or captured if a slotted drain is installed while operating individually without a median barrier?
- How will the size of a slotted inlet influence the interception capability of the slotted drain while operating without a median barrier?
- If surface water is not 100% been intercepted by the slotted drains while operating without a median barrier, will a concrete median barrier that is installed adjacent with a slotted drain, promote the interception capabilities of the slotted drain?
- What adjustments can be made to the proprietary slotted drains to improve the interception capabilities of the drain?

- How can the slotted drains be installed on a safe and cost-effective way for maximum effectiveness to remove surface water?

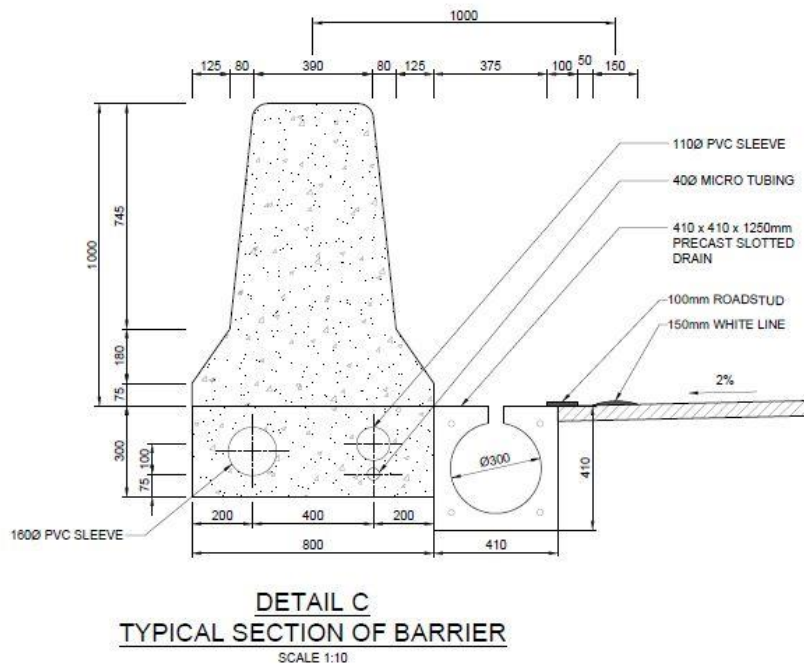


**Figure 1-1: Detailed cross section of the slotted drain installed adjacent to the median barrier**

To obtain answers to the above-mentioned questions, a research study was required to examine the interception capabilities of slotted drains while operating under the following two installation conditions:

- The operation of a slotted drain with an adjacent median barrier, which is installed horizontally within the pavement structure (with zero percent slope) with the median barrier, and
- The operation of a slotted drain without an adjacent median barrier, installed within the pavement structure at the same gradient as the cross slope of the pavement.

### 1.3 RESEARCH OBJECTIVES

The primary objective of the study was to examine the interception drainage capabilities of the proprietary slotted drains to determine the interception efficiencies of the proprietary slotted drains which SANRAL is considering implementing in the project. Also, to find informative answers to the uncertainties and questions specific to this case study.

**Other objectives were to:**

- Conduct a literature review to establish the state of practice about the implementation of slotted drains within the pavement structure to enhance surface drainage. A model study was also performed in order to construct an experimental model of a pavement with a slotted drainage system and adjustable features such as pavement slopes, slotted drain types and slotted drains operating with or without an adjacent barrier.
- Generate test data on the various flows (i.e. total input flow, intercepted flow and bypassed flow) of the individual slotted drain types for operating under different hydraulic conditions.
- Determine the efficiency of each test configuration as the ratio of total intercepted flow to total sheet flow.
- Provide informative and understandable explanation from the test results of slotted drain operations under different hydraulic conditions.
- Provide qualitative and quantitative feedback to SANRAL, regarding the implementation of these proprietary slotted drains in their project.

#### **1.4 SCOPE OF THE STUDY**

The only feature of surface drainage appurtenances investigated during the study was the interception drainage capabilities of slotted drain inlets under sheet flow conditions. Slotted drains operating in sump locations and the sensitivity to debris was only discussed in the literature as background. Therefore, as part of this study, debris tests and tests of slotted drains operating in sump conditions were not conducted.

The slotted drains being considered for the experiment in this research study was the property of a company called Salberg Concrete Products (Pty) Ltd. Similar generalized experimental models were developed according to these specifications of the proprietary slotted drains and only the top inlet part of the drains was re-constructed as a representative of the actual proprietary slotted drains required for testing. Since the actual proprietary slotted drain products were not tested in the study, the hydraulic capacity of the slotted drains, below the inlets, was not determined. Also, no structural analysis was performed in this study to assess the structural capacity (integrity) of the proprietary slotted drains.

Only efficiencies on sheet flow conditions were tested, and due to the scaling of the model, gutter flow from the side of the model was not implemented for testing assuming that SANRAL will install a long enough slotted length.

The effect of splash and spray caused by vehicles travelling during wet pavement conditions was very difficult to simulate during the experiment of study and was therefore ignored. Discussions made on the phenomenon of splash and spray was based only on the background knowledge obtained in the literature.

## **1.5 METHODOLOGY**

The methodology followed during the research study involved the following:

- A detailed literature review was conducted on pavement surface drainage. The implementation of slotted drains as surface drainage appurtenances, utilising the interception efficiencies of slotted inlets, was theoretically investigated and evaluated based on the research from existing literature.
- Experimental models were designed and constructed to simulate, under various assumptions, the implementation of slotted drains operating under two different installation conditions. The first installation condition was the operations of a slotted drain without an adjacent barrier, and the other installation condition was the operations of a slotted drain with an adjacent barrier.
- The pavement models were tested by using various variables for the two different test conditions which include: the slotted drain characteristics, pavement slope configurations and the volume of sheet flow applied.
- Test data was recorded and analysed to determine the interception efficiencies of the slotted drains. The experimental results were presented in tables, and graphical illustrations (graphs) were used to depict the field conditions in practice that were tested for during the experiment.
- Conclusions were clearly stated on the findings obtained from the experiment and recommendations were documented for future research in this field.

## **1.6 ORGANISATION OF THE REPORT**

The following chapters and appendixes constructed the report:

- Chapter 1 is the introduction of the report. It provides general background to pavement surface drainage and includes the problem statement (based on a case study), objectives, methodology; and scope of the study.
- Chapter 2 serve as literature review of pavement surface drainage focussing on surface drainage theories and concepts, drainage appurtenances and relevant model studies for experimenting.
- Chapter 3 is a description of the experimental methodology followed to gather test data of the interception capabilities of slotted inlets on constructed pavement models. The test set up, conditions, parameters and model operations are all discussed in this chapter.



- Chapter 4 discussed the data collection process during the experiment of the study. This analysis chapter is a discussion of the test limitations, findings and observations made during the experiment.
- Chapter 5 serves as a conclusion to the study and includes recommendations for future research on the topic of slotted drainage systems.
- Chapter 6 is a list of references as acknowledgement for the work and information of other authors, used in this study.
- Appendix A contains the nomographs of previous studies used as background knowledge and is linked to the literature review of the study.
- Appendix B contains data tables of all the test results obtained during the experimental part of the study.

## **2. LITERATURE REVIEW**

This chapter provides an informative overview of pavement drainage and technically review different surface drainage systems, specifically slotted drains, operating in the field. The literature review discusses the guidelines, findings and test procedures of existing literature of slotted drainage systems. The literature review aimed to gain an understanding of different pavement surface drainage concepts and the operations of the pavement surface drainage systems in the field. The knowledge of slotted drainage systems obtained from the literature was used to evaluate the hydraulic drainage capabilities of slotted drains operating in practice.

### **2.1 INTRODUCTION TO PAVEMENT DRAINAGE**

The improvement of pavement drainage in critical environmental conditions may increase the lifespan of the pavement significantly as undrained pavement conditions are responsible for accelerated distress, premature reduction in structural capacity and early failure of a pavement structure. Therefore, the implementation of a suitable and effective drainage system is essential in any pavement design.

The drainage of a pavement structure involves two aspects namely surface drainage and subsurface drainage. Surface drainage is the process of removing rainwater that fell on a pavement surface and flowing slope down in the form of a thin film of water. Surface drainage aims to reduce the possibility of water infiltrating into the pavement's foundation layers and improves the safety of traffic. By removing the surface runoff from the pavement as quickly as possible with the proper drainage systems, this can be achieved. Then again, subsurface drainage entails the removal of water within the layers of a pavement which infiltrate through the cracks, joints and pores of the pavement surface. Although it is essential for any pavement designer to consider both surface and subsurface drainage during pavement design, subsurface drainage was not being discussed in this dissertation and falls outside the scope of the study.

Two phenomena associated with surface drainage and the risk of water ponding on a pavement surface is hydroplaning and splash and spray. These phenomena are defined as follows:

### **2.2 HYDROPLANING**

Hydroplaning, also identified as aquaplaning, is the loss of contact between the tyres of a vehicle and the surface of the pavement when a vehicle moves fast enough to drive on a thin film of water. The water film on the pavement surface reduces the pavement skid resistance which can lead to a total loss of a vehicle

steering ability. Aquaplaning is classified into two main categories; dynamic and viscous aquaplaning which is described individually as follows (Chesterton, 2006):

- **DYNAMIC HYDROPLANING**

Dynamic aquaplaning may occur without a change in vehicle acceleration during rainfalls when a water layer forms on the pavement surface. When a vehicle is travelling through a water layer, the tyres push the water away and cause small waves to form in front of it. The waves propagate to the side of the tyres or escape through the tyre tread pattern. With an increase in vehicle speed, the water wave has less time to avoid the upcoming tyres and water becomes highly pressurised between the tyres and the pavement surface. The separation between the tyres and the pavement surface occur when the water pressure is equal to the downwards force of the vehicle resulting in the loss of traction. As the tyre loses contact with the pavement surface, it loses angular momentum and causes the tyre to spin uncontrolled.

- **VISCOUS HYDROPLANING**

Viscous aquaplaning may occur at any vehicle speed on very thin water films due to the viscous properties of water. The viscous forces within a water film affect the interaction interface between the tyres of a vehicle and texture of the pavement surface. Lateral and longitudinal vehicle acceleration may cause a vehicle to slide since the friction between the tyre and the pavement surface reduces. Therefore, the macrotexture of the pavement surface and the tread pattern of a vehicle tyre are crucial in absorbing and diffusing flow paths to remove the water film on the pavement surface. Other than dynamic aquaplaning, typical locations for viscous aquaplaning to occur is at areas where decelerating is common such as intersections or curves.

### **2.2.1 CONTRIBUTING FACTORS TO HYDROPLANING**

The tendency of hydroplaning to initiate is directly proportional to the thickness of the water film on the pavement surface and hydroplaning is affected by several countable factors depicted in Figure 2-1, adapted from Chaithoo and Allopi (2012). These factors can either alter the water film thickness on the pavement surface itself or affect the driving sensitivity to the thickness of the water film on the pavement surface.

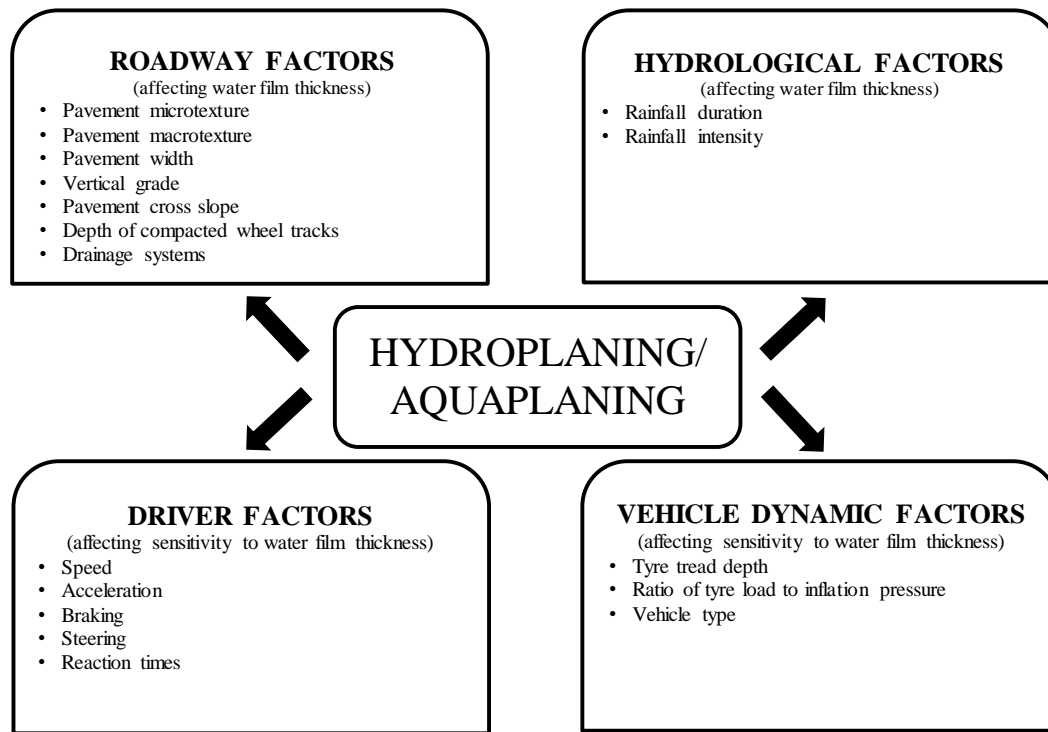


**Figure 2-1: Hydroplaning factors (Chaithoo and Allopi, 2012)**

### 2.2.1.1 ROADWAY FACTORS

The geometric design of the pavement structure and the surface texture of the upper layer have a substantial effect on the ability to decrease the water depth when rainwater flows over on the pavement surface.

The geometry of a pavement (its vertical grade and cross slope) controls the speed of sheet flow on the surface, while the pavement width or length of the water flow path on the pavement surface, determine the period that the pavement can accumulate rainwater. Longer flow paths cause water to stay longer on the pavement surface which increases the flow depths and initiating hydroplaning to exist. Superelevation changes and steep longitudinal grades may result in longer water flow paths and ultimately the flow depth.

Laminar free surface flow conditions may be assumed if the water surface is below the top of the aggregate macro asperities (Gallaway et al., 1975). However, the classification and state of surface flow on pavements are discussed in paragraph 2.5.2. The pavement surface texture allows rainwater to fill between the interstices of the aggregates and provides a flow path for drainage. As the water depth increases beyond the tops of the asperities of the aggregate, the water will sheet flow down the slope of the pavement to the edge of the pavement and into a drainage catchment area as illustrated in Figure 2-2.



**Figure 2-2: Sheet flow on the pavement surface (privately captured)**

Drainage systems such as concrete channels, kerbs, and grate inlets are installed to collect and remove accumulated surface water on the pavement. Installation locations, as well as efficient maintenance operations of these drainage systems, are vital to minimise ponding water in trafficking areas and reduce the risk for hydroplaning.

#### **2.2.1.2 ENVIRONMENTAL FACTORS**

During highly intensive or long durational rainfall events, surface drainage can become problematic. The water runoff and water film thickness increase when the rainfall intensity increases. The rainwater fills the interstices of the surface aggregates and water tends to pond on the surface of the pavement. The ponding water on the pavement surface improves the risk for hydroplaning and excessive vehicle splash and spray to occur.

#### **2.2.1.3 DRIVER FACTORS**

The driving behaviour of road users such as reaction times, braking, acceleration, steering abilities and vehicle speed plays an integral part for hydroplaning to occur during wet pavement conditions. The minimum vehicle speed to initiate hydroplaning is dependent on the water film thickness as well as other vehicle characteristics such as vehicle weight and tyre conditions.

#### **2.2.1.4 VEHICLE DYNAMIC FACTORS**

Vehicle types and tyre conditions are also an important hydroplaning factor. The weight of a vehicle determines the magnitude of uplift force required to bring separation between the pavement surface and the

tyres of the vehicle. The tyre pressure determines the contact area between the tyres and the pavement surface as it influences the weight to area ratio of a vehicle's tyre. The tyre tread depth has the same effect on hydroplaning as the macrotexture depth of aggregates. Deeper tyre treads allow water to migrate into the tyre grooves and away from the contact area when a vehicle drives on a thin film of water. This ensures that a vehicle remains in contact with the pavement surface. The law specifies a minimum tyre tread depth and a maximum vehicle speed, however, the minimum vehicle weight and tyre pressure are not defined, and safety factors need to be considered during the pavement design process to minimise possible hydroplaning risks.

In summary, all these influencing factors discussed should be considered during the pavement design to maintain adequate drainage requirements at which potential hydroplaning can be minimised.

### **2.3 SPLASH AND SPRAY**

Another safety concern associated with wet pavement conditions are the “splash and spray” effect, which generally leads to visibility problems for road users. When a vehicle travels on a wet pavement surface, the tyres of the vehicle accumulate the water from the pavement surface and spread clouds of small droplets into the air. Road users in passing vehicles or road users travelling behind other vehicles have very poor visibility and may not be able to observe other traffic through the cloud of spray, while the road users generating the splash and spray are unable to see the vehicles behind them.

Rungruangvirojn and Kanitpong (2010) have measured the visibility loss, due to splash and spray from different traffic loads, on various pavement types. Results have shown that the type of pavement surface has a significant influence on the visibility loss due to splash and spray as some pavement surfaces can accommodate more surface water than other. It was also recorded that more splash and spray was generated by heavy vehicles compared to passenger vehicles, which depends on the travelling speed of the vehicle and the water depth on the pavement surface.

### **2.4 WATER FILM THICKNESS**

A water film on the pavement surface involves the reduction of contact friction between the tyres of a vehicle and the pavement surface. Figure 2-3, adapted from Anderson et al., (1998), is an illustration of a water film with a specific thickness, which flows across a pavement surface. Accordingly, the water film thickness (WFT), mean texture depth (MTD) and total water flow are all defined as follows (Anderson et al., 1998):

- The WFT is the thickness of water film above the tops of the aggregate asperities;
- The MTD is affected by the macrotexture or roughness of the coarse aggregates in the pavement surface. When the water is below the MTD of the surface, the water is trapped between the asperities of the aggregate and does not contribute to the total water flow on the pavement and;
- The water flow layer (Y) is where flow or drainage occurs and may be determined as the WFT plus the MTD.

The WFT also referred to as the water film depth (WFD) can be predicted with two types of previously developed methods (models) which include empirical and analytical methods. Empirical methods consist of empirical data and equations to accurately predict the water film depth, while analytical methods consist of mathematical models which represent the hydrodynamic interaction between sheet flow and the tyre of a vehicle. The implementation of both these types of methods have proven credible results, but for this study, only the most common prediction methods were discussed in the literature review for background on the determination of water film depths on a pavement structure.

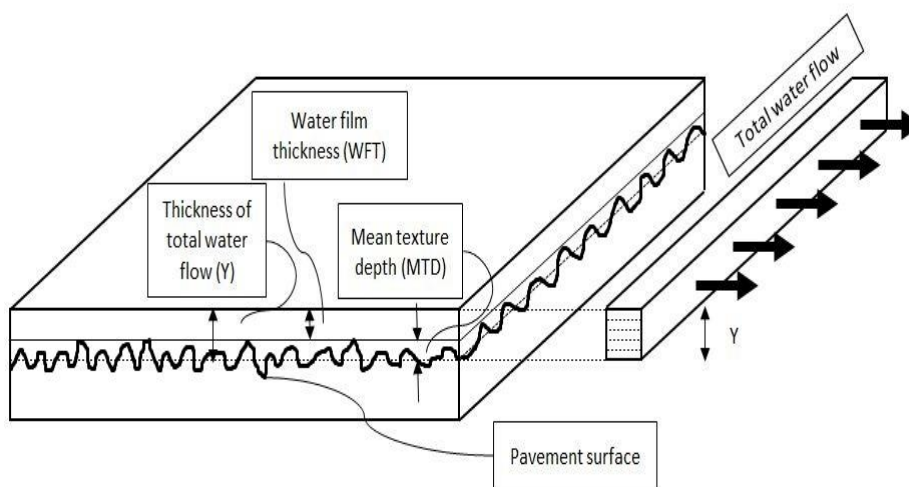


**Figure 2-3: Definition of water film thickness (Anderson et al., 1998)**

#### 2.4.1 PREDICTION METHODS (MODELS)

The two common prediction methods reviewed in the literature are:

- Road Research Laboratory (RRL) method and;
- Gallaway method.

### 2.4.1.1 ROAD RESEARCH LABORATORY (RRL)

The Road Research Laboratory examined the water film depth on rolled asphalt and brushed concrete surfaces. A method developed by the RRL (Russam & Ross, 1968), to accurately estimate the water depth on the pavement surface and consequently predict the water film depth for aquaplaning to initiate. The RRL method is defined by two concepts, the gradient (slope) and distance (length) of the drainage flow on the pavement surface. The drainage flow path length is the minimum distance that the water must flow from the point at which it falls on the surface to the edge of the pavement and is measured along its flow path slope which depends on a combination of the pavement width, cross slope and longitudinal slope.

The RRL method is an approved method to determine the water film depth on South African pavements and thus the same formulas, but with different symbols, is used in the South African National Road Agency Limited's (SANRAL) drainage manual (SANRAL, 2013). It is interesting to note that this method does not include any allowance for the texture depth for the corresponding pavement surface. The following equations are used and adapted from the SANRAL's drainage manual (SANRAL, 2013) to estimate the water film depth on a pavement surface according to the RRL method:

**To calculate the slope of the flow path (laminar flow conditions are assumed):**

$$S_f = \sqrt{n_1^2 + n_2^2} \quad \text{Equation 2-1}$$

Where:

- $S_f$  = flow path slope (%)
- $n_1$  = pavement crossfall (%)
- $n_2$  = pavement gradient (%)

(The flow path slope is determined assuming a planar road surface, without superelevation.)

**To calculate the length of the flow path (laminar flow conditions are assumed):**

$$l_f = W * \frac{S_f}{n_1} = W * \sqrt{1 + \left(\frac{n_2}{n_1}\right)^2} \quad \text{Equation 2-2}$$

Where:

- $l_f$  = length of flow path (m)
- $W$  = pavement width (m)
- $n_1$  = pavement crossfall (%)
- $n_2$  = pavement gradient (%)



**The water flow depth can consequently be determined as:**

$$d = 4.6 * 10^{-2} * (l_f * I)^{0.5} * (S_f)^{-0.2} \quad \text{Equation 2-3}$$

Where:

- d = water flow depth (mm)
- $l_f$  = length of flow path (m)
- I = rainfall intensity (mm/h)
- $S_f$  = energy slope of flow path (%)

The SANRAL drainage manual (SANRAL, 2013) also provided an alternative method from which these values can be obtained graphically using a nomograph. The nomograph is depicted in Appendix A, Chart 1.

NAASRA (1974) states that water depths ranging between 2.5mm to 5mm are enough to cause friction loss between tyres and the pavement surface without actual aquaplaning to occur. However, the critical water film depth for aquaplaning to initiate may vary between 4mm to 10mm depending on other characteristics of the pavement surface (NAASRA, 1974).

The SANRAL Drainage Manual (SANRAL, 2013) recommends that the water film thickness or water flow depth (d) on the pavement surface during a 1:5 year storm should not exceed 6mm to prevent any aquaplaning risks. The minimum slope along a flow path ( $S_f$ ) should be 2 percent and 2.5 percent for wider pavement surfaces for effective surface drainage. The goal for any pavement designer should thus be to minimise the flow path length ( $l_f$ ), consequently, to reduce the flow depth on the pavement surface to a maximum of 6mm.

Chaithoo and Allopi (2012) however developed a software tool to assist authorities and geometric designers with pavement drainage analysis considering various hydraulic factors. According to their surface drainage calculations, the following were confirmed in their study concerning water flow depths (d):

- The flow depth will increase when the width of the road increases or the road gradient increases and;
- The flow depth will decrease if the road cross fall increases.

The shortest flow path lengths occurred when the pavement gradient (longitudinal slope) is a minimum, and the water can drain transversely across the pavement width. Longer flow path developed with steeper

pavement gradients (longitudinal slopes) when the water flow parallel with the travel direction (Chaithoo and Allopi, 2012).

#### 2.4.1.2 GALLAWAY METHOD

Gallaway et al., (1979) developed a different empirical method for the United States Department of Transportation in cooperation with the Federal Highway Administration (FHWA) to accurately predict the water film depth (WFD) on a pavement surface. This method, detailed in the Texas Department of Transportation's (TxDOT) hydraulic design manual (Ken Bohuslav, 2004) is an empirical relationship between the drainage flow path length, the pavement slope, the rainfall intensity and the mean texture depth of the pavement surface.

The WFD is initially calculated with the Gallaway equation according to a specific rainfall intensity and designed pavement geometry. The calculated WFD is then utilised in a supportive equation to determine the required vehicle speed at which aquaplaning may occur. The design vehicle speed is finally compared with the aquaplaning vehicle speed and adjusted if necessary, to ensure safe driving conditions during a design storm. This equation, however, is only valid for speeds up to 95km/hr and Gallaway (1979) and Oakden (1977) recommended that the WFD on a pavement surface should be limited to a maximum depth of 4mm.

**The Gallaway equation is as follows:**

$$WFD = z * \frac{TXD^{0.11} * L^{0.43} * I^{0.59}}{S^{0.42}} - TXD \quad \text{Equation 2-4}$$

Where:

- WFD = water film depth above the top of the surface asperities (mm)
- z = constant (0.01485)
- TXD = mean pavement texture depth (mm, 0.5mm for design)
- L = length of drainage path (m)
- I = rainfall intensity (mm/h, with a minimum of 50mm/hr)
- S = Slope of drainage path (%)

(The values for the variables provided, was obtained from TxDOT's hydraulic design manual (Ken Bohuslav, 2004).

Chesterton et al., (2006) have compared the water film depth results obtained from the RRL method with the water film depths results obtained from the Gallaway method. The Gallaway equation constantly gave

lower water film depth values than the conservative RRL equation. It was assumed that it was possible since the Gallaway method has taken the mean texture depth and wider variations of pavement types into account when the empirical relationship was initially developed.

## **2.4.2 CONTROLLING WATER FILM THICKNESS**

Anderson et al. (1998) have studied the different techniques to control water film thickness on pavement structures. The following three most promising techniques were identified and discussed in their study:

- Controlling the pavement geometry;
- Implementing textured pavement surfaces (asphalt, grooved concrete, ultra-thin friction course (UTFC)) and;
- Installing effective drainage appurtenances.

### **2.4.2.1 CONTROLLING PAVEMENT GEOMETRY**

The drainage capacity of the pavement structure is primarily determined by its surface geometry (Anderson et al., 1998). Geometry factors such as cross slopes and superelevations may be altered to maximise surface drainage within the general design criteria for road safety, geometric design, driveability and appearance. SANRAL (2002) have developed geometric design guidelines for designers to use on any road, especially national roads designed within the domain of South African national roads, which limits the degree to which pavement geometry may be used to minimise water film thickness.

The longitudinal slope of the pavement also referred to the road gradient, has a minimum and maximum allowable criterion essential for adequate drainage and safety regulations respectively. Flat slopes may not drain surface water adequately, while steeper slopes may cause safety risks, heavy traffic flows and driver discomfort. The American Association of State Highway and Transportation Officials (AASHTO), (2011) recommend a minimum road gradient of 0.5 percent for highways or streets with restricted cross slope drainage due to the curb installations to ensure proper surface drainage. At vertical sag curves, a minimum slope of 0.3 percent within 15m of the low point of the curve should be maintained (Brown et al., 2009). Maximum road gradients are established based on the performance and operational characteristics of particularly larger vehicles as well as the topographical area of the pavement. Road gradients affect the speed of the vehicle travelling on the road and Committee of State Road Authorities (1988) recommends the following maximum gradients for specific design speeds and topography (flat, rolling and mountainous terrains) shown in Table 2-1.

**Table 2-1: Maximum gradients (Committee of State Road Authorities, 1988)**

Design Speed (km/h)	Topography		
	Flat	Rolling	Mountainous
60	6%	7%	8%
80	5%	6%	7%
100	4%	5%	6%
120	3%	4%	5%

The rate at which the cross slope of the pavement changes is an essential element in the cross section design to control water film thickness and improve surface drainage. Cross slopes may be described as a camber, a high point in the centre of the pavement with two slopes downwards towards both edges of the pavement or a cross fall, a single continuous slope from shoulder to shoulder of the pavement. Slope adjustments for drainage design should be well considered as the steepness of the cross slope mainly affects vehicle control and driving behaviour. Minimum slope grades are also implemented to ensure adequate surface drainage. The Committee of State Road Authorities (1988) prescribes a preferable cross slope steepness of two percent for adequate drainage and a maximum three percent in areas with heavy rains and where the longitudinal gradient is equal to zero. Brown et al. (2009) recommends a maximum pavement cross slope of four percent.

AASHTO (2011), states that cross slopes steeper than two percent require conscious effort for steering and vehicle control and implies that cross slopes steeper than two percent is not desirable on high-speed paved highways. AASHTO's studies showed that as the longitudinal slope increase, the pavement cross slope should also be increased to shorten the water flow distance and to remove the water more rapidly from the pavement surface.

At horizontal curves, the rate of maximum superelevation implemented on highway pavements may be affected by four factors: climate conditions (i.e. frequency and intensity of rainfall), terrain conditions (i.e. flat, rolling and mountainous areas), region of pavement (i.e. rural or urban areas) and the frequency of slow-moving vehicles whose operations are affected by high superelevation rates (AASHTO, 2011). The superelevation of a pavement controls the driving conditions and water drainage on the surface. High superelevations cause slower vehicle speeds as the drivers need to steer up the slope. The maximum superelevation used in the design of South African rural roads is 10% (Committee of State Road Authorities, 1988). According to AASHTO (2011), the highest superelevation rate typically used for highway design is also 10%, depending on the design speed of the pavement.

Another important geometry element in drainage design is the transition distance, also known as the runoff length, changing from a usually crowned pavement (camber) to a superelevated pavement (cross fall). This causes the pavement to be level, and special attention is required for surface drainage in transitions areas.

#### **2.4.2.2 IMPLEMENTING TEXTURED PAVEMENT SURFACES**

Approximately 80% of the pavements in South Africa have seal surfaces, either as an initial surfacing or as a reseal (SANRAL, 2014). Other surfacing layers in South Africa include asphalt, asphalt concrete (AC) and wearing courses. These surfaces layers have specific engineering properties to provide adequate skid resistance between the tyres of a vehicle and the pavement surface. Surfaces have different roughness and angularities which affect the water film thickness as well as the resistance to water flow.

The increase in texture depth of the pavement surface enhances surface drainage by providing a reservoir for water within the macrotexture of the pavement surface. Permeable (porous) pavements however have a pervious asphalt or concrete surface layer that allows surface water to drain through the pavement surface. The under lying layers of the pavement act as a storage reservoir for the infiltrated water and the depth and materials used in these pavement layers determines the storage capacity of the water. Water finally leaves the underground reservoir through a drain. Generally, for adequate surface drainage, the water infiltration rate in the granular layers of a porous pavement should exceed 12.7mm/hr (0.5in/hr), (Sample et al., 2013).

Concrete pavement surfaces can be broom swept (tined) or grooved. Grooving should be done parallel to the slope of the pavement to create active surface flow channels for water to flow into catchment areas. However, this is not always practical for super elevated pavements sections with alternating longitudinal and cross slope sections, given that the slope of the water flow path changes and is usually skewed to the direction of traffic. This hampers the effectiveness of grooves as drainage channels on the pavement surface.

Once these grooves begin to overflow, a water film will accumulate for sheet flow to occur which contributes towards the increase in water film thickness. Studies have shown that once the pavement is flooded and the grooves are filled with water, the grooves become inactive to reduce the water film thickness. Once submerged, there is no improvement in the hydroplaning tendency for a grooved pavement surface compared to a similar section with a broom swept surface without grooves (Anderson et al., 1998).

Gallaway et al. (1971) found that an increase in surface texture caused a decrease in water flow depths for a given rainfall intensity, cross slope and drainage length. However, this effect was more prominent for lower rainfall intensities and flatter cross slopes.

### 2.4.2.3 INSTALMENT OF EFFECTIVE DRAINAGE APPURTENANCES

The geometry factors such as the cross slope and superelevation of the pavement were traditionally designed to control water flow on the pavement surface. However, drainage appurtenances are still required to remove the excessive amount of surface water. Drainage appurtenances such as grate inlets and slotted drains are implemented in the drainage design of the pavement to control the volume of water on the pavement surface adequately. Depending on the geometry of the pavement, drainage appurtenances are placed at the outer edge, the median, transversely or across the carriageways of the pavement to capture excessive surface water. The implementation of these drainage systems specific slotted drains is discussed in the remaining paragraphs of the literature review.

## 2.5 SLOTTED DRAINS

Many configurations of slotted drains exist and can be produced by several manufacturers globally and in South Africa. Manufacturers provide detailed descriptions of the drains as well as the application procedures for the use of it. Slotted drains are commonly known as pipe segments cut along its longitudinal length as an opening and often spaced with bars perpendicular to the pipe opening to form slotted inlets. Slotted drains can be installed within a pavement structure to intercept sheet flow on the pavement surface without any additional water channelling devices required. This means that the surface water can directly be intercepted by the slotted inlets and then transported through its pipe sections into a discharge unit. A typical example of a slotted drain inlet is depicted in Figure 2-4.

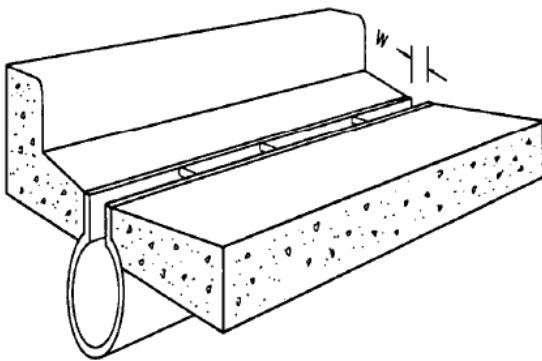


**Figure 2-4: Slotted drain inlet (Brown et al., 2009)**

### 2.5.1 THE FUNCTIONALITY OF SLOTTED DRAINS

Slotted drain designs have unique features and functional principles to remove sheet flow from the pavement surface adequately. In basic terms, slotted drains are installed within a pavement structure to

function on its own or are installed within the pavement structure to operate with a concrete barrier placed along the slotted drain's longitudinal length, as schematically illustrated in Figure 2-6 (A) and Figure 2-6 (B) respectively. The judgement to implement a median barrier with a slotted drain or not is still debatable but usually depends on the geometric design of the pavement and total width of the pavement. Commonly on South African highways with more than two undivided carriageways, some slotted drains are installed in the centre of the pavement and operate with a median concrete barrier along its length as pictured in Figure 2-5.

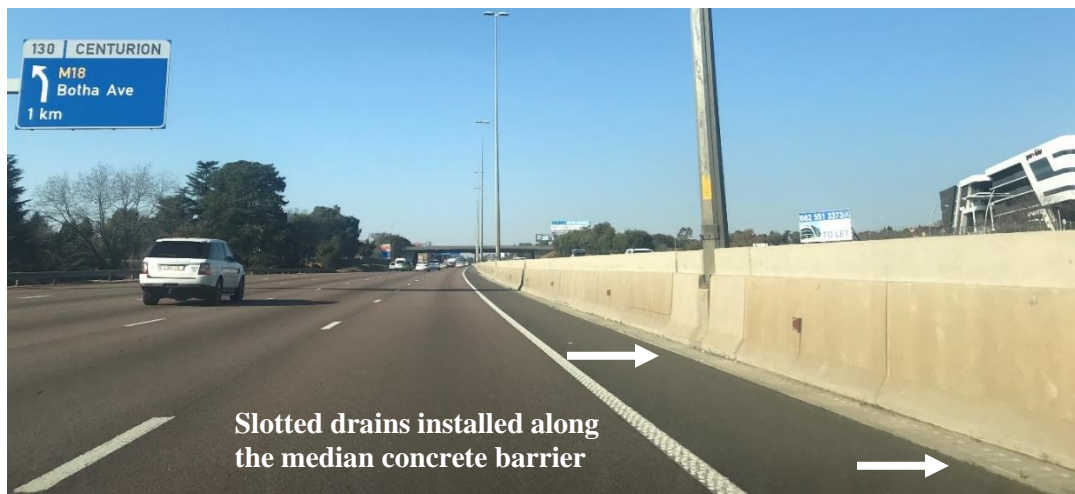


**Figure 2-5: Slotted drain installations on N1 highway near Centurion (privately captured)**

By referring to the schematic cross sections in Figure 2-6, the two operational scenarios are distinguished as follows:


- Scenario A is a slotted drain installation within the pavement structure with a median barrier placed along the longitudinal length of the slotted drain. Both the slotted drain and the concrete barrier are installed horizontally (with zero percent slope) regardless of the pavement's cross slope. The concrete barrier will prevent the un-intercepted surface water to flow across to the opposite side of the pavement width.
- Scenario B is a slotted drain installation within the pavement structure operating independently without a concrete barrier. The slotted drain is installed along the same gradient as the cross slope or superelevation of the pavement. Storm water which is not intercepted by the slotted drain will flow across the pavement width to the opposite carriageway.

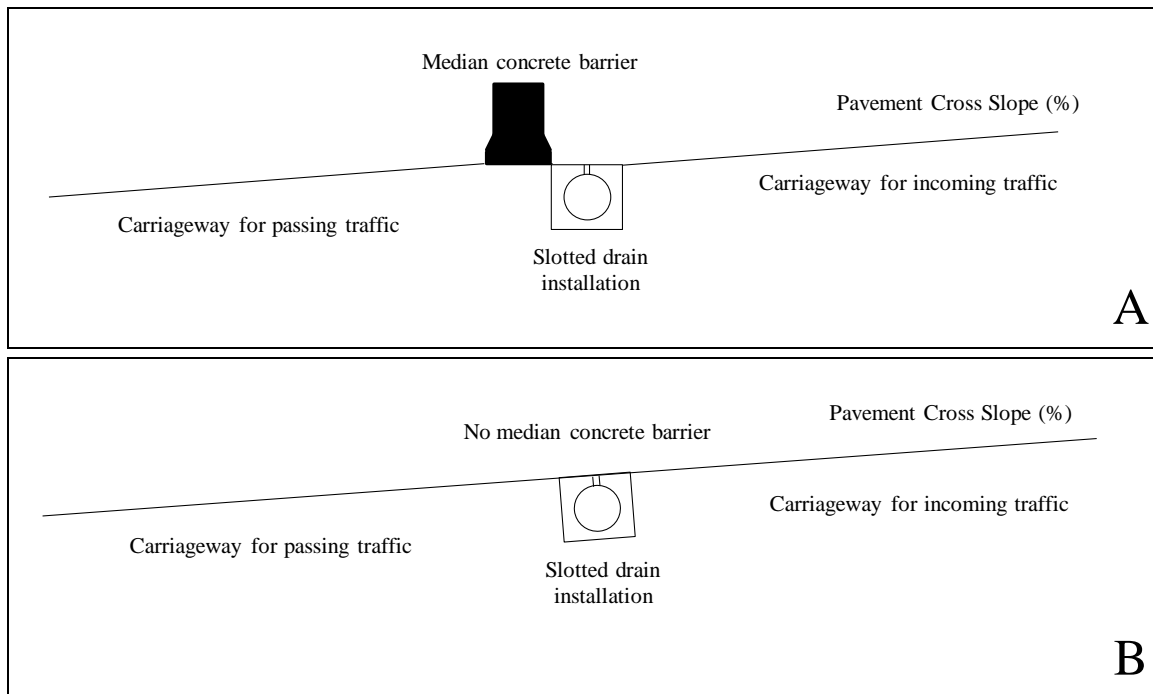





**Figure 2-6: Cross section of the installation scenarios of slotted drains: (A) - with median barrier; (B) - without median barrier**



Various installation scenarios of slotted drains are globally implemented within pavement structures nowadays. Table 2-2 provides a few examples of case studies where these drains are implemented to operate under unique pavement and environmental conditions.

**Table 2-2: Slotted drain case studies**

<u>INSTALLATION DESCRIPTIONS AND ADVANTAGES</u>	<u>VISUAL ILLUSTRATION AND REFERENCE</u>
<p><b>Case study – Indianapolis, Indiana</b></p> <p><b>Surface drainage upgrades</b></p> <ul style="list-style-type: none"> <li>• Surface drainage is allowed between the inside lane barrier and shoulder;</li> <li>• Provide an obstruction free, single grade roadside;</li> <li>• Promote the drainage effectiveness of the inside shoulder and improve highway safety;</li> </ul>	 <p>(Contech Engineered Solutions, 2017)</p>



<p align="center"><b><u>INSTALLATION DESCRIPTIONS AND ADVANTAGES</u></b></p>	<p align="center"><b><u>VISUAL ILLUSTRATION AND REFERENCE</u></b></p>
<p align="center"><b>Case study – Dallas, Texas</b></p> <p align="center"><b>IH30 Roadway improvements</b></p> <ul style="list-style-type: none"> <li>• Slotted drains are installed in a concrete pavement to collect surface run-off in a high trafficking area;</li> <li>• Concrete barriers are installed along the slotted drains.</li> <li>• Slotted drains are installed at a transitional superelevated section of the roadway.</li> </ul>	 <p align="center">(Contech Engineered Solutions, 2018)</p>
<p align="center"><b>Case study – Phoenix, Arizona</b></p> <p align="center"><b>The Ridge at Lookout Mountain</b></p> <ul style="list-style-type: none"> <li>• Slotted drains are installed next to a roadway on a mountain ridge;</li> <li>• Slotted drains are designed as a combination of a curb and slotted inlet drainage system.</li> </ul>	 <p align="center">(Contech Engineered Solutions, 2018)</p>
<ul style="list-style-type: none"> <li>• Installed at zero to shallow road gradients;</li> <li>• No hard shoulders constructed as the side slope act as a barrier;</li> <li>• Slotted drain is designed to assist in self-cleaning of debris;</li> <li>• Designed to withstand heavy vehicle loading</li> </ul>	 <p align="center">(StatonBonna, 2012)</p>

<u>INSTALLATION DESCRIPTIONS AND ADVANTAGES</u>	<u>VISUAL ILLUSTRATION AND REFERENCE</u>
<p><b>Gauteng Freeway Improvement Projects (GFIP)</b></p> <ul style="list-style-type: none"> <li>• Slotted drains installed at longitudinal slopes at freeway sections;</li> <li>• Installed adjacent to a concrete median barrier;</li> <li>• Barrier improves overall highway safety by separating the incoming from the passing traffic.</li> </ul>	 <p>(Privately captured)</p>
<p><b>Kimberley Airport, Runway drainage</b></p> <ul style="list-style-type: none"> <li>• Slotted drains installed on airport runways to remove surface water;</li> <li>• Reduce hydroplaning risks initiating from high travelling airplane speeds;</li> <li>• Slotted drains can withstand heavy airplane loads.</li> </ul>	 <p>(Privately captured)</p>

### 2.5.2 THE HYDRAULICS OF SURFACE FLOW

To examine the operation of slotted drains in practice, it is valuable to understand the basic principles of open channel flow, also known as free surface flow. For the purpose of the study, the only type and state of free surface flow, studied and explained in the literature, was a steady uniform flow and laminar flow condition.

Open channel flow is the term to describe a specific cross sectional flow having a free surface and is subjected to atmospheric pressure (Chaudhry, 2007). Free surface flow can be classified into various types according to the change in flow velocity or flow depth with regards to time and space. Steady uniform flow on the pavement surface occurs when the flow velocity or flow depth is constant during the time domain under consideration within a given length of a pavement section (Te Chow, 1959). This, however, is very

difficult to determine on a pavement surface in practice, as rain intensities may vary in very small areas at any given time.

The state or behaviour of free surface flow is affected by both viscosity forces and gravity forces relative to the inertial forces of the flow. Depending on the magnitude of viscosity forces relative to inertia forces, the flow behaviour can be described as laminar, turbulent or transitional (Te Chow, 1959). During laminar surface flow conditions, the viscosity forces are more dominant relative to the inertial forces. The water particles tend to move in definite smooth sheets or paths across the pavement surface while the thin layers of water seem to slide over one another (Te Chow, 1959).

Two fundamental numerical depth-velocity relationships of free surface flow which governs the operation of slotted drains in practice are the Manning equation and the Froude number (Fr) of the approaching surface flow. These two relationships can be used to predict or compare observed test data and are described as follows:

- **MANNING'S EQUATION**

The numerical relationship for uniform flow conditions (i.e. no change in roughness, slope and flow rate along the water flow path) on pavement section is defined with the Manning's equation. In such sections, the Manning equation can be applied to determine the flow depth when the energy grade line is set equal to the channel pavement slope ( $S_f=S_0$ ), (SANRAL, 2013).

**Manning's n equation is as follows:**

$$Q = V * A = \frac{A * R^{\frac{2}{3}} * S_f^{\frac{1}{2}}}{n} \qquad \text{Equation 2-5}$$

Where:

- Q = flow rate (m<sup>3</sup>/s)
- V = flow velocity (m/s)
- A = cross sectional area (width x height), (m<sup>2</sup>)
- R = hydraulic radius (R=A/P, where P is the wetted perimeter), (m)
- S<sub>f</sub> = friction slope (energy grade line), (m/m)
- n = Manning's roughness coefficient (s/m<sup>1/3</sup>)

- **FROUDE NUMBER (Fr)**

SANRAL (SANRAL, 2013), classified a slotted drain as a drop outlet or a type I outlet. Drop outlets (Type I outlets), feeds surface run-off and discharge the stormwater into an underground drainage system. Grids are usually placed over the opening of these outlets to prevent safety hazards for pedestrians and traffic. Drop outlets perform either under subcritical approach flow condition or supercritical approach flow conditions (SANRAL, 2013). Under these mentioned flow conditions, slotted drains can operate as a weir or as an orifice and the Froude number is required to determine whether the approaching flow is subcritical or supercritical.

The Froude Number (Fr) of the approaching surface flow is the ratio between the inertial and gravitational forces of flow (Chaudhry, 2007).

**The Froude number is calculated as follows:**

$$Fr^2 = \frac{V^2}{g \cdot D} = \frac{Q^2 \cdot B}{g \cdot A^3} \quad \text{Equation 2-6}$$

Where:

- Fr = Froude number
- V = average cross sectional flow velocity (m<sup>3</sup>/s)
- D = hydraulic depth (m)
- Q = flow rate (m<sup>3</sup>/s)
- B = flow width (free surface width which is in contact with the atmosphere), (m)
- g = gravitational acceleration (9.81m/s<sup>2</sup>)
- A = cross sectional area (m<sup>2</sup>)

- **SUBCRITICAL APPROACH FLOW**

Subcritical approach flow conditions are applicable when the Froude number is smaller than one, (Fr<1). During subcritical flow conditions, a flow disturbance may occur upstream or downstream (Comport et al., 2009), which the outlet flow may either be free-flow or drowned (submerged). The broad-crested weir formula may be applied for free outflow conditions, and the orifice formula may be applied for drowned conditions to determine the flow rates of the oncoming surface water (SANRAL, 2013).

**For free outflow conditions:**

$$Q = C_D \cdot b \cdot H \cdot \sqrt{g \cdot H} \quad \text{Equation 2-7}$$

Where:

Q	=	flow rate (m <sup>3</sup> /s)
C <sub>D</sub>	=	discharge coefficient (0.6)
b	=	total width of flow (m)
H	=	energy head (flow depth), (m)
g	=	gravitational acceleration (9.81m/s <sup>2</sup> )

**For drowned (submerged) flow conditions:**

$$Q = C * F * A * \sqrt{2 * g * H} \quad \text{Equation 2-8}$$

Where:

Q	=	flow rate (m <sup>3</sup> /s)
C	=	inlet coefficient (0.6 for sharp edges or 0.8 for rounded edges)
F	=	blockage factor (say 0.5)
A	=	effective cross sectional plan area of the opening (m <sup>2</sup> )
H	=	total energy head (water depth) above the grid (m)

- **SUPERCritical APPROACH FLOW**

Supercritical approach flow conditions are applicable when the Froude number is greater than one, (FR>1). During these conditions, the flow disturbance can only occur in the direction of flow (Comport et al., 2009). In practice, it becomes more complex to deal with supercritical approach flows. It can be dealt with, however, by implementing a drain opening in the direction of flow, at least the same area as the sectional area of the incoming sheet flow stream. The drain outlets should be operating free (individually) to prevent a possible hydraulic jump which influences the upstream water depth, i.e. increasing the water flow depth on the pavement surface (SANRAL, 2013).

According to additional literature, Brown et al. (2009) state that slotted drains operate as a weir for flow depths below 50mm and as an orifice for flows greater than 120mm, between these depths transition flow exists.

### **2.5.3 THE INTERCEPTION CAPACITY AND EFFICIENCY OF SLOTTED DRAINS**

The interception capacity of an inlet is described as the maximum amount of flow intercepted by the inlet under a set of conditions and is affected by the inlet size (length and configuration) and the volume of water (flow depth) approaching the slot opening. The interception efficiency of an inlet (E) is the ratio between

the total amount of water flow intercepted and the total amount of flow approaching the inlet, expressed as a percentage. This is dependent on the inlet type (length, width, curb opening etc.), the flow depth, the gutter flow velocity and the pavement slopes (longitudinal and transverse (cross) slopes). With increasing flow rates, the interception capacity will increase to some degree. The opposite applies to the interception efficiency which will decrease with the increasing flow rates and decrease when the flow width is greater than the slotted inlet width (Brown et al., 2009).

The interception efficiency of an inlet and the bypass flow can be determined using the following basic equations (Brown et al., 2009):

**To calculate the interception efficiency:**

$$E = \frac{Q}{Q_i} * 100 \quad \text{Equation 2-9}$$

Where:

E = interception efficiency (%)

Q = total flow (m<sup>3</sup>/s)

Q<sub>i</sub> = intercepted flow (m<sup>3</sup>/s)

The bypass flow or carry overflow is defined as the flow that is not intercepted by the slotted inlet and is determined as follows:

**To calculate the bypass flow:**

$$Q_b = Q - Q_i \quad \text{Equation 2-10}$$

Where:

Q<sub>b</sub> = bypass flow (m<sup>3</sup>/s)

Q = total flow (m<sup>3</sup>/s)

Q<sub>i</sub> = intercepted flow (m<sup>3</sup>/s)

#### 2.5.4 DISADVANTAGES OF SLOTTED DRAINS

The implementation of slotted drains on pavements has potential disadvantages. Slotted drains are highly susceptible to clogging from debris (Figure 2-7), and the implementation of slotted drains in environments where significant sediment and debris are presented is not recommended, as severe ponding can develop on the pavement surface, creating safety hazards for pavement users (Brown et al., 2009). Design

procedures with regards to the installation, spacing and location of the slotted drains on pavements surfaces should, therefore, be well considered.



**Figure 2-7: Clogging of slotted inlets (privately captured)**

Cleaning of slotted inlets can be relatively easy but should be maintained on a regular basis in high sediment areas. Special equipment is used such as cleaning paddles or cleaning brushes which matches the shape and the profile of the bottom of the drain for cleaning smaller slotted drains. A water compressor can also be used to clean more significant drains where a high force of water and air is blown into the slotted inlets to remove clogging materials. Debris is then manually removed from the catch basin. The unpredictability of debris to clog can become a problem as heavy stormwater can easily transport sediments and debris over a large pavement area to cause clogging of the slotted inlets.

Slotted drains, subjected to traffic loads within trafficking areas, are likely to settle and causing unevenness on the roadway surface. Figure 2-8 is an example of such typical problematic scenario occurred on the GFIP freeway sections. Figure 2-9 is also an illustration of a slotted drain installation used to drain surface water on a block paving pathway and is subjected to direct traffic. Special precautions are required for the structural support of the drains within the travel lanes; however, the structural capacities of slotted drains are beyond the scope of the study.





**Figure 2-8: Slotted inlet cover failure and settlement (privately captured)**



**Figure 2-9: Damaged slotted inlets (privately captured)**

As a result of these disadvantages, a safe and cost-effective application of slotted drains is still required for slotted drains to operate efficiently when being installed as drainage systems on pavements.

## **2.6 RELEVANT STUDIES ON SURFACE DRAINAGE**

Several hydraulic studies have been done to determine the hydraulic characteristics of drain inlets with different configurations. To accomplish one of the objectives of the research study, it was necessary to



examine the physical models and tests procedures of the relevant studies of slotted inlets, to obtain sufficient knowledge to construct an experimental model to obtain accurate test results.

## **2.6.1 HYDRAULIC CAPACITY AND EFFICIENCY OF SLOTTED DRAINS**

### **2.6.1.1 UNITED STATES BUREAU OF RECLAMATION**

A hydraulic study was conducted by the United States Bureau of Reclamation (USBR) for Federal Highway Administration (FHWA) on a simplified hydraulic design of a slotted drain installation in the field. FHWA investigated the performance of slotted drain inlets in practice to maximise pedestrian and bicycle safety to accomplish the following (Pugh, 1980):

- To determine the total slotted length necessary to intercept 100% of the surface flow;
- To determine the interception efficiencies of slotted inlets for different sheet flow depths;
- To determine the slotted inlet ability to handle debris without clogging;
- To determine the interception efficiencies of slotted inlets operating in sag (sump) locations and;
- To determine the interception efficiencies of the slotted inlets with partial flow conditions in situations where the flow is captured by only a downstream portion of the slotted length.

Both total flow interception and partial flow interception measurements were done to obtain the interception efficiency and capacity of the slotted drain inlets. The USBR varied different input parameters including slot widths, type of transverse slot bars, curb distances, discharges, roughness and slope conditions (cross slope, longitudinal slope, and the slot to curb back slope).

The USBR (Burgi et al., 1977) and (Pugh, 1980) used a full-scale test facility which consists of a hydraulic roadway flume with a slotted drain installed along the length of the pavement. A movable curb design was implemented to allow distance variations between the slotted inlet and the curb face. A prototype roadbed was constructed with 1.22m x 2.44m Permaply sheets which had a total roadbed dimension of 2.44m x 18.3m. The roadbed was supported with beams underneath which could be raised and lowered as a unit according to different slope configurations. Longitudinal slopes were adjusted with a chain hoist which was driven by a gear motor while the cross slopes were adjusted with automobile-type screw jacks.

The roadbed surface was initially treated with epoxy paint, and a specific sand particle size was applied to the wet paint to obtain a specific roughness. Marine varnish and a larger sand particle size were added afterwards. Repeated roughness tests were conducted by applying various slopes and flows. It was

confirmed by using Manning's equation that the treated surface has an acceptable manning's roughness coefficient very close to the actual roughness of an asphalt pavement (Pugh, 1980).

The laboratory sump delivered gutter flow through pumps to a head box situated at the upstream end of the roadbed width. The gutter flow could enter the inlet either as frontal flow or side flow. Frontal flow approached the inlet in line with the width of the inlet and side flow occurred outside the width of the inlet.

A sluice gate controlled the water flow velocity and water depth in front of the head box. An upstream approach was required to assure uniform flow conditions. A portable point gauge was used to measure the water depth at several locations upstream of the slotted inlet to assure uniform flow conditions were applied from the gutter flow. Sheet flow was also applied along the length of the pavement through manifolds connected to a pipe with evenly spaced holes. Pugh (1980) states that a unit discharge of 0.216l/s per meter is similar to a rainfall intensity of 343mm/h over a 21.9m wide pavement. Water pressure in the manifolds was regulated with valves to ensure uniform flow was obtained. The following equation was used to relate the sheet flow on the roadbed surface, and it was stated to be accurate within five percent (Pugh, 1980).

**To calculate sheet flow in a flow range between 0.01 ft<sup>3</sup>/s/ft and 0.04 ft<sup>3</sup>/s/ft. (0.086l/s/m and 0.345l/s/m):**

$$q = (0.023 * \log_{10} * P) - 0.011 \quad \text{Equation 2-11}$$

Where:

- q = sheet flow (ft<sup>3</sup>/sec), (multiply by 0.02832 for m<sup>3</sup>/s)  
 P = manifold pressure (kPa), (multiply by 0.14504 for Psi)

Flow passing the slotted inlets was captured in a weir box constructed underneath the test facility at the downstream side of the roadbed. The bypass flow was subtracted from the total supplied flow to determine the flow intercepted by the slotted inlet. The bypass flow was measured with three calibrated devices inside the weir box, depending on the volume of water passing the slots. The devices were (Burgi et al., 1977):

- Contracted weir (0.61m high) for flows larger than 0.007m<sup>3</sup>/s;
- 90° V-notch weir for flows varying between 0.007m<sup>3</sup>/s to 0.002m<sup>3</sup>/s and;
- Small volumetric tank for flows below 0.005m<sup>3</sup>/s.

Table 2-3 summarises the various model features and parameters that were varied during the hydraulic tests of Pugh (1980).

**Table 2-3: Model characteristics and test conditions (Pugh, 1980)**

MODEL FEATURE	UNIT	TEST CONDITION		
Roadbed width	m	2.44		
Roadbed length	m	18.3		
Slotted drain length	m	17.1		
Slotted drain inlet widths	mm	25.4	44.45	63.5
Type of transverse bars	-	Solid vertical	Solid 45 °angle	Double Hexagonal
Transverse bar spacing	mm	101.6		152.4
Manning's roughness of surface	s/m <sup>1/3</sup>	0.016-0.017		
Longitudinal slope	%	0-9		
Cross slope	%	1-6		
Flow type	-	uniform		
Gutter flow supply system capacity	m <sup>3</sup> /s	0.15		
Sheet flow supply system capacity	l/s/m	0.345		
Curb distances	mm	0	88.9	177.8

The following equations were calibrated in the data analysis and can be used to calculate the drainage capabilities of slotted drains (Brown et al., 2009). These equations were also used to develop similar charts (nomograph) from the test results, depicted in Appendix A:

**To calculate the slotted drain inlet length for total flow interception with a uniform cross slope (also depicted in Chart 2 in Appendix A):**

$$L_T = k_u * Q^{0.42} * S_L^{0.3} * \left(\frac{1}{n * S_x}\right)^{0.6} \quad \text{Equation 2-12}$$

Where:

$L_T$  = slotted inlet length to intercept 100% of the gutter flow (m)

$k_u$  = constant (0.817)

$Q$  = gutter flow (m<sup>3</sup>/s)

$n$  = Manning's roughness coefficient (s/m<sup>1/3</sup>)

$S_L$  = longitudinal slope (m/m)

$S_x$  = cross slope (m/m)

For slotted drains in depressed gutter sections an equivalent cross slope  $S_e$  should be applied to Equation 2-12 instead of the uniform cross slope,  $S_x$ . This is defined where the cross slope of the gutter (shoulder) differ

from the pavement cross slope. The ratio of flow in the depressed section to total gutter flow,  $E_o$ , needs to be calculated initially to determine the equivalent cross slope accordingly. This can be determined by Brown et al. (2009):

**To calculate the ratio of flow in the depressed section to total gutter flow:**

$$E_o = \frac{Q_w}{Q} = 1 - \left(1 - \frac{W}{T}\right)^{2.67} \quad \text{Equation 2-13}$$

Where:

- $E_o$  = ratio of flow in the depressed section to total gutter flow
- $Q_w$  = flow in width (m<sup>3</sup>/s)
- $Q$  = total gutter flow (m<sup>3</sup>/s)
- $W$  = width of depressed gutter (m)
- $T$  = total spread of water (m)

**To calculate the equivalent cross slope for depressed gutter sections:**

$$S_e = S_x + (S'_w * E_o) \quad \text{Equation 2-14}$$

Where:

- $S_e$  = equivalent cross slope (m/m)
- $S_x$  = cross slope (m/m)
- $S'_w$  = cross slope of gutter measured from the cross slope of pavement (m/m)
- $E_o$  = ratio of flow in the depressed section to total gutter flow

**To calculate the slotted drain interception efficiency shorter than the length required for total interception (also depicted in Chart 3 in Appendix A):**

$$E = \left(1 - \left(\frac{L}{L_T}\right)^{1.8}\right) * 100 \quad \text{Equation 2-15}$$

Where:

- $E$  = interception efficiency (%)
- $L$  = slotted drain inlet length (m)
- $L_T$  = slotted inlet length to intercept 100% of the gutter flow (m)

The USBR summarised the following qualitative findings in their research studies (Pugh, 1980):

- Slotted drains intercept flow more efficiently in the upstream portion of the slot inlet, while wider slot widths are more efficient at higher slope configurations;
- At steep slopes, higher inlet efficiencies were obtained at longer inlet lengths than shorter lengths;
- For all slopes tested, the three slot widths (25.4mm, 44.45mm and 63.5mm) intercept nearly all the sheet flow up to the system flow capacity of 0.345l/s per meter flow and therefore have little effect on the 100% interception length for slotted inlets;
- For a design discharge of 0.216l/s per meter, waterfalls entirely through the slot inlets as weir flow without overflowing the slot to the opposite curb side of the inlet;
- Larger curb to inlet distances are less efficient at high discharges compare to low discharges. More surface area is available at the curb side of the inlet to accumulate overflowing water and tend to flow longitudinally down the slope of the roadbed rather than into the slot inlet;
- For a 100% flow interception, a roadway roughness with a manning n value of 0.0165s/m<sup>1/3</sup> results in an 18% reduction on average n required slotted length, compared to a roadway roughness of 0.009s/m<sup>1/3</sup>;
- The interception efficiencies for different types of transverse bars and slot widths are the same for small slopes and discharges;
- The addition of sheet flow combined with the gutter flow has little effect on the 100% interception length of the slotted inlets and;
- A small amount of splash and spray occurred from the transverse spacers at steep slope configurations during the sheet flow tests with a maximum flow depth recorded as 14.2mm.

#### **2.6.1.2 SIGMA BETA CONSULTING ENGINEERS**

Another study was completed by Sigma Beta Consulting Engineers (SBCE) at the University of Stellenbosch in South Africa on a median drainage system with slot inlets. In the unpublished report of Gouws (1993), there was limited literature available with connection to the test facility and procedures for the testing of these drainage systems.

It was found, however, that various vertical inlet slots were tested in a 400mm wide by 200mm deep rectangular wooden box to determine the interception drainage capacity of drainage slots at different water depths and longitudinal slopes (Gouws, 1993).

A mathematical model was developed by Gouws (1993) to calculate the total inlet length (or a total number of slots) required to capture the pavement surface runoff flowing alongside the median barrier (Gouws, 1993). The SBCE have the following hydraulic criteria in their mathematical model, which is also depicted in Figure 2-10:

- Gouws (1993) assumed constant energy over the slot openings (Te Chow,1959):
  - The flow will pass through its critical depth at the first slot, for sub-critical flow conditions. (Critical energy was used to determine flow depths at remaining slots.)
  - A Uniform flow depth was assumed at the first slot, for supercritical flow conditions. (Uniform energy was used to determine flow depths at remaining slots.)

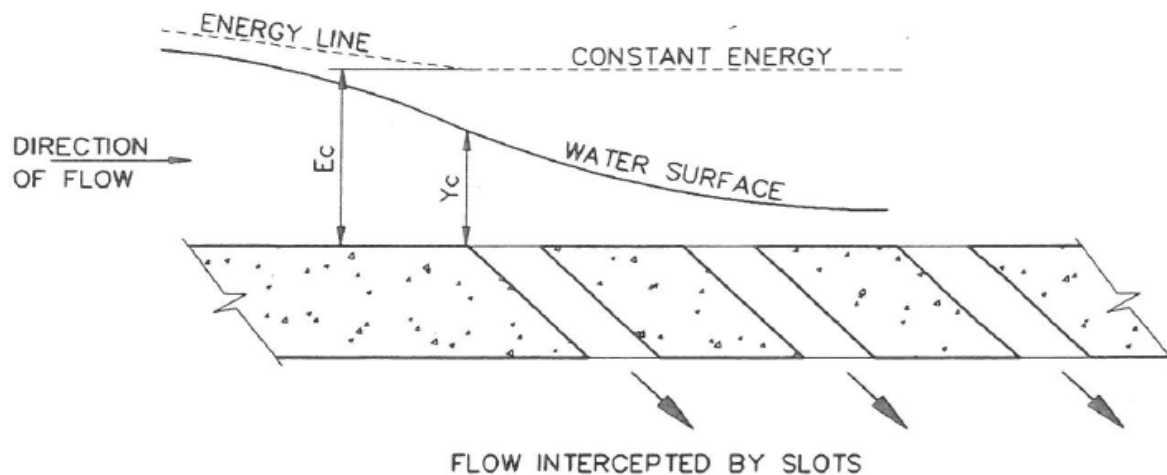


**Figure 2-10: Assumed water and energy profile for sub-critical flow (Gouws, 1993)**

The orifice formula was applied for subcritical submerged flow conditions to calculate the flow passing through any slot. After extensive testing, this mathematical model was calibrated with the results of the laboratory tests and to find a correlation between the mathematical model and the laboratory test results; a Froude number correction factor was incorporated.

**Flow through a slot opening was calculated as follows:**

$$Q = \frac{C_a * C_b * A * \sqrt{2 * g * y}}{Fr^{0.3}} \quad \text{Equation 2-16}$$

Where:

Q = flow through a slot opening (m<sup>3</sup>/s)

$C_a$	=	inlet coefficient (0.6 for sharp edges and 0.8 for rounded edges)
$C_b$	=	blockage factor (1 for laboratory tests and 0.5 for design)
$A$	=	area of slot opening ( $m^2$ )
$g$	=	gravitational acceleration ( $9.81m/s^2$ )
$y$	=	water depth (m)
$Fr$	=	Froude number immediately upstream of the first slot (1 for sub-critical approach flow and $\frac{v}{\sqrt{g*y}}$ for supercritical approach flow where $V$ is the approach velocity)

A reasonable agreement was found between the proposed mathematical model and the laboratory tests over the first slot. Accordingly, SBCE developed a design chart (nomograph), to allow pavement designers to determine the total length of slots required, for any combination of longitudinal slope, cross slope, shoulder runoff and width, to drain surface water flowing alongside the median barrier. This chart is depicted in Appendix A, Chart 4.

The SBCE concluded the following in their study (Gouws, 1993):

- At low water flows, vertical slots were not as effective as significant upwards spray developed as the water impacted the opposite side of the slots;
- Consequently, slot inlets inclined at  $45^\circ$ , were tested and their observations showed that  $45^\circ$  inclined slots prevented the water from spraying upwards and;
- The Froude number and upstream flow depth play a significant role in the determination of interception capacities through the drainage slots.

### 2.6.2 SLOTTED DRAINS IN SAG (SUMP) LOCATIONS

Water flow paths in sag locations are usually longer compared to flat tangent sections where water is more likely to pond on the pavement surface of these sections. Water runoff builds up at the absolute low point of the sag curve due to the decreasing change in longitudinal grade approaches zero from both sides of the curve. Additional time is required to adequately drain the pavement surface as the drainage runoff doubles due to the runoff from both sides of the curve. The slotted drains should be designed accordingly, with an adequate inlet capacity to accommodate the increase in water runoff.

Special attention is required when placing slotted drains in sag location. Slotted inlets have more potential to intercept debris from the longer water runoffs and clogging makes it less practical to drain the surface

water at the lower points of the curve. The operation of slotted drains in sag locations is outside the scope of the study and is only discussed in the literature to understand precisely how slotted drains operating in practice under different environmental conditions.

### 2.6.2.1 UNITED STATES BUREAU OF RECLAMATION

The USBR conducted an additional study for the FHWA on the operation characteristics of slotted drains in sag (sump) locations (Brown et al., 2009). Slotted inlets in sag locations can either operate as a weir or an orifice depending on the water depth as described previously. Results indicate that the orifice equation can be used to calculate flow capacities of slots in completely submerged sump conditions (Pugh, 1980).

The same test facility was used to test the performance of slotted drains in sump locations, as described previously in paragraph 2.6.1.1. Some additional adjustments were made to the original test facility. A scale model, with a scale ratio of 1:1.75, was used with the different slotted inlets widths to obtain flow depths up to 254mm high. A Froude scale relationship of 4.051 was used for discharge purposes. An additional 203.2mm high barrier was added to the pavement section of the test facility, situated across the roadway at the downstream side of the head box. The barrier was assumed to be at the bottom of a sag curve with the roadway set on a longitudinal slope of 0.2 percent with alternating cross slopes. Different flows were applied from the head box until submerged conditions were reached at the slot inlet in front of the barrier. Measurement concluded that a slot inlet performed on a similar manner at low discharges as if a slot inlet is installed on a grade (Pugh, 1980).

The following empirical equations were developed through data analysis from the test results and may be used for slotted drain calculations in sag location (Brown et al., 2009):

**The following equation can determine the interception capacity of a slotted inlet with lower water depths of about 60mm and depending on the slot width, performing as a weir:**

$$Q_i = C_w * L * d^{1.5} \qquad \text{Equation 2-17}$$

Where:

- $Q_i$  = interception capacity flow (m<sup>3</sup>/s)
- $C_w$  = weir coefficient, varies with different flow depths and slot lengths (typically 1.4)
- $L$  = slot length (m)
- $d$  = depth at slot inlet measured from the normal cross slope (m)



**The following equation can determine the interception capacity of a slotted inlet with water depths greater as 120mm and the slot performing as an orifice:**

$$Q_i = C_o * L * W * \sqrt{2 * g * d} \quad \text{Equation 2-18}$$

Where:

- Q<sub>i</sub> = interception capacity flow (m<sup>3</sup>/s)
- C<sub>o</sub> = orifice coefficient (typically 0.8)
- L = slot length (m)
- W = width of slot (m)
- g = gravitational acceleration (9.81m/s<sup>2</sup>)
- d = water depth at slotted inlet for d > 0.12m (m)

According to Equation 2-17 and Equation 2-18 above, Chart 5 in Appendix A was developed to obtain graphical solutions for the weir and orifice flow conditions, and it also indicates that the transition between the weir flow and orifice flow can occur at different water depths.

## 2.7 SCALING OF PHYSICAL HYDRAULIC MODELS

The experimental part of all the above-mentioned studies was completed by testing physical constructed pavement models with slotted drainage systems in a laboratory. To implement the relevant testing equipment on a pavement section in practice with high traffic volumes, can be very difficult and a huge safety concern. Thus, hydraulic models can be constructed on scale as an accurate presentation of the actual pavement structure operating with a slotted drainage system in practice.

A physical constructed model which represents a real-world prototype model can produce fatal findings if a set of pre-operational analysis such as inspection analysis, dimensional analysis and calibrations, is not accurately done during the model construction.

The parameters between a physical hydraulic model and the real-world prototype model may differ due to measurement, model or scale effects. In short, these effects can be described as follows (Heller, 2011):

- Measurement effects may occur due to inaccurate measurement techniques used for the data generation of the model as well as the prototype;
- Model effects may occur due to incorrect model feature replications including geometries, parameters inputs and properties; and

- Scale effects may occur when key force ratios are not kept constant between the scaled model and prototype.

Geometric, kinematic and dynamic similarities between the physical model and the prototype model are essential to minimise these effects. The geometrical scale chosen for the pavement section of the generalised model is a critical consideration so that the flow depth applied on the model is not too small. Minimal flow depth may be confused with laminar flow conditions even though the applied flow is turbulent. A glassy and smooth flow surface may appear as laminar flow conditions, but this phenomenon may be due to insufficient flow velocity to form capillary waves on the flow surface (Chaudhry, 2007). This misconception may lead to unreliable test results.

Hydraulic modelling, more generally in open-channel hydraulics, requires dynamic similarities where all force ratios in the two systems are identical (Heller, 2011). In order to obtain these dynamic similarities, a Froude or Reynolds ratio is usually implemented. The Froude similarity is applied in circumstances of free surface flow where gravity and the inertial forces are dominant and thus implemented to ensure that gravity forces between the physical and prototype model are identical. The Reynolds similarity is applied in unusual circumstances where viscous and inertial forces are dominant and thus implemented to ensure that the viscous forces between the physical and prototype model are identical.

In conclusion, water on a pavement surface can become a serious safety concern as hydroplaning and splash and spray can occur at minimum water depths which are influenced by various factors, much more than just the water on the surface itself. Adequate drainage systems should be implemented to remove surface water effectively and early as possible to prevent safety risk and deterioration of the pavement structure. The implementation of slotted drainage systems is a promising drainage technique, but a condemned topic of pavement drainage in South Africa. Minimum research was found on slotted drains operating with pavements with unique design, geometric, and environmental conditions in the domain of South Africa. Consequently, the exact interception drainage capabilities of slotted drains operating within South African pavements are relatively inconclusive and required future investigation. Several other studies were done on slotted drains outside South Africa and the valuable findings and recommendations obtained, was used as a supportive platform for further research on slotted drains on South African pavement structures. The insightful knowledge gained from the literature of various references is used to construct a physical model for experimentation that will yield accurate test results to examine slotted drains operating in practice.

### **3. EXPERIMENT METHODOLOGY**

#### **3.1 INTRODUCTION**

An experiment was performed at the hydraulic laboratory of the University of Pretoria on constructed pavement models with slotted drainage systems operating within a pavement structure in practice. Two different slotted drain installations were tested during the experimental part of the study which includes a total of 120 tests. The operational conditions of the tested slotted drains were:

- A slotted drain operating with a concrete barrier adjacent to the longitudinal length of the slotted drain installed to remove surface water from a pavement; and
- A slotted drain operating individually without a concrete barrier, installed to remove the surface water from a pavement.

The experimental methodology and the development of physical models to obtain representative test results on the interception capabilities of slotted drains are described in this chapter and include the following:

- Proprietary slotted drain specifications;
- Test parameters;
- Model descriptions and construction;
- Experimental set up and model operations;
- Flow measuring devices;
- Test procedures.

#### **3.2 PROPRIETARY SLOTTED DRAIN SPECIFICATIONS**

The Consulting Engineers of the SANRAL project (as discussed in the case study in Chapter 1), have suggested implementing slotted drains of a specific manufacturer, Salberg Concrete Products (Pty) Ltd, as a possible surface drainage system of future pavement projects. Salberg Concrete Products (Pty) Ltd was established in 1972 and manufacture a full range of South African Bureau of Standards (SABS) approved precast concrete products for the construction industry. Salberg specialised in precast sewer, stormwater systems and is specifically a well-known manufacturing company for precast slotted drains.

Salberg manufactures various types of slotted drains with unique operating principles and interception drainage capabilities. Salberg's concrete slotted drains evaluated in this study were 1.250m long precast sections and consist of a pipe diameter with an opening at the top along its longitudinal length, which performs as a slot inlet to intercept surface water. The drains are manufactured in three different diameter

sizes with corresponding slot inlet widths. The concrete inlet is chamfered at  $45^\circ$  on both sides of the top ends of the inlet for possible improvement of the interception capabilities of the drains. A cross sectional design of Salberg's slotted drains is shown in Figure 3-1 with its dimensions summarised in Table 3-1.

The weight and size of the precast slotted drain sections made it to some extent unpractical to test the actual products in the hydraulic laboratory of the University. It was decided to construct generalised full-scale models of the proprietary slotted drains with the same inlet dimensions as the actual products, which included the drain width ( $W$ ), (i.e.  $W_x$ ,  $W_y$  and  $W_z$ ), the slot width ( $S_w$ ) and the slot depth ( $S_d$ ), as illustrated in Figure 3-1. The fact that only the interception capabilities of the slotted drains were examined during the study and not the hydraulic capacity of the drains itself, resulted that only the top part of the Salberg slotted drains were reconstructed. This entails a full-scale reconstruction of all the features of the slotted drain above the Section A-A line in Figure 3-1.

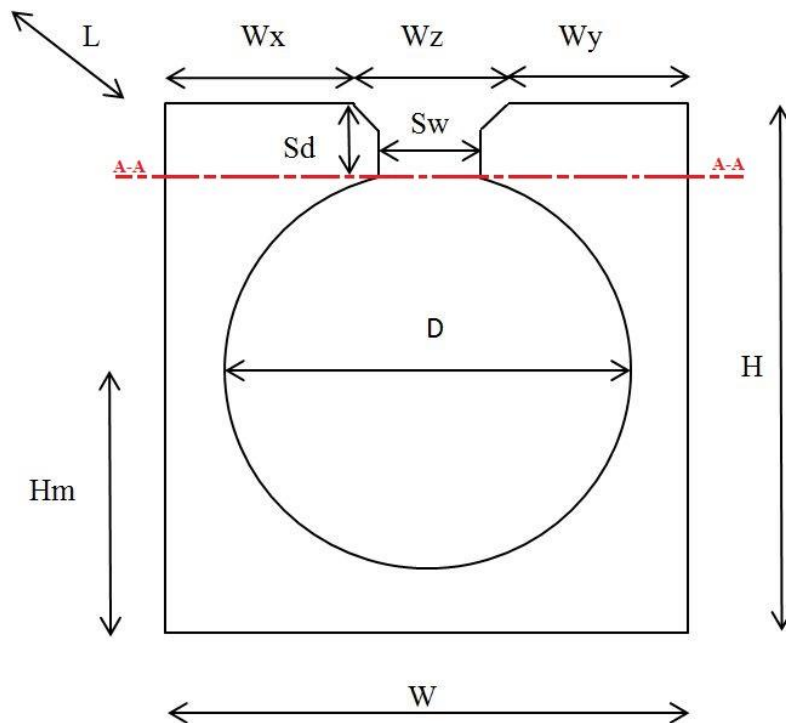


**Figure 3-1: Cross section design of the propriety slotted drain**

**Table 3-1: Slotted drain dimensions and specifications**

<b>DIMENSIONS</b>	<b>TYPE OF SLOTTED DRAIN</b>		
	<b>Slotted drain 150</b>	<b>Slotted drain 300</b>	<b>Slotted drain 450</b>
<b>D (mm)</b>	150	300	450
<b>H (mm)</b>	260	410	600
<b>W (mm)</b>	255	410	600
<b>L (mm)</b>	1250	1250	1250
<b>Wx(mm)</b>	97.5 (98)	165	250
<b>Wy (mm)</b>	97.5 (98)	165	250
<b>Wz (mm)</b>	60	80	100
<b>Sd (mm)</b>	55	55	75
<b>Sw (mm)</b>	20	40	60
<b>Hm (mm)</b>	130	205	300
<b>Mass (kg)</b>	163	312	720

### **3.3 TEST PARAMETERS**

During the model study and testing of the slotted drains, it was essential to take specific parameters into consideration that might affect the interception capabilities of the slotted drains. Some parameters were varied to determine the exact influence that the factors will have on the interception efficiencies of the drains, and others were held constant for consistent test conditions throughout the experiment. These parameters were implemented and altered according to the recommendations of previous studies, the SANRAL project field conditions and the standards of pavement design criteria of South Africa as discussed in the literature. This includes the following:

- Pavement surface texture;
- Concrete surface texture of the pre-cast slotted drain;
- Longitudinal slopes;
- Cross slopes;
- Slotted drains operating with or without a median barrier;
- Rainfall intensities and
- Width of the slotted inlet.

### **3.3.1 PAVEMENT AND PRECAST CONCRETE SURFACE TEXTURES**

The surface area of the constructed models was modified to obtain a surface texture roughness similar to the roughness of asphalt and precast concrete. Te Chow (1959) indicated a normal roughness coefficient (Manning's  $n$ ) of  $0.013\text{s/m}^{1/3}$  for smooth asphalt surfaces and  $0.016\text{s/m}^{1/3}$  for rough asphalt surfaces for open channel flow. The normal roughness coefficient for precast concrete, similar to a trowel finish was stated as  $0.013\text{s/m}^{1/3}$  (Te Chow, 1959). In other literature from Engman (1986), a Manning roughness coefficient for sheet flow smaller or equal than 0.1ft on smooth surfaces including concrete and asphalt, are specified as  $0.011\text{s/m}^{1/3}$ .

The average roughness coefficient of the pavement models was determined from the mean texture depth (MTD) of the pavement surfaces that were estimated by following the sand patch test method (Committee of State Road Authorities, 1984). The test procedures of the sand patch test are discussed in paragraph 3.7.1 in this chapter.

### **3.3.2 LONGITUDINAL SLOPE**

The longitudinal slopes of the pavement models were adjusted to simulate the grade changes at vertical sag and crest curves in the field. The longitudinal slopes were adjusted following the design specification of the SANRAL project. Longitudinal slopes were varied between a minimum value of one percent and a maximum value of six percent.

### **3.3.3 CROSS SLOPE**

The cross slopes of the pavement models were adjusted to simulate the change in superelevation at horizontal curves in the field. The cross slopes were adjusted in accordance with the design specification of the SANRAL project. Cross slopes were varied between a minimum value of one percent and a maximum value of six percent.

### **3.3.4 MEDIAN BARRIER**

The installation of the slotted drains to operate with a median barrier and without a median barrier in the field was simulated individually with two separate pavement models. The simulation of these two operational scenarios implemented in the experiment is discussed in paragraph 3.4.

### **3.3.5 RAINFALL INTENSITY**

The rainfall intensity was simulated with the volume of water which was applied to the surface of the pavement model as sheet flow. The volume of water applied for a given period (l/s) during the experiment was converted to typical rainfall intensities that can occur on different pavements widths in practice.

### **3.3.6 WIDTH OF THE SLOTTED INLET**

The widths of the slotted drain inlet were varied to determine the interception efficiency of each inlet width. The three different slotted widths that were tested and compared with one another were (also listed in Table 3-1):

- 20mm inlet width;
- 40mm inlet width and
- 60mm inlet width.

## **3.4 MODEL DESCRIPTIONS AND CONSTRUCTION**

Two different types of models were constructed to evaluate the two different installation conditions of slotted drains in practice. The first type of model, (Type I), was the primary pavement test model which represented the proposed slotted drain installation of the SANRAL project. A Type I model was constructed to simulate the operation of a slotted drain without an adjacent median barrier, which functions with the same gradient as the cross slope of the pavement. The second type of model, (Type II), was constructed to simulate the operation of a slotted drain adjacent to a median barrier, which functions with the same gradient as the median barrier (horizontally to the cross slope of the pavement with a zero percent slope). Three of each type of models was constructed according to the three individual sizes of the proprietary slotted drains.

The model construction was performed at the Experimental Farm of The University of Pretoria. Each constructed model consists of a pavement section with a slotted drainage inlet and a water catchment system fixed under the slotted inlet. The models were placed on portable and adjustable support footings to accommodate the different pavement slope configurations. The features of the constructed models were modified and scaled based on Salberg's slotted drains operating in real-world circumstances to ensure feasible test conditions. Figure 3-2 and Figure 3-3 are schematic illustrations of the constructed Type I and Type II model respectively, followed by the general model dimensions specified in Table 3-2 and Table 3-3.

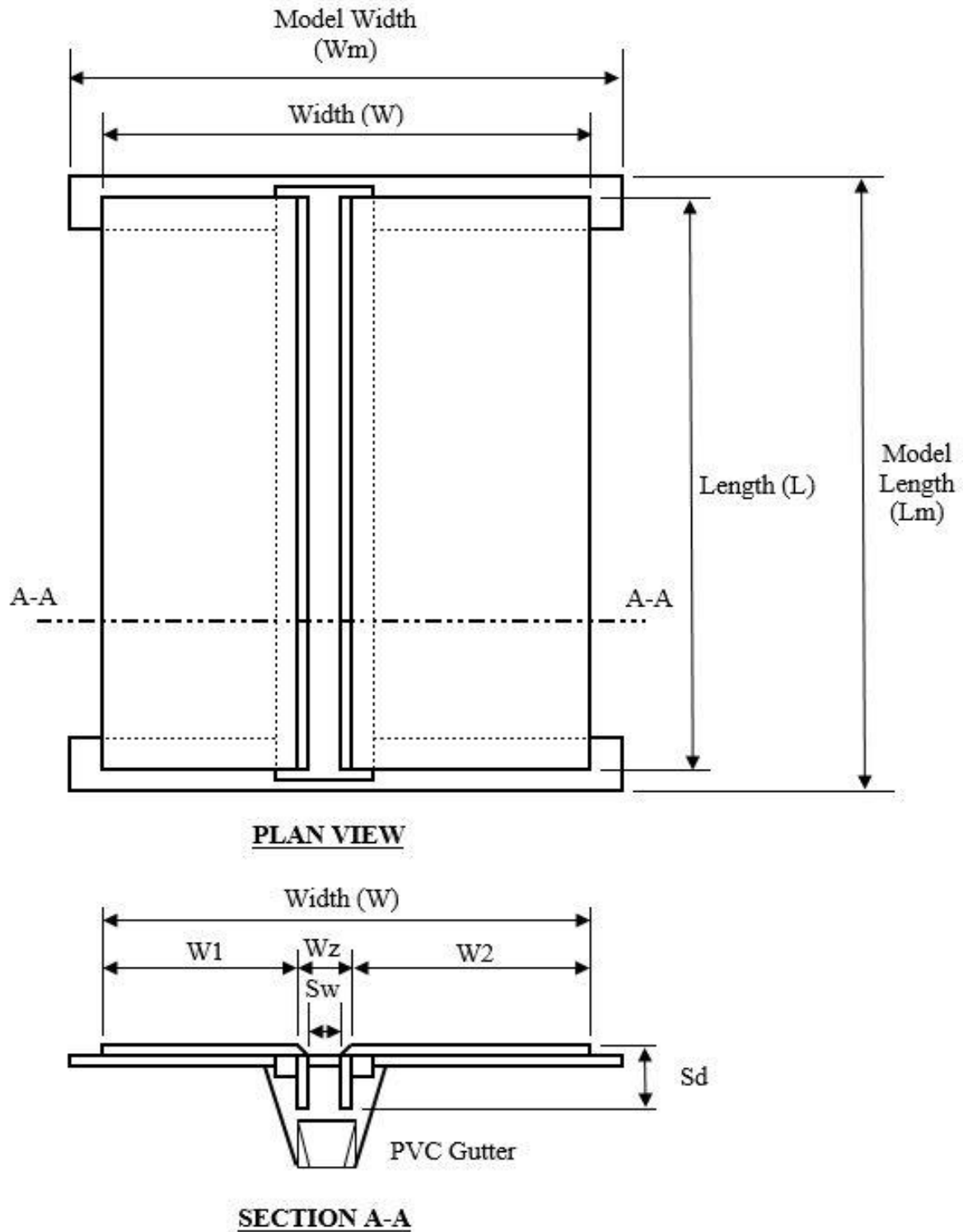


Figure 3-2: Type I Model design



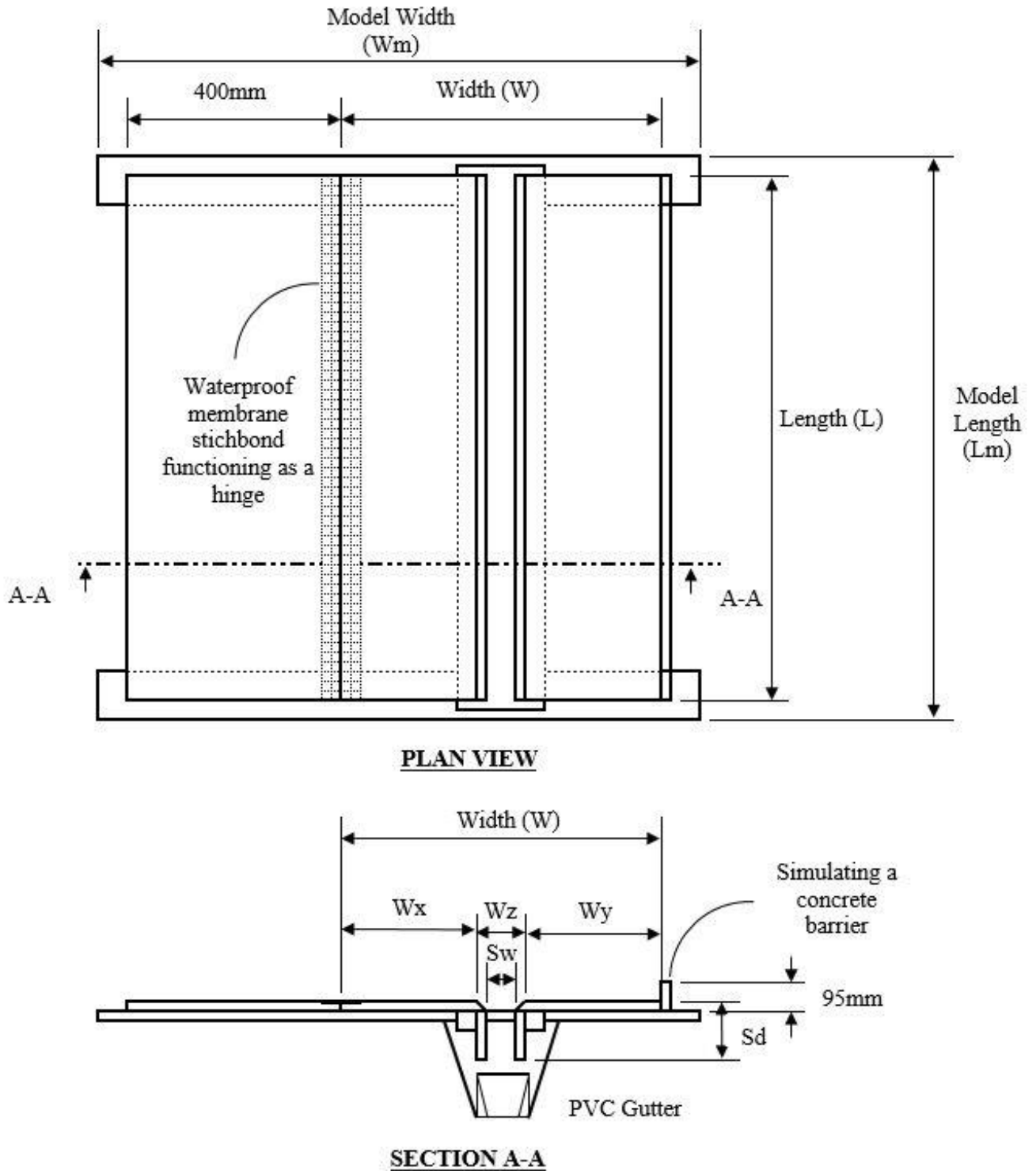


Figure 3-3: Type II Model design

**Table 3-2: Type I Model dimensions**

<b>DIMENSIONS</b>	<b>TYPE I MODEL (Slotted drain 150)</b>	<b>TYPE I MODEL (Slotted drain 300)</b>	<b>TYPE I MODEL (Slotted drain 450)</b>
<b>Lm (mm)</b>	2740	2740	2740
<b>Wm (mm)</b>	1500	1500	1500
<b>L(mm)</b>	2440	2440	2440
<b>W(mm)</b>	1220	1240	1260
<b>W1 (mm)</b>	480	480	480
<b>W2 (mm)</b>	680	680	680
<b>Wz (mm)</b>	60	80	100
<b>Sw (mm)</b>	20	40	60
<b>Sd (mm)</b>	55	55	75

**Table 3-3: Type II Model dimensions**

<b>DIMENSIONS</b>	<b>TYPE II MODEL (Slotted drain 150)</b>	<b>TYPE II MODEL (Slotted drain 300)</b>	<b>TYPE II MODEL (Slotted drain 450)</b>
<b>Lm (mm)</b>	2740	2740	2740
<b>Wm (mm)</b>	980	1080	1230
<b>L(mm)</b>	2440	2440	2440
<b>W (mm)</b>	255	410	600
<b>Wx (mm)</b>	98	165	250
<b>Wy(mm)</b>	98	165	250
<b>Wz(mm)</b>	60	80	100
<b>Sw (mm)</b>	20	40	60
<b>Sd (mm)</b>	55	55	75

The overall dimensions of the two types of models (Lm, Wm and L) were determined according to the maximum water flow path length and width of spread if water will be applied to the surface of pavement section of the models. As indicated in the literature the water flow path and width of spread is affected by the different combinations of the longitudinal slope and cross slope of the pavement. For any combination between these two experimental variables, the slope of the flow path, as well as the maximum flow path length, was calculated to determine the ideal designed dimensions of the models. Calculations were made

based on the SANRAL drainage manual (SANRAL, 2013), Equation 2-1 and Equation 2-2 in the literature review. Practical model dimensions were chosen consequently so that all surface water will approach the slotted inlets to be captured and measured, with a minimum volume of water overflowing off the sides of the models.

Oil treated shutter boards with general dimensions of 1.22m x 2.44m x 0.02m were used to construct the models and were cut into the required designed dimensions. The type I and II models were assembled differently to simulate the two slotted drain operational scenarios.

The pavement section and the slotted inlet of the type I models were fixed to adjust as a unit on the support footings for different slope configurations. Differently from the type II models, where the pavement section was partially fixed to the slotted inlet with a stitch bond fabric membrane. The membrane performed as a hinge which allowed the pavement section to adjust independently from the slotted inlet system on the support footings to simulate the second installation condition. More additions were made to the type II models to simulate the operation with a median barrier. A small piece of shutter board with a height of 95mm was fixed at the end of the slotted inlet, which represents the bottom part of the median barrier in practice (Figure 1-1). A 2.44m long Polyvinyl chloride (PVC) gutter was fixed to the bottom of the drainage inlet for both type I and II models to capture intercepted surface water for flow measurements.

The pavement section of all the constructed models was modified to obtain a surface roughness close to the roughness of an asphalt surface. The surface of the pavement section of the models was coated with rubberised bitumen paint. According to previous findings and recommendations from the study of Burgi et al. (1977), sand with specific particle diameter sizes was applied to wet paint to obtain a specified surface roughness of asphalt. A similar approach was followed. Sand was sieved to obtained sand particle sizes between one and two millimetres and washed afterwards to remove the dust before it was added to the wet bitumen rubberised paint, (Figure 3-4). The paint with the sand particles was left to dry, and the excess sand was removed from the treated surface. Some sand particles didn't cling to the painted surface, and another paint layer and sand was required to fill the uneven visible areas, (Figure 3-5). Finally, a last layer of paint was applied to cover all sand patches and to obtain smooth presentable asphalt-like surface.



**Figure 3-4: Pavement surface treatment**

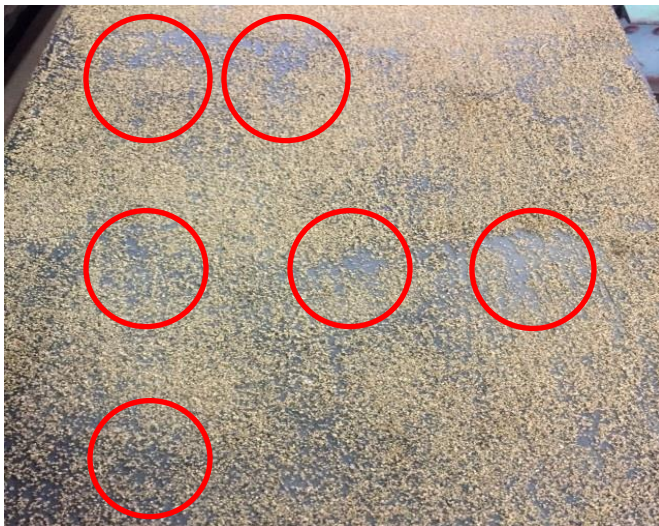


**Figure 3-5: Visible uneven sand patches**

A similar process was followed for the surfaces of the slotted inlets. Instead of rubberised bitumen paint, the surfaces of the slotted inlets were treated with a silver Enamel paint and sand. This resulted in slightly different surface roughness than the pavement sections. The surface roughness regarding mean texture depths (MTD) was determined for each constructed model. The different surface colours made it convenient to distinguish visually between the surface of the pavement sections and slotted inlets of the models. An illustration of the completed constructed type I and II model can be seen in Figure 3-6 and Figure 3-7 respectively.

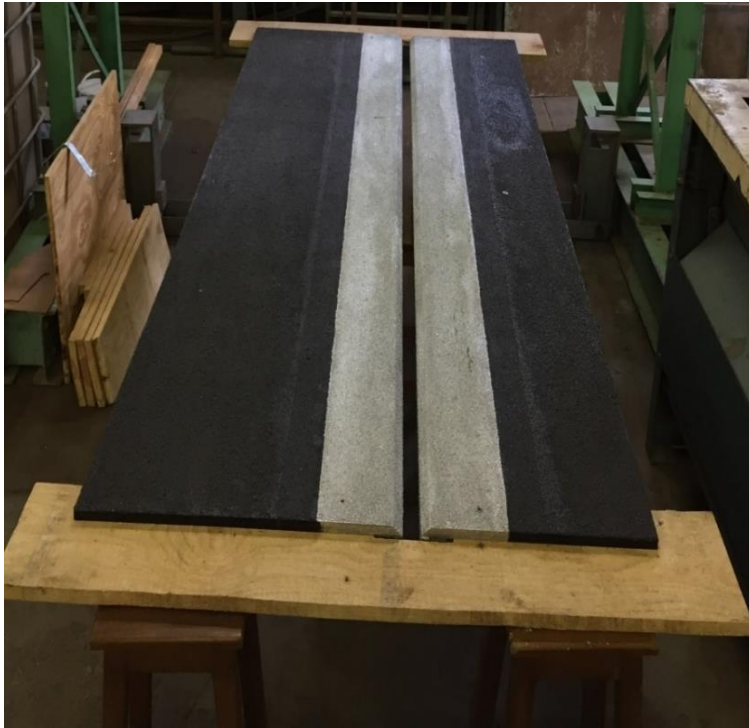


**Figure 3-6: Constructed Type I model**



**Figure 3-7: Constructed Type II model**

### 3.5 EXPERIMENTAL SET UP AND MODEL OPERATIONS

The experiment consists of two different model set ups each with unique objectives. The hydraulic laboratory of the university provided ample space to set up the constructed models individually on the adjustable footings next to a large sump built into the laboratory floor, which served as a water reservoir for the experiment. Figure 3-8 is a schematic illustration of the experimental set up in the laboratory with the main principle features listed in Table 3-4. Each experimental set up consists of a water supply system (i), water catchment area (ii), a pavement model (iii) and a water drainage system (iv) to capture and measure the intercepted sheet flow. Flow measurement devices (D and L) were installed to measure the supplied flow of the supply system and the intercepted flow of the drainage system, which formed part of the data collection process.

**Table 3-4: Principle features of experimental set up.**

PRINCIPLE FEATURE	POSITION	PRINCIPLE FEATURE	POSITION
<b>WATER SUPPLY SYSTEM (i)</b>		<b>WATER CATCHMENT AREA (ii)</b>	
Submersible Pump	A	Shade netting	E
Valve 1 (bypass valve)	B	Perforated pipe outlet	F
Valve 2 (control valve)	C	Rubber insertion	G
Flow meter 1	D	Adjustable support footings	H
<b>CONSTRUCTED PAVEMENT MODEL (iii)</b>		<b>WATER DRAINAGE SYSTEM (iv)</b>	
Adjustable support footings	J	Flow meter 2	L
Treated pavement surface	K	Goose neck flow outlet	M

#### 3.5.1 WATER SUPPLY SYSTEM (i)


A water supply system was required to deliver water from the sump to the surface of the pavement models as a simulation of sheet flow on a pavement surface in practice. A V2200F submersible pump (A), with its pump specifications detailed in Table 3-5, was used to deliver water from the sump through pipes and valves into a self-constructed catchment area before it could overflow onto the pavement sections of the models.

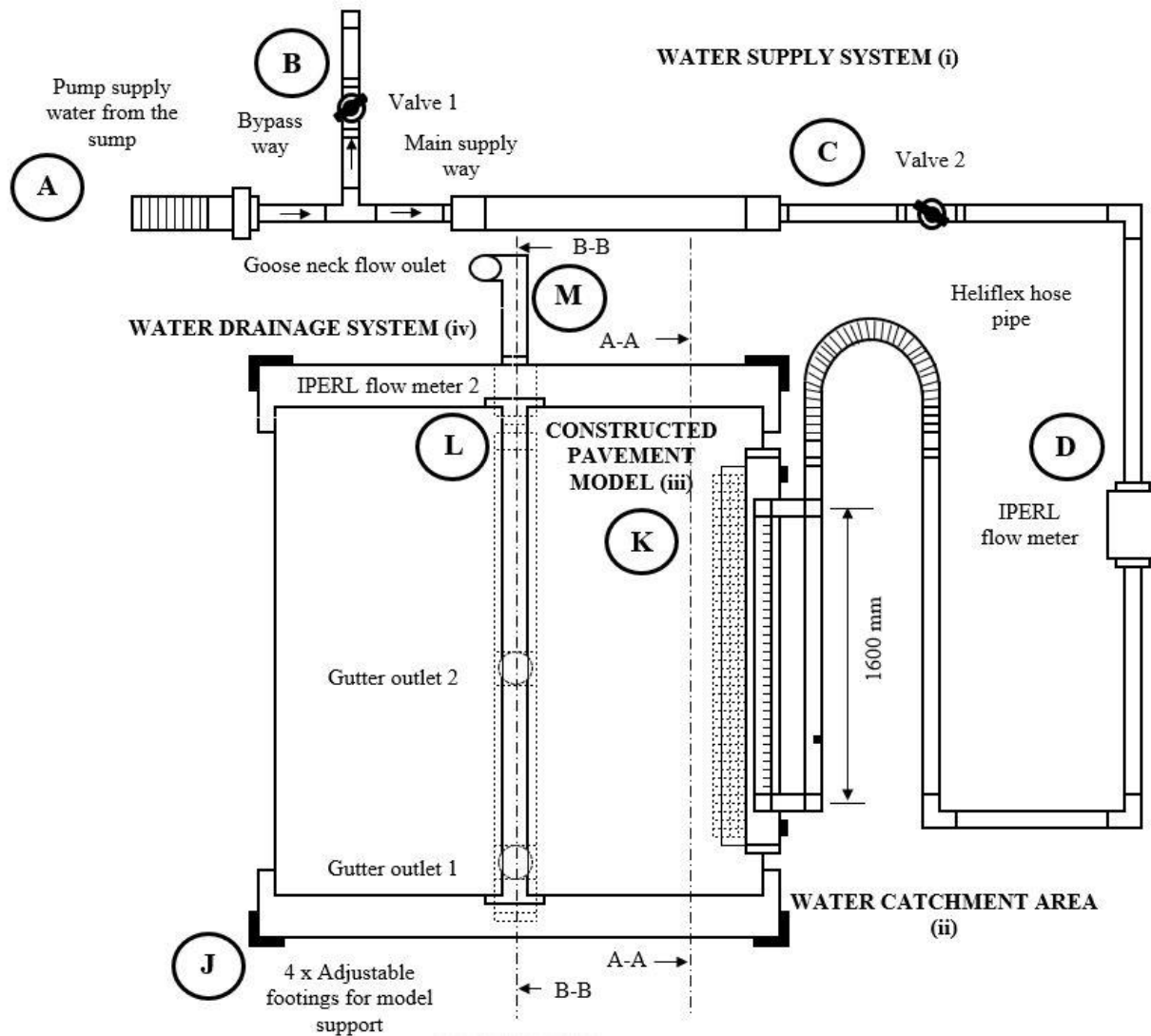


**Figure 3-8: Principle features of test set up (schematic)**

The water was fed through the network of pipes, including a small section Heli flex hose pipe and was discharged into the catchment area through a perforated pipe section (F), which was placed inside the water catchment area. Two PVC ball valves were used to control the volume of water applied to the experimental models. Referring to Figure 3-8, Valve 1 (B), was manually operated to bypass the excess volume of water to discharge back into sump of the laboratory. Valve 2 (C) was manually operated to vary the volume of water delivered through the pipe network into the water catchment area. A flow meter (D) was connected to the pipe system to measure the volume of water supplied to the pavement models at any given time.

**Table 3-5: Pump specifications**

<b>Pump Model</b>	V2200 (F)	 <p>(Pumps for Africa, 2017)</p>
<b>Power (kW)</b>	2.2	
<b>Outlet diameter (mm)</b>	76	
<b>Voltage (V/Hz)</b>	220/50	
<b>Maximum flow (m<sup>3</sup>/h)</b>	38	
<b>Maximum head (m)</b>	16	
<b>Weight (kg)</b>	33.5	
<b>Dimension (mm)</b>	590 x 230 x 330	

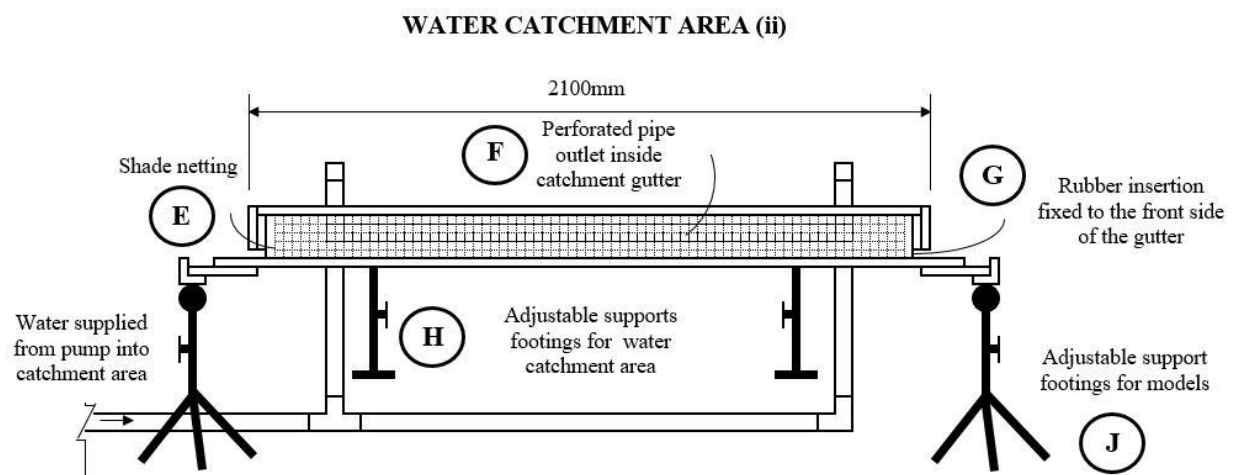


**Figure 3-9: Principle features of the water catchment area, Section A-A**

### 3.5.2 WATER CATCHMENT AREA (ii)

The self-constructed water catchment area, schematically illustrated in Figure 3-9, was a 1.6m long gutter section fixed to two adjustable footings as supports (H). The catchment area was located just above the pavement section of the models and was able to be raised and lowered as required for the different slope configurations of the models. The catchment area was angled by manually tilting it slightly askew, for the



water to flow evenly over the side of the gutter onto the pavement section of the models. A rubber insertion strip (G), was sealed to the frontal side of the gutter to prevent water leaking underneath the gutter and off the pavement model. Shade netting (E), was fixed to the frontal side of the gutter to further reduce water turbulence exiting the gutter and to enhance sheet flow conditions on the model surfaces. The individual features of the water supply system as described above may be seen in Figure 3-10 and Figure 3-11.



**Figure 3-10: Water catchment features (A)**

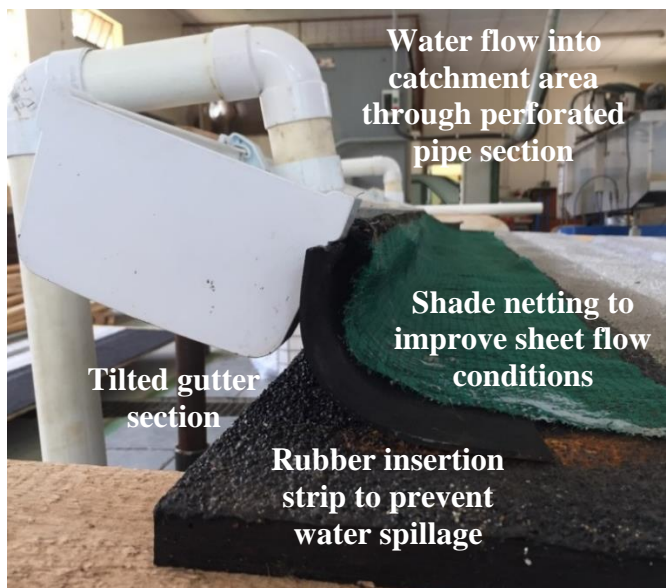


**Figure 3-11: Water catchment features (B)**

### 3.5.3 WATER DRAINAGE SYSTEM (iv)

The water that overflows the catchment area was able to sheet flow on the treated pavement surface (K) towards the slotted inlets of the models. The sheet flow which was intercepted by the slotted inlets was captured in the gutter constructed underneath the slotted inlets of the models. A drainage system, schematically illustrated in Figure 3-12, was connected to two gutter outlets to effectively drain the intercepted water without overflowing the gutter. Another flow meter (L) was connected to a pipe on the drainage system to measure the total volume of water intercepted by the slotted inlet for a specific period. Any water not intercepted by the slotted inlet would flow directly into the sump below the installation. A gooseneck flow outlet (M) was connected at the end of the drainage pipe network to ensure the drainage pipe was flowing full for accurate flow measurements. The drainage water was also discharged into the sump creating a closed loop system.

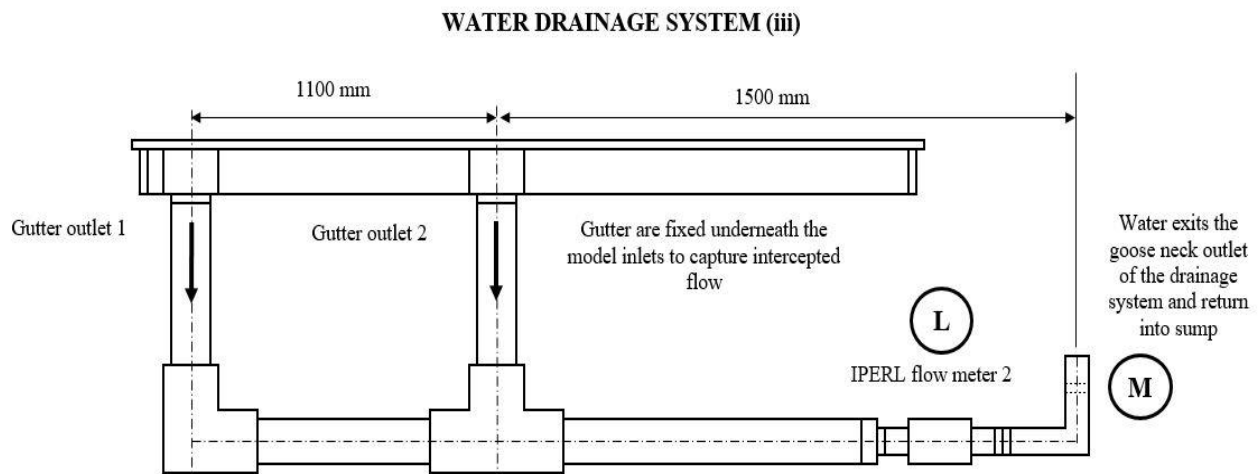


**Figure 3-12: Principle features of the water drainage system, section B-B**

The experimental test set up for both the type I and II models are depicted in Figure 3-13 and Figure 3-14 respectively.

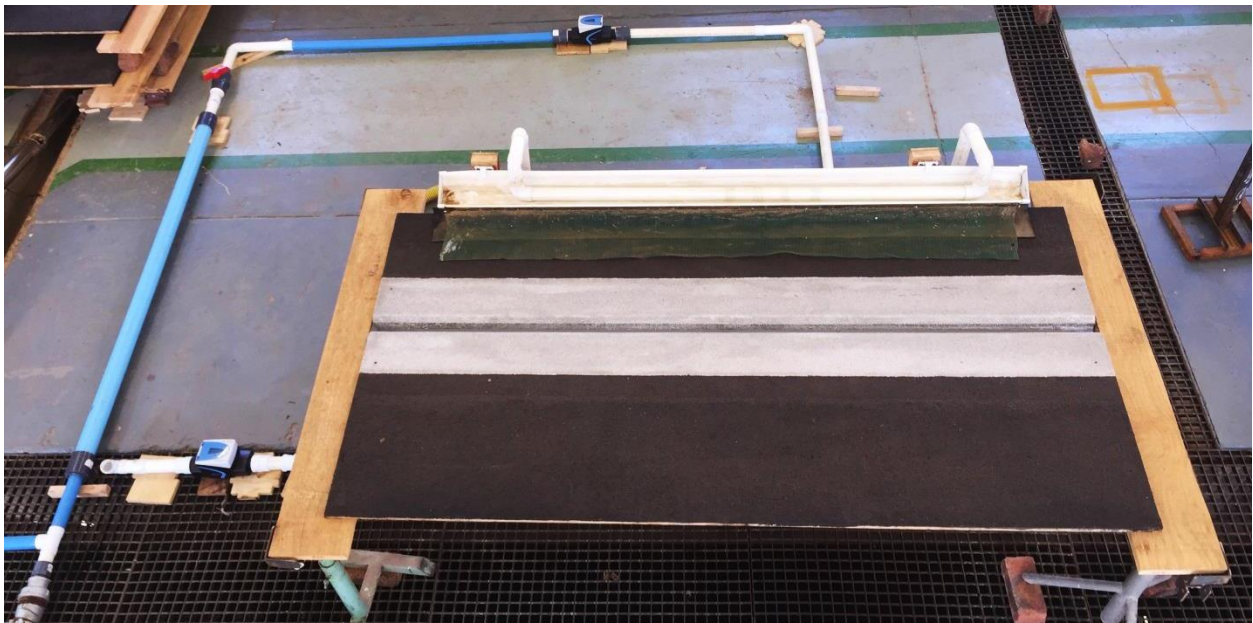


**Figure 3-13: Test set up for the Type I models**

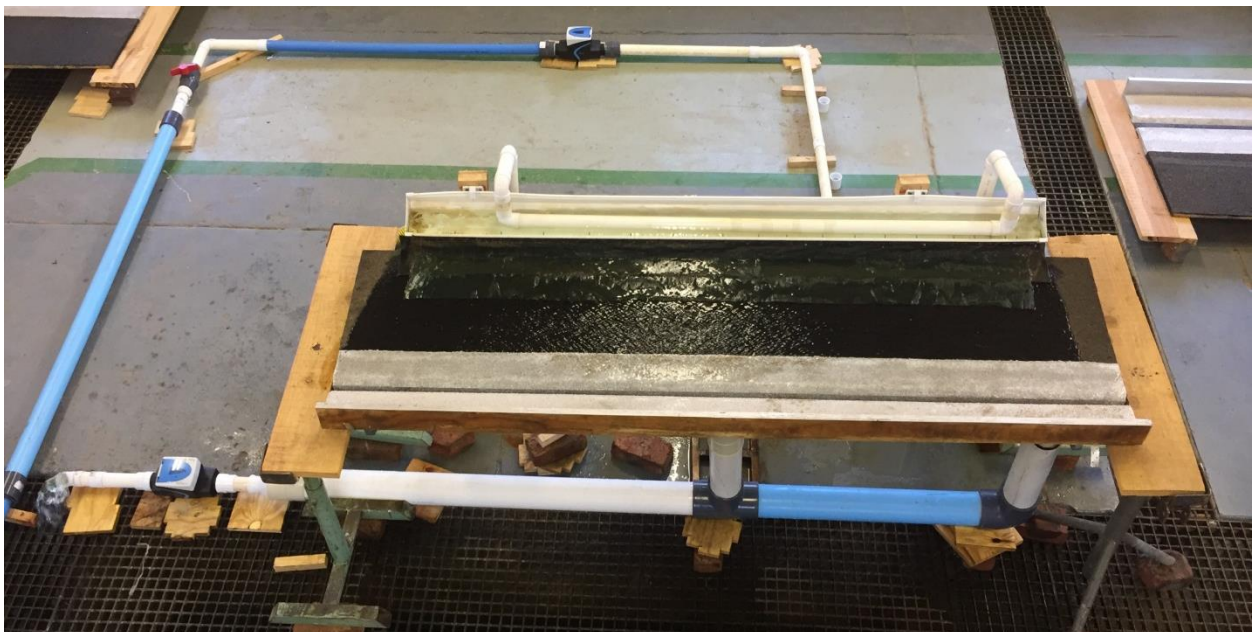


**Figure 3-14: Test set up for the Type II model**

### **3.6 FLOW MEASURING DEVICES**

Two Sensus IPERL flow meters were used in the experimental set up for the required flow measurements. IPERL has approved certification to deliver constant flow measurements (with accuracy within +/- 2 percent) with convenient installation requirements as it can be connected in any orientation without the

need for a linear pipe lead. These static electromagnetic meters use remnant magnetic field technology to measure very low flow rates. The principle of magnetic-inductive flow measurements is illustrated in Figure 3-15. In basic terms, the magnetic field acting on the water which flows through the flow meter generates an electrical voltage which is proportional to the velocity of the water passing through the flow meter.

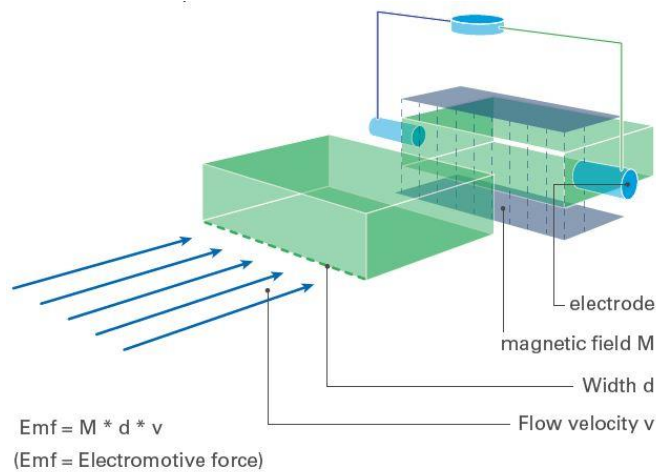


**Figure 3-15: The principle of magnetic-inductive flow measurements (Sensus, 2018)**

### 3.6.1 DEVICE SET UP

The two IPERL flow meters were connected to the water supply system and water drainage system respectively, to measure the volume of water supplied onto the pavement models and the volume of water captured by the inlets of the pavement models independently. The interception efficiencies for different test configurations were determined accordingly which form part of the data collection of the research.

### 3.6.2 VERIFICATION OF MEASUREMENTS

Before the actual experimenting commenced, it was required to verify if the flow readings, given by the two individual IPERL flow meters for the unique experimental set up, are indeed accurate. An additional flow measurement method was applied to measure the volume of water manually, utilising a simple bucket test. Firstly, the time to fill a bucket with a small amount of water leaving the drainage system outlet was recorded. The bucket was then weighed to determine the exact volume of water inside the bucket to ultimately obtain a flow rate by dividing the volume of water inside the bucket with the time it took to fill the bucket, (Figure 3-16).





**Figure 3-16: Bucket test**

The flow rate obtained by the bucket test was compared individually with the two flow readings from IPERL meters.

The flow measurement verification was done in ten-minute intervals for five different flow rates. Different flows were obtained by opening or closing the valve (C) of the supply system, and the system could reach stable flow conditions before measurements were taken. Controlled supervision also ensured that no water losses occurred, while all the supplied water entering the pavement model was captured in the drainage system of the set up. Flow measurements have been recorded four times per interval before an average flow rate was determined for the three flow measurement methods per interval. The average flow rates for each flow measurement, calculated from the five pre-set supplied flows, were tabulated in Table B-1, in Appendix B.

The flow measurement verifications were done for flows up to two litres per second (2.0l/s) as water spillages during the bucket test produced inaccurate flow measurements compared to the two IPERL flow meters. The average flow rates of the three different flow measurements are summarised in Table 3-6. The accuracy between the minimum and maximum flow rate measurement per interval was also determined and tabulated. The flow rate measurements between 0.3l/s to 2.2l/s, obtained during the five flow verification intervals, were determined to be accurate within two percent.

**Table 3-6: Summary of average flow rates**

Interval no	Average flow rates (l/s)			Accurate within (%)
	Flow rate 1	Flow rate 2	Manually measured flow rate	
1	0.343	0.341	0.345	1.11
2	0.548	0.546	0.544	0.75
3	0.989	0.981	0.998	1.63
4	1.622	1.600	1.605	1.37
5	2.161	2.139	2.134	1.23

### 3.7 TEST PROCEDURES

#### 3.7.1 SAND PATCH TEST PROCEDURE

As mentioned in paragraph 3.3.1, the surface texture depths of all the constructed pavement models were determined by using the sand patch test method described in the Technical Methods for Highways (TMH) 6 (Committee of State Road Authorities, 1984). The following sand patch test procedures were followed:

- Two parallel chalk lines were drawn over the length of the pavement test surface about 500mm apart, (Figure 3-17);
- A 250ml container was filled with fine sand and levelled off at the top of the container without compacting the sand;
- The sand was poured in a zig-zag pattern between the two chalk lines, (Figure 3-18);
- The sand was spread with a ruler to the greatest possible length without crossing the chalk lines;
- The length of sand spread was measured to the nearest 5mm (Figure 3-19) and
- The texture depth was calculated for the model surfaces to the nearest 0.001mm, by using the following equation:

**To calculate texture depth:**

$$T_d = \frac{A}{1000 \cdot B} \quad \text{Equation 3-1}$$

Where:

- $T_d$  = texture depth (mm)
- A = volume of sand (ml)
- B = area covered with sand (m<sup>2</sup>)

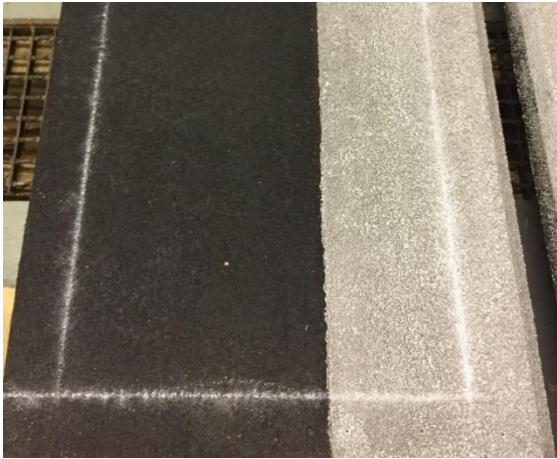


**Figure 3-17: Area marked with chalk**



**Figure 3-18: Sand spread in a zig zag pattern**



**Figure 3-19: Sand patch length measurement**

### 3.7.2 EXPERIMENTAL TEST PROCEDURES

After the necessary preparations were made for the experiment including the model constructions, the experimental set up and flow verifications of the flow meters, the testing commenced. The following experimental test procedures were followed for all individual pavement test models and illustrated in relative figures:

- Different flows were applied to the surface of the pavement model by opening or closing valve 2, (C), of the supply system. A smooth sheet flow surface runoff was obtained before the flows were recorded, (Figure 3-20);
- Flow was measured by the flow meters (D and L), every 180 seconds for four consecutive times per applied flow rate;
- Flow depths were measured with a digital vernier gauge across the width of the sheet flow at three different positions: the left, middle and right for the specifically applied sheet flow, (Figure 3-21);
- The different slope configurations of the pavement model were implemented by adjusting the heights of the support footings, (J), individually to pre-calculated heights for the specific model set up. The model elevations were measured with a measuring rod (Figure 3-22) to confirm the heights required for the specific slope configuration;
- The footings of the water catchment area were adjusted with the slope heights of the models so that the water can exit the catchment area at the most elevated side of the pavement surface for water to flow towards model inlets without flowing off the sides of the model, (Figure 3-23);
- Once the specific slope of the pavement model was obtained, the test procedure was repeated for different flows in a similar manner, (Figure 3-24);
- A small droplet of liquid dye was applied to the sheet flow of the elevated pavement to obtain a visual illustration of the slope of the flow path as a result of the different implemented slopes, (Figure 3-25);



**Figure 3-20: Sheet flow on the pavement model surface**





**Figure 3-21: Flow depth measurements**

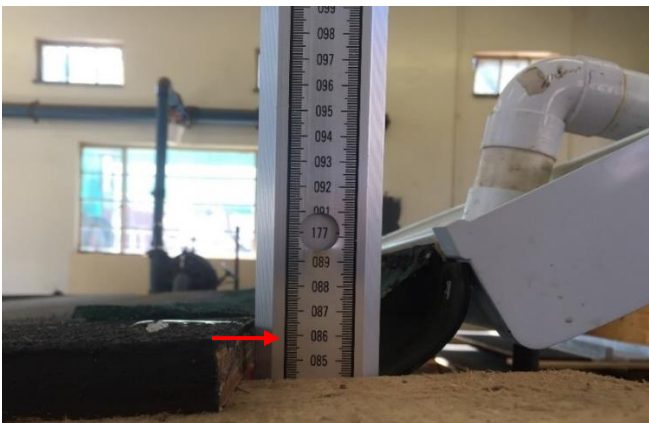


**Figure 3-22: Model height measurements for specific slope configuration**



**Figure 3-23: Water catchment area lifted with model slope adjustments**

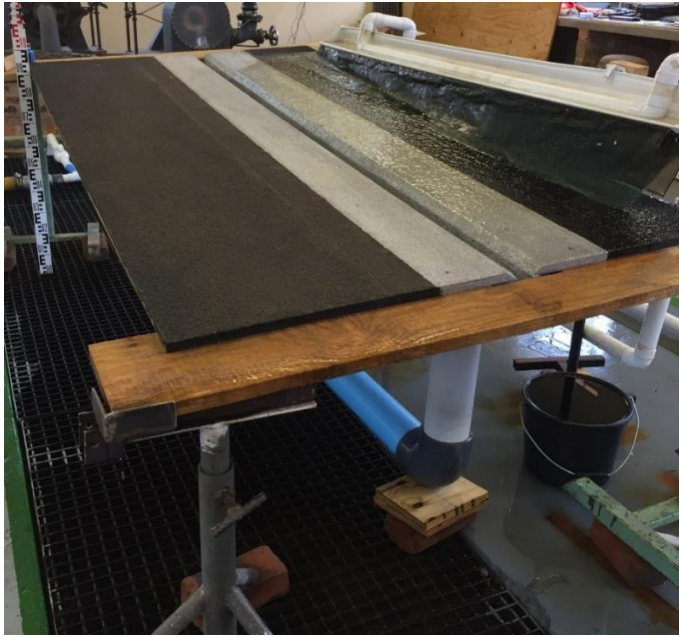


**Figure 3-24: Pavement model elevated at a specific slope configuration**



**Figure 3-25: Blue dye applied to indicate water flow path slope**

The following test conditions, summarised in Table 3-7, were implemented during the experimental methodology to examine the interception capabilities of the slotted inlets of the constructed models:

**Table 3-7: Test conditions**

<b>MODEL FEATURE</b>	<b>UNIT</b>	<b>TEST CONDITION</b>		
<b>Roadbed width</b>	<b>m</b>	0.5		
<b>Roadbed length</b>	<b>m</b>	2.44		
<b>Slotted drain length</b>	<b>m</b>	2.44		
<b>Slotted drain inlet widths</b>	<b>mm</b>	20	40	60
<b>Mean texture depth (MTD) of pavement surface</b>	<b>mm</b>	0.628		
<b>Longitudinal slope</b>	<b>%</b>	0-6		
<b>Cross slope</b>	<b>%</b>	1-6		
<b>Simulated flow type</b>	<b>-</b>	sheet flow		
<b>Approximate sheet flow supply capacity</b>	<b>l/s</b>	3.0		

The process of gathering informational data by following the experimental methodology described in this chapter will further be discussed and analysed in the following chapters.

## **4. DATA COLLECTION AND ANALYSIS OF RESULTS**

### **4.1 INTRODUCTION**

The data collection procedure followed during the experiment of this study is presented and discussed in this chapter. The effect of different slope elevations, slotted inlet widths and the installation conditions of slotted drains operating within a pavement structure in the field are compared, analysed and discussed. Consequently, valuable conclusions could be made regarding the interception efficiency of slotted drains operating under various conditions in the field.

### **4.2 TEST LIMITATIONS**

Several test limitations during the test procedures and data collection process have been identified. These include:

- Initially, two ultra-sonic flow meters were used for the data collection of the experiment, but unrealistic and imprecise flow measurements were recorded. Two volumetric flow meters were used instead which produced much more realistic test results.
- The amount of water applied on to the pavement models was limited to a maximum flow rate of approximately 3.0l/s. For flow rates higher than the test flow capacity, major water spillages occurred as the hydraulic capacity limit of the drainage system was reached.
- Interception efficiency tests were conducted for maximum longitudinal and cross slopes of six percent.
- Flow paths with calculated slopes lower than two percent were not tested to analyse the interception capabilities of the slotted drains, as a requirement for a minimum slope of a flow path should exceed two percent (SANRAL, 2013).
- Water depths were only recorded on the type I model with the 20mm inlet width and only for a zero longitudinal slope with varying cross slope test set ups. Once the longitudinal slopes were implemented to a test set up, the water catchment area was elevated in comparison with the test model to ensure that the sheet flow does not spill off the sides of the pavement models as the water flow path changed. Different flow depths were recorded over the width of a specifically applied sheet flow. It became challenging to measure these flow depths accurate, and this test procedure was discontinued.
- Once all the type I models were tested and observed that sheet flow was nearly 100% intercepted for all slot sizes, and slope configurations for the maximum applied sheet flow of the experiment. Only the smallest inlet size, the 20mm slot width, of the type II model was tested to determine whether the median barrier will influence the interception capabilities of the slotted drains.

### 4.3 SAND PATCH TEST RESULTS

Texture depths of the pavement surfaces were obtained by collecting sand patch test data from the six different constructed models, and the mean texture depth (MTD) data are summarised in Table 4-1. The calculated texture depth ranges between 0.585mm and 0.667mm and are presentative average texture depth is determined for six test models.

In Marriott & Jayaratne (2010) obtained from Webber (1971), an approximate relationship was related from the Colebrook White formula, between the absolute surface roughness,  $k_s$ , and the Manning's n coefficient. The Manning's n coefficient used in this study were determined accordingly by using the calculated average MTD of the pavement models surfaces in Equation 4-1.

**To calculate manning's coefficient using absolute surface roughness:**

$$n \approx \frac{k_s^{1/6}}{26} \quad \text{Equation 4-1}$$

Where:

n = Manning's coefficient (s/m<sup>1/3</sup>)

$k_s$  = absolute surface roughness ( $k_s$  = average MTD/1000), (m)

All calculations and conclusions in the study are made based on a pavement surface with an average texture depth of 0.628mm or a Manning's coefficient of 0.011s/m<sup>1/3</sup>.

**Table 4-1: Mean texture depth (MTD) results**

Model surfaces		Width (mm)	Length (mm)	Area (mm <sup>2</sup> )	Volume (mm <sup>3</sup> )	Mean texture depth, MTD (mm)
Type I model	20mm slotted width	500	750	375000	250000	0.667
	40mm slotted width	500	795	397500	250000	0.629
	60mm slotted width	500	805	402500	250000	0.621
Type II model	20mm slotted width	500	815	407500	250000	0.613
	40mm slotted width	500	765	382500	250000	0.654
	60mm slotted width	500	855	427500	250000	0.585
<b>Average mean texture depth (MTD) for the constructed model surfaces</b>						<b>0.628</b>

#### 4.4 INTERCEPTION EFFICIENCY TEST RESULTS

During the first series of tests, six slope combinations were tested for all type I models. Each slope combination was tested for five different applied sheet flows, and the complete records of the tests are presented in Appendix B. These tables provide the flow meter readings measured during each test for three, 180 second time intervals per applied sheet flow. The applied flow rates were measured with the flow meter at the water supply system (C) and intercepted flow rates were measured with the flow meter at the drainage system (L) of the test set up as explained previously. A simple calculation was done to determine the interception efficiency (%) of each test by dividing the intercepted flow rate (flow rate 2) by the applied flow rate (flow rate 1), also referred as Equation 2-9 in Chapter 2. Finally, an average applied flow rate, intercepted flow rate, and interception efficiency was determined for each test. These results for the three type I model tests are summarised in Table 4-2 to Table 4-4.

It was found that 98% to 100% of the applied sheet flow was intercepted by all the type I model inlets for all parameters tested. In other words, all the type I model inlets have the capability to intercept 98% to 100% of the sheet flow up to a capacity of approximately 3.0l/s for longitudinal and cross slopes up to six percent.

Due to the outcome of the first series of tests with all the test flow been intercepted, the second series of test was conducted but only the type II model with the 20mm slot width was tested. The same test parameters were implemented as for the type I models as explained and the obtained data is presented in Appendix B. The results of the type II model tests, summarised in Table 4-5, indicate that the outcome of these tests was similar to the type I models that have been tested.

It was found that the median barrier of the type II model did not have any effect on the interception capability of the inlet for the respective test parameters as all the sheet flow was intercepted without overflowing the inlet before the barrier could function. This outcome was expected to be the same for the other two type II models that were not tested.

**Table 4-2: Interception efficiency test results, Type I model with a 20mm slotted inlet width**

Slope configuration (%)		Average flow rates (l/s)		Interception efficiency (%)
Longitudinal slope	Cross slope	Applied flow	Intercepted flow	
0	2	0.650	0.644	99.15
		1.159	1.148	99.04
		1.881	1.856	98.62
		2.300	2.263	98.39
		2.922	2.872	98.29
0	4	0.420	0.419	99.56
		1.111	1.100	99.00
		1.559	1.546	99.17
		2.172	2.148	98.89
		2.987	2.952	98.82
0	6	0.617	0.613	99.40
		1.224	1.211	98.94
		1.611	1.594	98.97
		2.437	2.407	98.78
		2.993	2.950	98.58
2	6	0.570	0.567	99.35
		1.307	1.300	99.43
		1.907	1.887	98.93
		2.494	2.463	98.74
		2.970	2.917	98.19
4	6	0.691	0.685	99.20
		1.137	1.128	99.19
		1.633	1.617	98.98
		2.702	2.669	98.77
		3.002	2.961	98.64
6	6	0.698	0.693	99.20
		1.117	1.111	99.50
		1.802	1.789	99.28
		2.304	2.280	98.96
		3.011	2.961	98.34

**Table 4-3: Interception efficiency test results, Type I model with a 40mm slotted inlet width**

Slope configuration (%)		Average flow rates (l/s)		Interception efficiency (%)
Longitudinal slope	Cross slope	Applied flow	Intercepted flow	
0	2	0.841	0.837	99.56
		1.191	1.181	99.22
		1.861	1.839	98.81
		2.231	2.209	99.00
		2.959	2.930	99.00
0	4	0.700	0.694	99.21
		1.022	1.019	99.64
		1.330	1.317	99.06
		2.383	2.356	98.83
		3.009	2.989	99.32
0	6	0.900	0.893	99.18
		1.143	1.139	99.68
		1.687	1.681	99.67
		2.537	2.496	98.39
		3.063	3.006	98.13
2	6	0.793	0.789	99.53
		1.378	1.370	99.46
		1.915	1.893	98.84
		2.650	2.615	98.67
		3.080	3.020	98.08
4	6	0.830	0.824	99.33
		1.470	1.461	99.37
		2.006	1.985	98.98
		2.656	2.631	99.09
		2.987	2.959	99.07
6	6	0.719	0.715	99.49
		1.407	1.394	99.08
		1.985	1.954	98.41
		2.526	2.494	98.75
		2.974	2.933	98.63



**Table 4-4: Interception efficiency test results, Type I model with a 60mm slotted inlet width**

Slope configuration (%)		Average flow rates (l/s)		Interception efficiency (%)
Longitudinal slope	Cross slope	Applied flow	Intercepted flow	
0	2	0.806	0.800	99.31
		1.291	1.272	98.57
		1.533	1.519	99.03
		1.981	1.954	98.60
		2.946	2.891	98.11
0	4	0.778	0.772	99.29
		1.348	1.339	99.31
		1.735	1.715	98.83
		2.263	2.231	98.61
		3.078	3.024	98.26
0	6	0.963	0.959	99.62
		1.176	1.165	99.06
		1.637	1.615	98.64
		1.970	1.937	98.31
		2.893	2.843	98.27
2	6	0.807	0.802	99.31
		1.220	1.211	99.24
		1.546	1.528	98.80
		2.259	2.220	98.28
		2.967	2.941	99.13
4	6	0.639	0.633	99.13
		1.243	1.228	98.81
		1.389	1.372	98.80
		1.961	1.931	98.49
		3.070	3.013	98.13
6	6	0.637	0.631	99.13
		1.265	1.252	98.98
		1.517	1.504	99.15
		1.941	1.922	99.05
		3.046	2.989	98.12

**Table 4-5: Interception efficiency test results, Type II model with a 20mm slotted inlet width**

Slope configuration (%)		Average flow rates (l/s)		Interception efficiency (%)
Longitudinal slope	Cross slope	Applied flow	Intercepted flow	
0	2	0.656	0.652	99.44
		1.298	1.283	98.86
		1.739	1.715	98.62
		2.169	2.137	98.55
		3.037	2.993	98.54
0	4	0.531	0.526	98.96
		1.139	1.130	99.19
		1.743	1.724	98.94
		2.428	2.391	98.47
		3.024	2.972	98.29
0	6	0.578	0.576	99.68
		0.965	0.954	98.85
		1.674	1.652	98.67
		2.487	2.454	98.66
		2.965	2.920	98.50
2	6	0.715	0.709	99.22
		1.369	1.354	98.92
		1.930	1.896	98.27
		2.306	2.278	98.80
		3.002	2.967	98.83
4	6	0.756	0.750	99.27
		1.437	1.419	98.71
		1.830	1.806	98.68
		2.415	2.385	98.77
		3.026	2.987	98.72
6	6	0.624	0.619	99.11
		1.559	1.550	99.41
		1.898	1.883	99.22
		2.519	2.494	99.04
		2.972	2.933	98.69

To bring the experiment into perspective with real life pavement drainage scenarios, the sheet flow parameter was analysed to identify the typical rainfall intensities and water flow depths that occurred on different pavement widths in practice, for which the interception capabilities of the slotted inlets were tested during the experiment. The rational method (Equation 4-2) was implemented to determine different rainfall intensities for the applied sheet flow and other parameters tested. This relationship is

based on the law of conservation of mass with the assumption that the flow rate is directly proportional to the rainfall intensity and the contributing area of the catchment or water film (SANRAL, 2013) and is represented as follows:

**Rational method to calculate rainfall intensity:**

$$Q = \frac{C \cdot I \cdot A}{3.6} \quad \text{Equation 4-2}$$

Where:

- Q = peak flow (m<sup>3</sup>/s)
- C = run-off coefficient (C=1 for this study), (dimensionless),
- I = average rainfall intensity over a catchment (mm/hr)
- A = cross sectional area catchment/water film (A=L<sub>f</sub>/1000, slope of the flow path/m), (km<sup>2</sup>)
- 3.6 = conversion factor

In addition, the time of concentration, T<sub>c</sub>, which is defined as the required time for sheet flow with a uniform area to flow from the most distant point of a drainage area to the inlet of a catchment, were determined. The time of concentration (Equation 4-3) was used to determine the respective flow depths that will occur on the different pavement widths at the calculated rainfall intensities and were compared with the calculated flow depths obtaining from the RRL method (Equation 2-3), Gallaway method (Equation 2-4) and Manning's n method (Equation 2-5). The MTD and Manning coefficient determined during the sand patch test were used in the Gallaway and Manning's n method respectively to calculate these flow depths for pavements up to four carriageways taking that each carriageway is 3.6m wide.

**To calculate time of concentration, (SANRAL, 2013):**

$$T_c = 0.604 \left( \frac{r \cdot L}{\sqrt{S_{av}}} \right)^{0.467} \quad \text{Equation 4-3}$$

Where:

- T<sub>c</sub> = time of concentration (hours)
- r = roughness coefficient (0.02 for paved areas), (dimensionless)
- L = hydraulic length of catchment (length of the flow path), (km)
- S<sub>av</sub> = Slope of catchment (slope of the flow path), (m/m)

The results obtained during the process where the applied test sheet flows of the experiment were converted to actual rainfall intensities and flow depths that will occur on different pavements widths in practice are summarised in Appendix B.

From these tables, the rainfall intensities were plotted in Figure 4-1 against different water flow path lengths for the different applied sheet flows tested during the experiment. The flow path lengths which is a function of the pavement width and slope (cross and longitudinal), were determined from the slope configurations tested during the experiment but for different pavement widths in practice, by using Equation 2-1 and Equation 2-2.

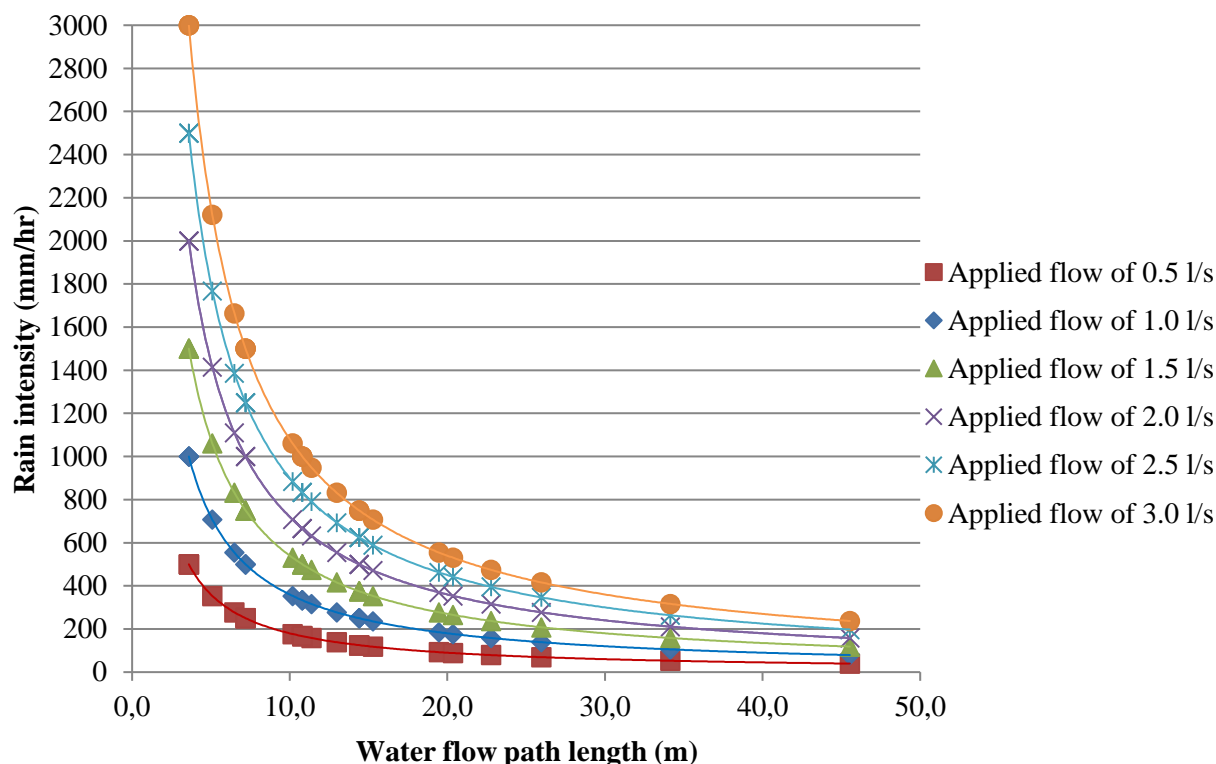


**Figure 4-1: Results of rainfall intensities and water flow path lengths - all applied test flows**

The graph illustrates that for the calculated flow paths between zero and 50m measured per meter flow width, typical rainfall intensities up to 3000mm/hr will occur on different pavement widths in practice for the applied sheet flows that were tested during the experiment. Also, from the interception tests results, the slotted inlets will intercept 98% to 100% of the sheet flow if long enough slotted drains are installed for these respective rainfall intensities.

The estimated flow depths per meter flow width that will occur on different pavement widths in practice, obtained from the different tested sheet flows during the experiment, are illustrated in Figure 4-2 to Figure 4-7. The calculated rainfall intensities occurred on different pavement widths, and slopes (Figure 4-1) were plotted against the estimated flow depths determined from the four methods mentioned above. The orange and red vertical lines represent the recommended maximum flow depth of 4mm for a 1:2 year storm (Oakden,1977) and maximum flow depth of 6mm for a 1:5 year storm on a pavement surface respectively (SANRAL, 2013), to prevent hydroplaning to occur.

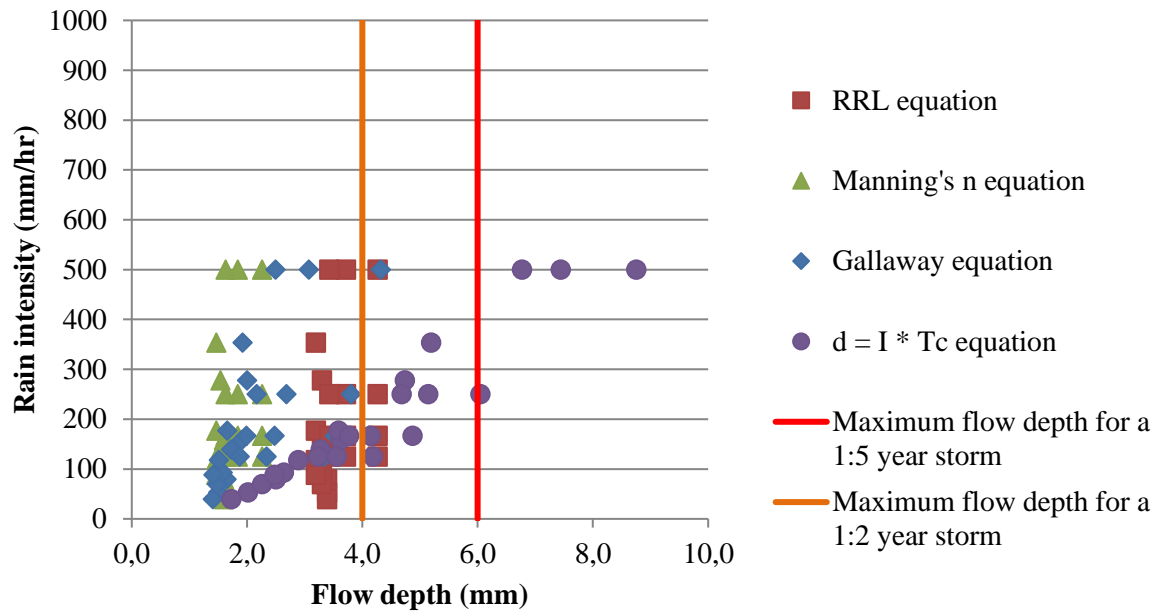


Figure 4-2: Rainfall intensities and flow depth results - 0.5l/s applied test flow

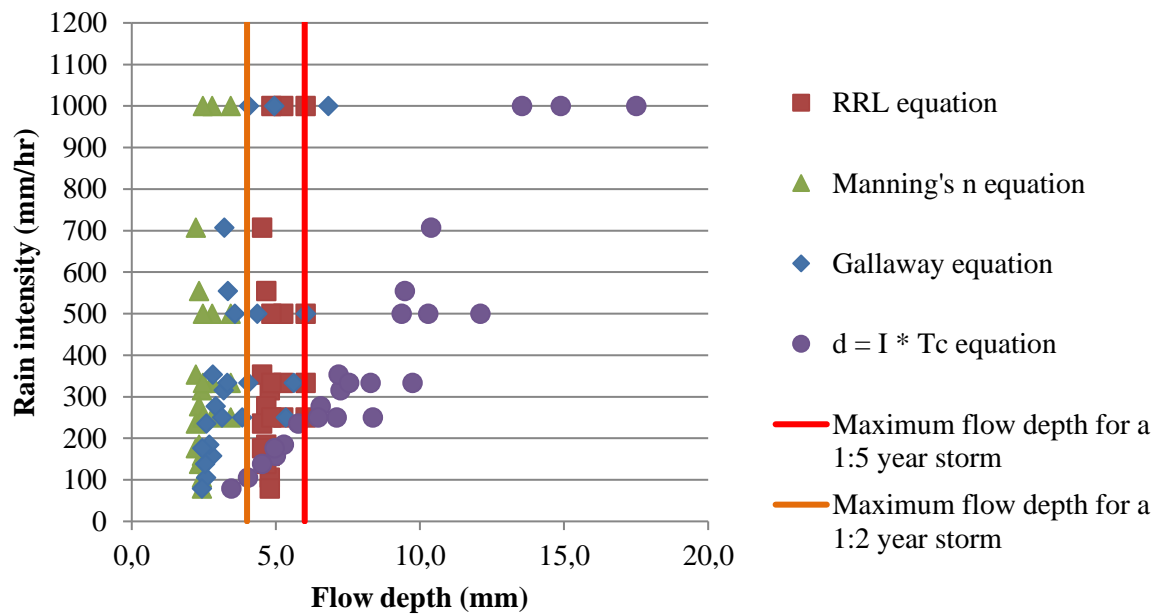


Figure 4-3: Rainfall intensities and flow depth results - 1.0l/s applied test flow

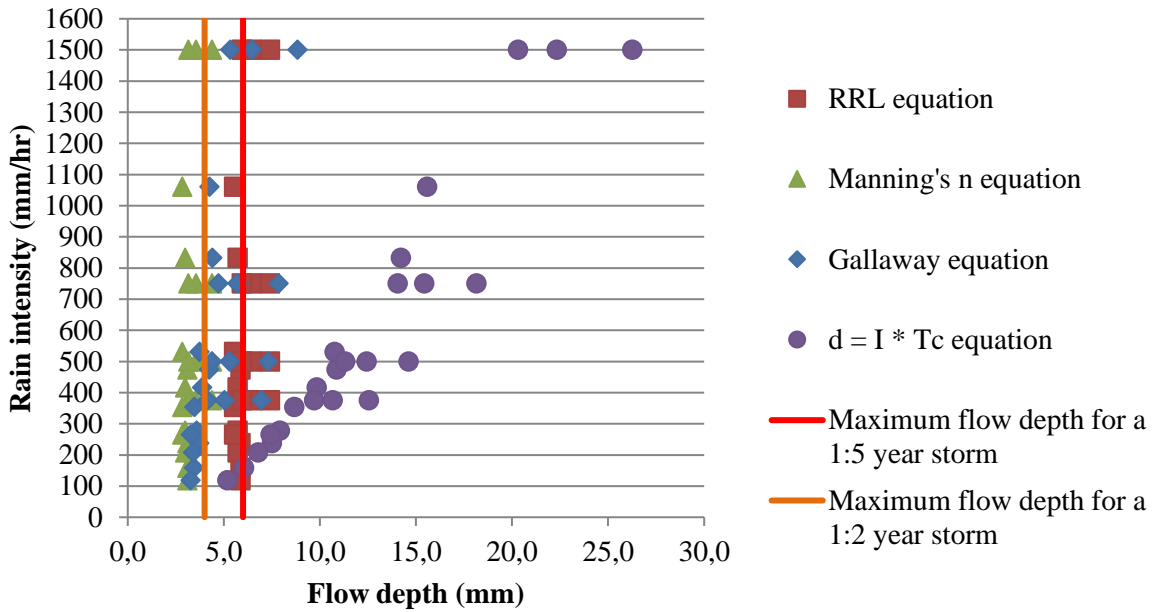


Figure 4-4: Rainfall intensities and flow depth results - 1.5l/s applied test flow

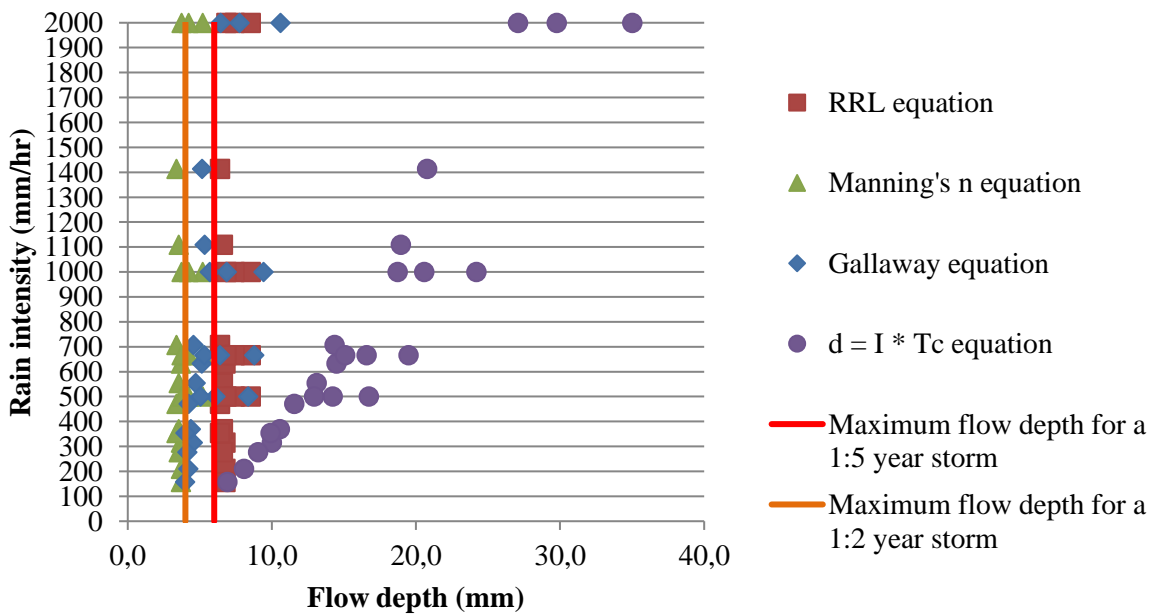


Figure 4-5: Rainfall intensities and flow depth results - 2.0l/s applied test flow

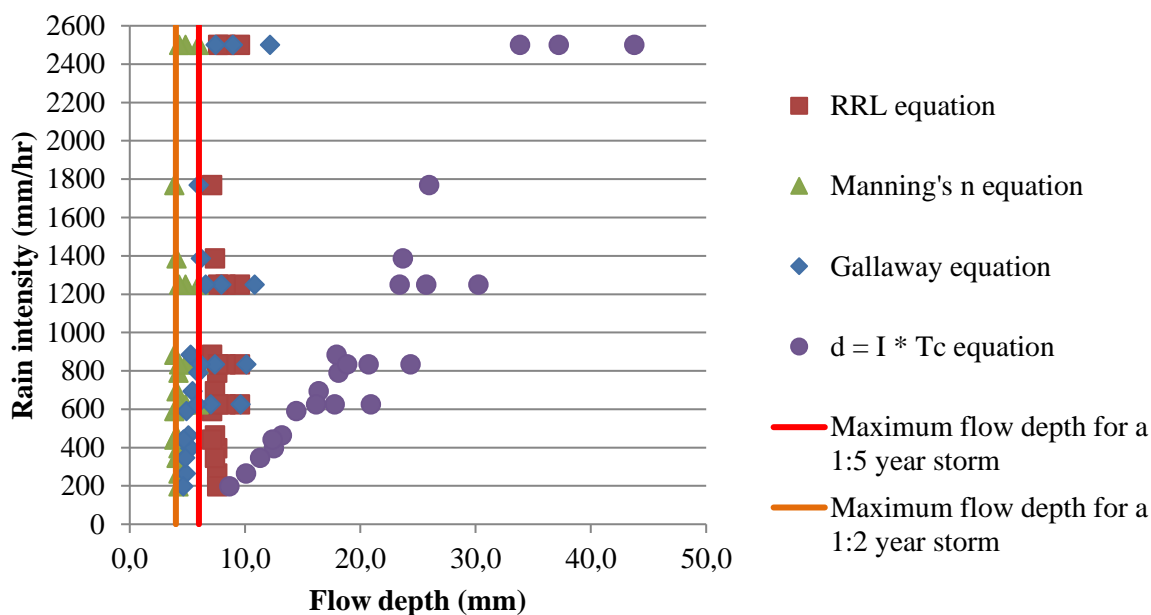


Figure 4-6: Rainfall intensities and flow depth results - 2.5l/s applied test flow

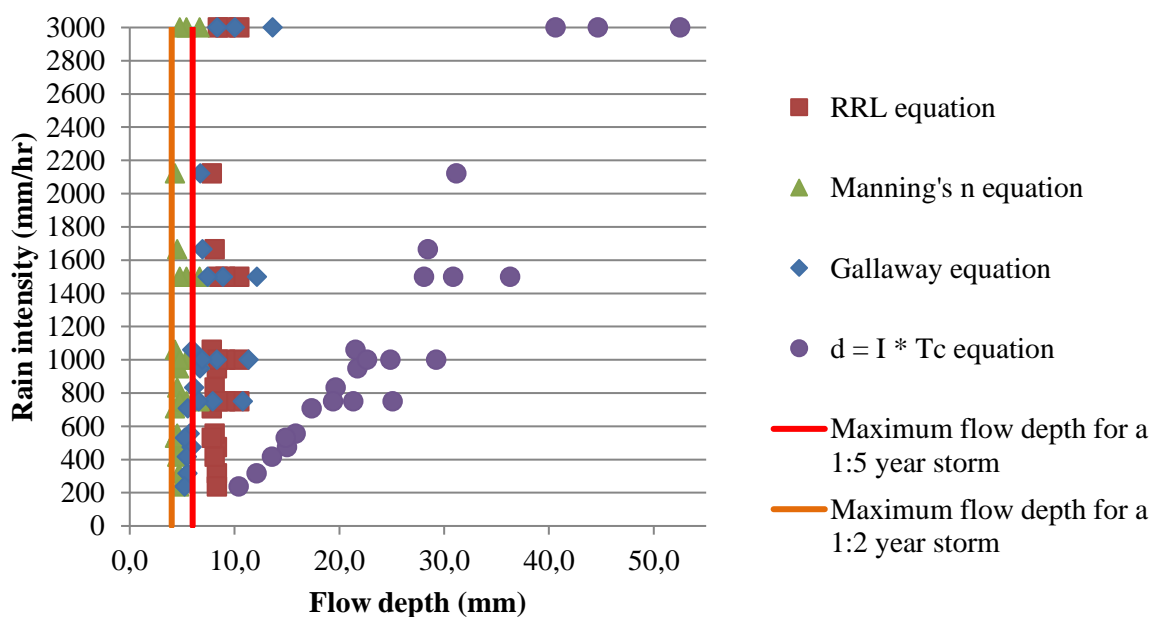


Figure 4-7: Rainfall intensities and flow depth results - 3.0l/s applied test flow

It is obvious to note from these graphs, comparing the four methods with each other, that the four equations provide different estimated flow depth values calculated from different rainfall intensities, pavement slopes and pavement widths. The method to determine the flow depth, using the time of concentration equation, provide unrealistic flow depths compared to the other flow depth estimating methods and thus were not considered for any conclusions made. It is important to note that the Manning's n equation does not take the pavement width or the length of the sheet flow path into

consideration to estimate the flow depth. Lower flow depths were estimated compared to the other methods.

In connection to the experiment and all the conditions tested, it is safe to say that all tested model inlets will intercept nearly 100% of the sheet flow for the different pavement widths and maximum estimated flow depths summarised in Table 4-6.

**Table 4-6: Maximum estimated flow depths**

Road width (m)	Maximum estimated flow depths (mm)		
	RRL method	Manning's n method	Gallaway method
3.6	10.5	6.7	13.6
7.2			12.1
10.8			11.3
14.4			10.8

For more clarity an example by referring to Figure 4-1, Figure 4-2 and Table B-26 are provided:

- On a pavement width of 3.6m with a cross and longitudinal slope creating a water flow path length of 3.6m per meter flow width, the following was determined:
  - For a tested sheet flow of 0.5l/s/m, a typical rainfall intensity of 500mm/hr was simulated.
  - The simulated rainfall intensity for this specific case can cause flow depths of up to 4.3mm per meter flow width, estimated by using the RRL and Gallaway method.
  - All tested model inlets will intercept almost 100% of the tested sheet flow for these simulated field conditions.

#### 4.5 WATER DEPTH MEASUREMENT RESULTS

Flow depth measurements were only taken for test set ups with longitudinal slopes at zero percent, as difficulties were experienced during the adjustment of the water catchment area. As previously mentioned, the water catchment area was adjusted during each slope configuration to ensure all the water that enters the pavement surface flow towards the model inlets without overflowing the side of the model. Special attention was required with the longitudinal slope adjustments where the catchment area was adjusted in such a manner that the water enters the most elevated part of the model surface. This ensured that no water spilt off the sides of the pavement model when the sheet flow was flowing down the slope towards the model inlets. This affected the flow depth and spread of sheet flow on the model surface drastically and making it almost impossible to measure accurate and constant flow



depths. Due to the flow depth variations measured during the first model tests regardless of the zero longitudinal slope set, flow depth measurement was not conducted for the remaining tests as planned.

The water depth measurements that were taken during the first model test of the experiment is summarised in Table 4-7. This table includes the flow depths obtained from different applied flow rates and slope configurations at the three measuring positions across the width of the sheet flow on the pavement model surface. Average flow depths were determined from the three depth measurements that were taken per test set up and applied sheet flow.

**Table 4-7: Flow depth measurement results - Type I model with 20mm slot inlet width**

Average applied flow rate (l/s)	Pavement cross fall (%)	Pavement gradient (%)	Pavement model width (m)	Length of flow path (m)	Slope of flow path (m)	Measured water depth (mm)			
	n <sub>1</sub>	n <sub>2</sub>	w	l <sub>f</sub>	S <sub>f</sub>	Left	Mid	Right	Ave
<b>0.650</b>	2	0	0.4	0.4	2	2.1	1.7	1.4	<b>1.7</b>
<b>1.159</b>						2.4	3.4	1.9	<b>2.6</b>
<b>1.881</b>						3.1	4.2	2.4	<b>3.2</b>
<b>2.300</b>						5.4	3.2	4.5	<b>4.4</b>
<b>2.922</b>						5.8	4.8	4.3	<b>5.0</b>
<b>0.420</b>	4	0	0.4	0.4	4	2.0	1.5	1.1	<b>1.5</b>
<b>1.111</b>						2.5	2.1	1.7	<b>2.1</b>
<b>1.559</b>						2.7	3.1	2.5	<b>2.8</b>
<b>2.172</b>						3.6	2.9	3.5	<b>3.3</b>
<b>2.987</b>						4.5	5.2	3.7	<b>4.5</b>
<b>0.617</b>	6	0	0.4	0.4	6	1.7	1.5	0.9	<b>1.4</b>
<b>1.224</b>						2.0	1.8	1.3	<b>1.7</b>
<b>1.611</b>						3.1	2.1	1.8	<b>2.3</b>
<b>2.437</b>						2.4	2.6	3.1	<b>2.7</b>
<b>2.993</b>						3.5	3.9	3.4	<b>3.6</b>

From these results, it is noticeable that different flow depths were measured across the width of any particular sheet flow, which means that the sheet flow entered some portions of the slotted inlets partially more than other parts of the inlets. This occurrence did not affect the interception efficiencies results of the tested model inlets as almost all the sheet flow was intercepted, refer to Table 4-3. The

average flow depths obtained from the respective these measurements also confirmed the findings in the literature of Chaithoo and Allopi (2012), which include that:

- The water flow depth increases as the applied test sheet flow increases for the specific test set up;
- The water flow depth decreases as the cross slope increases for constant applied sheet flow.

No judgement could be made regarding the effect that different longitudinal slopes will have on the water depths on the pavement model surfaces as this parameter was kept constant during the flow depth measurements.

#### 4.6 GENERAL OBSERVATIONS

Throughout the experiment, controlled supervision and general observation were required to confirm that all the flow measurements that were obtained are logical and accurate. Similar observations were recorded between the type I and type II models being tested regardless of the slotted inlet sizes or slope configurations. These observations were photographed and are depicted in Figure 4-8 and Figure 4-9 respectively. For all applied sheet flow up to its test capacity of approximately 3.0l/s, the following was noticeable:

- All the test models with different inlets sizes and slope configurations have intercepted all the sheet flow with no water overflowing the slot inlets.
- The sheet flow applied to a specific test model has entered the slotted inlets at different flow depths in the width of the inlet. The effect of sheet flow entering the slotted inlets at different partial flow depths has not affected the interception capabilities of all the tested models;
- The chamfered inlets allowed the sheet flow to flow smoothly over the edge of the inlets into the drainage system without any water spilling to the opposite side of the pavement model.
- Hardly any splash and spray were noticed during the experiment for all inlets tested;



**Figure 4-8: Almost 100% sheet flow interception observed for all applied sheet flow**



**Figure 4-9: Intercepted sheet flow captured in drainage system**

In addition, for the type I model with the 20mm slotted inlet, a cross slope set to six percent and longitudinal slope of zero percent, the bypass valve (B) was closed, and applied flow of 5.24l/s was recorded. Even in this extreme case, it was observed that the 20mm slotted inlet intercepted all the applied sheet flow.

#### **4.7 COMPARISON WITH PREVIOUS STUDIES**

The operation of the pavement model and the experimental set up was conducted based on the guidance and test procedures of individual studies completed by Burgi et. al. (1977), Pugh (1980), Gouws (1993) and Comport et. al. (2009). The test conditions implemented during the experiment and the results obtained, compared closely to the other tests conducted in previous studies and include the following:

- Pugh (1980) and Masch (1978) stated in Pugh (1980), also applied sand and paint to their pavement model surfaces and obtained similar pavement roughness's with Manning's  $n$  values of  $0.015\text{s/m}^{1/3}$  to  $0.016\text{s/m}^{1/3}$  and  $0.011\text{s/m}^{1/3}$  to  $0.012\text{s/m}^{1/3}$  respectively. Comport et. al. (2009) created a model street section with an average manning's roughness of  $0.015\text{ s/m}^{1/3}$  in their study. In this study, an average pavement roughness of  $0.011\text{s/m}^{1/3}$  was calculated.
- For all slope tested, Pugh (1980) have recorded that nearly all sheet flow was intercepted by slotted inlets with 25.4mm, 44.45mm and 63.5mm slot sizes, but for a much smaller flow capacity of only 0.345l/s per meter flow width. A design discharge of 0.216l/s per meter falls entirely through the slotted inlets without overflowing the slots. In this study, a flow capacity of approximately 3.0l/s (1.5l/s per meter) was applied, and nearly 100% of this sheet flow was intercepted by the inlets for all parameters tested.
- Slotted drains consist of a continuous open inlet as in this study, caused almost no splash and spray compared to other inlets designs tested in previous studies. Inlets spaced with transverse bars

(Gouws, 1993) and Pugh (1980) caused a relative amount of upwards spray to develop when sheet flow entered the inlets at steep slopes. However, slotted inlets inclined at 45° can prevent water from spraying upwards as sheet flow can approach inlet more smoothly (Gouws, 1993).

- The maximum flow depth of 14.2mm was recorded at steep slopes from a previous study of Pugh (1980) with a small amount of splash from the transverse inlet spacers. According to the calculation of the prediction methods in this study, a maximum flow depth of 6.7mm (RRL method), 10.5mm (Manning's n method) and 13.6mm (Galloway method) per meter flow width, was simulated during the experiment for the applied sheet flows that can develop in practice. Almost no upwards spray occurred at the model inlets during the experiment.
- No comparisons could be drawn regarding the operation of the concrete barrier compared to curb inlets in other studies as all the sheet flow was intercepted before the barrier could be in operation.

## 5. CONCLUSIONS AND RECOMMENDATIONS

In this chapter, the conclusions and recommendations made during the evaluation of the interception drainage capabilities of slotted drains operating in practice are discussed. All the findings and conclusions that were made is based on the interception drainage capability of a proprietary slotted drain design and are presented in the following two sections respectively:

### 5.1 CONCLUSIONS

The data collected, and the analysis performed during the experiment of the study provide informative findings on the performance of slotted drains as surface drainage systems operating within South African pavements. The uncertainties arose to implement slotted drainage system in the SANRAL project and in practice, as stated in Chapter 1, are also discussed based on the outcome of the research project.

A full-scale undistorted pavement model with slotted inlets tested during the experiment, provide valuable test results for conclusions to be drawn on the interception drainage capabilities of slotted drains, based on the following field conditions tested:

- Salberg Concrete Products (Pty) Ltd slotted drain design with inlet sizes (widths) of 20mm, 40mm and 60mm respectively;
- Pavement surfaces with approximate mean texture depths (MTD) of 0.628mm or a Manning's coefficient of  $0.011\text{s/m}^{1/3}$ ;
- Pavement slopes, including longitudinal slopes and cross slopes, varying between a minimum of zero percent and a maximum of six percent;
- Slotted drains operating individually and operating with a medium concrete barrier placed along its longitudinal length;
- Simulated rainfall intensities up to 3000mm/hr calculated per meter flow width for pavement widths of 3.6m, 7.2m, 10.8m and 14.4m in practice;
- Simulated flow depths up to 6.7mm (RRL method), 10.5mm (Manning's n method) and 13.6mm (Galloway method) calculated per meter flow width by utilising tests parameters in the respective prediction models.

The following conclusions were drawn regarding the interception drainage capabilities of the slotted drains being evaluated during this study:

- All tested slotted inlets with individual slot widths of 20mm, 40mm and 60mm effectively intercepted nearly 100% of the sheet flow tested with a flow capacity of approximately 3.0l/s ( $0.003\text{m}^3/\text{s}$ ) for

longitudinal and cross slopes up to six percent, regardless of operating with or without an adjacent barrier. Thus, for the sheet flow capacity tested, the size of the slotted inlet being tested had no effect on the interception efficiency of the inlet as all the sheet flow were nearly intercepted.

- Comparing the performance of slotted inlets of the constructed pavement model during the experiment to other model studies in the literature, a similar outcome was reported. Pugh (1980) have recorded that nearly all sheet flow was intercepted by slotted inlets for a flow capacity of only 0.345l/s per meter flow width.
- The effect of sheet flow entering the slotted inlets at different flow depths did not affect the interception capabilities of all the inlets tested during the experiment.
- Almost no upwards spray was recorded during the experiment as the sheet flow approached the inclined inlets smoothly and fell entirely into the continuous open inlet without any transverse spacers causing an upwards spray.
- The simulation of placing a concrete median barrier along the longitudinal length of the slotted inlets during the experiment, did not affect the interception capabilities of the inlets as all the sheet flow was intercepted before the barrier could be in operation.
- It was found that almost all the surface water will be intercepted by the slotted drains operating individually without a median barrier on pavement surfaces with similar field conditions been tested and therefore the most cost-effective installation of the slotted drains will be without a median barrier. The median barrier, however, can be installed alongside a slotted drain in practice to promote safer driving conditions. A median barrier can prevent splash and spray risks for passing vehicles by blocking all the clouds of spray caused by surface water accumulated under a vehicle's tyres. The water droplets that get trapped against the barrier can then flow down the barrier and be intercepted by the slotted inlets.
- Depending on the width of the pavement that influences the flow path length of surface water, calculations showed that the sheet flow applied on the pavement models during the experiment simulates rainfall intensities up to 3000mm/hr in the field. All slotted inlets tested under these selected pavement conditions during the experiment will sufficiently intercept almost 100 % of these sheet flow water in practice if long enough slotted drains are installed.
- According to the prediction methods to calculate water film depths on pavement surfaces from the experimental test conditions (RRL method, Gallaway method and Manning's n method), it was determined that flow depths higher than the 6mm recommended by SANRAL (2013) as the maximum flow depth in a 1:5 year storm to prevent any safety risks, were simulated during the experiment. All slotted inlets tested during the experiment will sufficiently remove nearly 100% of the surface water for all these simulated flow depths during a storm in the field.

- The installation of the slotted drains in the middle of the existing pavement and in areas within minimum traffic exposure to the drain itself is concluded to be a safe and efficient method to remove surface water on wider pavements in South Africa with similar pavement conditions being tested as all the sheet flow were nearly intercepted.

## 5.2 RECOMMENDATIONS

As in most research studies, further work is required in this field of study. Recommendations were made as useful guidance for future studies on this specific topic.

The actual testing and observation of slotted drains operating within a pavement with specific geometric designs and under actual field conditions in practice will serve the best to verify the soundness of experimental results. In real life pavement situations, travelling vehicles can cause small successive surface flow waves that influence the speed and depth of the approaching sheet flow on a pavement surface as well as splash and spray to occur. The effect of splash and spray is complicated to simulate during experimental procedures to draw any accurate conclusions regarding the benefit of slotted drains operating with an adjacent concrete barrier in practice.

Another investigation to consider for future research of the interception drainage capabilities of slotted drains is to determine the minimum slot width required to intercept 100% of sheet flow under various pavement conditions. Narrow slot widths are more susceptible to clogging than wider slot widths, but this can benefit manufactures to develop optimum slotted drain design that will intercept surface water efficiently with minimal manufacturing costs.

The construction of a more powerful and portable model structure can improve the testing conditions that are less time-consuming during measurements, calibrations and different model set ups. Using one universal testing facility rather than different individual models for experimenting will emphasise simplicity and the ease of operation to complete more tests in a reasonable amount of time. This will allow the testing of different test parameters in greater detail, for example, higher pavement slopes, higher sheet flow rates, different slotted drain design, different pavement surface texture (concrete pavement, seals etc.).

Consequently, this will possibly result in more presentable experimental data to develop comprehensive mathematical formulae describing the interception drainage capabilities (efficiencies) of slotted inlets by utilising all dependent testing parameters as input variables per specific drain design.

## 6. REFERENCES

American Society of State Highway and Transportation Officials. 2011. *A Policy on Geometric Design of Streets and Highways*. 6<sup>th</sup> ed. Washington DC, United States of America. ISBN: 978-1-56051-508-1.

Anderson, D.A., Huebner, R.S., Reed, J.R., Warner, J.C. & Henry, J.J. 1998. *Improved Surface Drainage of Pavements*. National Cooperative Highway Research Program (NCHRP) Web Document 16 (Project 1-29). Pennsylvania Transportation Institute.

Brown, S.A., Schall, J.D., Morris, J.L., Doherty, C.L., Stein, S.M. & Warner, J.C. 2009. *Hydraulic Engineering Circular (HEC) No. 22 Urban Drainage Manual*. 3<sup>rd</sup> ed. Publication No. FHWA/NHI-10-009. Federal Highway Administration, Department of Transportation. United States of America.

Burgi, P.H. & Gober, D.E. 1977. *Bicycle-Safe Grate Inlets Study, Volume 1-Hydraulic and Safety Characteristics of Selected Grate Inlets on Continuous Grades*. Federal Highway Administration, Report No. FHWA-RD-77-24. U.S. Department of Interior, Bureau of Reclamation. Denver, Colorado.

Chesterton, J., Nancekivell, N. & Tunnicliffe, N. 2006. *The Use of the Gallaway Formula for Aquaplaning Evaluation in New Zealand*. Transit New Zealand and New Zealand Institute of Highway Technology (NZIHT) 8th Annual Conference.

Committee of State Road Authorities, 1984. *Technical Methods for Highways 6 (TMH6) – Special methods for testing roads*. The Department of Transport. Pretoria, South Africa

Committee of State Road Authorities, 1988. *Technical Recommendation of Highways 17 (TRH17) – Geometric Design of Rural Roads*. Division of Roads and Transport Technology, CSIR. Pretoria, South Africa.

Comport, B.C., Thornton, C.I. & Cox, A.L. 2009. *Hydraulic Efficiency of Grate and Curb Inlets for Urban Storm Drainage*. American Society of Civil Engineers. Colorado State University.

Comport, B.C. & Thornton, C.I. 2012. *Hydraulic Efficiency of Grate and Curb Inlets for Urban Storm Drainage*. Journal of Hydraulic Engineering. DOI: 10.1061/ (ASCE) HY.1943-7900.0000552.



Contech Engineered Solutions, 2017. 'Slotted drains drainage products'. Available: <http://www.conteches.com/products/pipe/corrugated-metal-cmp/slotted-drain.aspx> [Accessed: 22 June 2017].

Contech Engineered Solutions, 2018. 'Dallas IH30 Roadway Improvements'. Available: <http://www.conteches.com/KnowledgeCenter/CaseStudies/CaseStudyDetails?articleId=1408> [Accessed: 15 May 2018].

Contech Engineered Solutions, 2018. 'The Ridge at Lookout Mountain'. Available: <http://www.conteches.com/KnowledgeCenter/CaseStudies/CaseStudyDetails?articleId=1400> [Accessed: 14 May 2018].

Chaithoo, D.B. & Allopi, D.R. 2012. *A Software Tool Approach to Re-evaluating Superelevation in Relation to Drainage Requirements and Vehicle Dynamics—a Case Study*. South African Transport Conference (SATC). 9-12 July 2012.

Chaudhry, M. H. 2007. *Open Channel Flow*. 2<sup>nd</sup> ed. Springer Science and Business Media. New York, USA. ISBN 978-0-387-30174-7.

Dawson, A. 2008. *Water in Road Structures Movement, Drainage and Effects*. Nottingham Transportation Engineering Centre. University of Nottingham, UK. DOI 10.1007/978-1-4020-8562-8.

Engman, E.T. 1986. *Roughness coefficients for routing surface runoff*. Journal of Irrigation and Drainage Engineering 112 (1). American Association of Civil Engineering. New York, USA. pp. 39–53.

Gallaway, B.M., Ivey, D.L., Ross Jr, H.E., Ledbetter, W.B., Woods, D.L. & Schiller Jr, R.E. 1975. *Tentative Pavement and Geometric Design Criteria for Minimizing Hydroplaning*. Federal Highway Administration, Report no. FHWA-RD-75-11. Texas Transportation Institute, Texas A&M University. College station, Texas.

Gallaway, B.M., Schiller Jr, R.E. & Rose, J.G. 1971. *The Effects of Rainfall Intensity, Pavement Cross Slope, Surface Texture, and Drainage Length on Pavement Water Depths*. Federal Highway Administration, Report no.138-5. Texas Transportation Institute, Texas A&M University. College station, Texas.

Gallaway, B.M., Ivey, D.L., Hayes, G., Ledbetter, W.B., Olson, R.M., Woods, D.L. & Schiller Jr, R.E. 1979. *Pavement and Geometric Design Criteria for Minimizing Hydroplaning*. Federal Highway Administration, Report No. FHWARD-79-31. Texas Transportation Institute, Texas A & M University. College station, Texas.

Gouws, C. H. 1993. 'Hydraulic Design of the Proposed Median Drainage System for National Route N17'. Unpublished Report. Stewart Scott Inc. Toll highway development co. (Pty) Ltd. Van Wyk and Louw. ROCLA.

Heller, V. 2011. *Scale Effects in Physical Hydraulic Engineering Models*. Journal of Hydraulic Research 49:3, 293-306. DOI: 10.1080/00221686.2011.578914.

Izzard, C. F. 1946. *Hydraulics of Runoff from Developed Surfaces*. Highway Research Board (HRB) Proc., Vol. 26.

Ken Bohuslav, P.E. 2004. *Hydraulic Design Manual*. Texas Department of Transportation (TxDOT) Texas.

Masch, F. D. 1978. *Limited Capacity Studies on Armco Slotted Drain Pipes*. Reported for Armco Steel Corporation.

Marriott, M.J. & Jayaratne, R. 2010. *Hydraulic roughness – links between Manning's coefficient, Nikuradse's equivalent sand roughness and bed grain size*. Proceedings of Advances in Computing and Technology, (AC & T). The School of Computing and Technology 5th Annual Conference. University of East London, pp. 27-32.

National Association of Australian State Road Authorities (NAASRA). 1974. *Drainage of Wide Flat Pavements*. Sydney, Australia.

New Zealand Transport Agency, 2014. *Preferred Method for Calculating Road Surface Water Run-off in New Zealand*. Technical Memorandum: Road Design Series. TM-2505 (01/2014).

Oakden, G.J. 1977. *Highway Surface Drainage, Design Guide for highways with a positive collection system*. Ministry of works and development. New Zealand.

Pugh, C.A. 1980. *Bicycle-Safe Grate Inlets Study, Volume 4 – Hydraulic Characteristics of Slotted Drain Inlets*. Federal Highway Administration, Report No. FHWA-RD-79-106. U.S. Department of Interior, Bureau of Reclamation. Denver, Colorado.

Pugh, C.A. 1980. *Bicycle-Safe Grate Inlets Study, Volume 5 – Hydraulic Design of General Slotted Drain Inlets*. Federal Highway Administration, Report No. FHWA-RD-80-081. U.S. Department of Interior, Water and Power Resources Service. Denver, Colorado.

Pumps for Africa, 2017. ‘Submersible sewage and Dirty water dumps’. Available: <http://pumpsforafrica.co.za/ht-v2200f-pump.html> [Accessed: 12 September 2017].

Road Traffic Management Corporation (RTMC). 2018. *Road Fatality Report for 2017*. Centurion, South Africa.

Rungruangvirojn P & Kanitpong K. 2010. *Measurement of Visibility Loss due to Splash and Spray: Porous, SMA and Conventional Asphalt Pavements*. International Journal of Pavement Engineering. Vol. 11, No. 6, December 2010, 499–510.

Russam, K. & Ross, N.F. 1968. *The Depth of Rain Water on Road Surfaces*. Road Research Laboratory, Ministry of Transport Report No. LR 23625pp.

Sample, D. & Doumar, L. 2013. *Best Management Practice Fact Sheet 7: Permeable Pavements*. Virginia Cooperation Extension, Publication 426-126. Virginia State University.

Sensus, 2018. ‘IPERL (International) water meters’. Available: <https://sensus.com/products/iperl-international/> [Accessed: 11 April 2018].

South African National Roads Agency Limited (SANRAL). 2002. *Geometric Design Guidelines*. Council for Scientific and Industrial Research (CSIR). Pretoria, South Africa.

South African National Roads Agency Limited (SANRAL). 2013. *Drainage Manual*. 6<sup>th</sup> edition. Pretoria, South Africa. ISBN 978-0-620-55428-2.

South African National Roads Agency Limited (SANRAL). 2014. *South African Pavement Engineering Manual (SAPEM)*. 2<sup>nd</sup> edition. Pretoria, South Africa. ISBN 978-1-920611-00-2.

Stanton Bonna, 2012. 'Slotted drain benefits'. Available:

<https://www.stanton-bonna.co.uk/drainage-systems/slot-drains/> [Accessed: 27 May 2018].

Te Chow, V. 1959. *Open Channel Hydraulics*. McGraw-Hill Book Company, Inc. New York, USA.

Webber, N.B. 1971. *Fluid Mechanics for Civil Engineers*. S.I. edition. CRC pressbook. London, New York. ISBN 9780412106002

Yu, U.S. & McNown, J.S. 1963. *Runoff from Impervious Surfaces*. Contract Report No. 2-66. U. S. Army Engineer Waterways Experiment Station, Corps of Engineers.

## A. APPENDIX A

The flow depth ( $d$ ) on the pavement surface during rain pour with a specific rainfall intensity ( $I$ ), can graphically be determined with the nomograph in Chart 1. If the cross slope ( $n_1$ ), gradient ( $n_2$ ) and the width ( $W$ ) of the pavement are known, the water flow path slope ( $S_f$ ) and water flow path length ( $l_f$ ) can easily be determined with Equation 2-1 and Equation 2-2 respectively. Consequently, the water flow depth ( $d$ ) can be read directly off the chart by connecting the intercepted lines of the known variables, starting in the upper right-hand quadrant of the chart and moving counter clockwise.

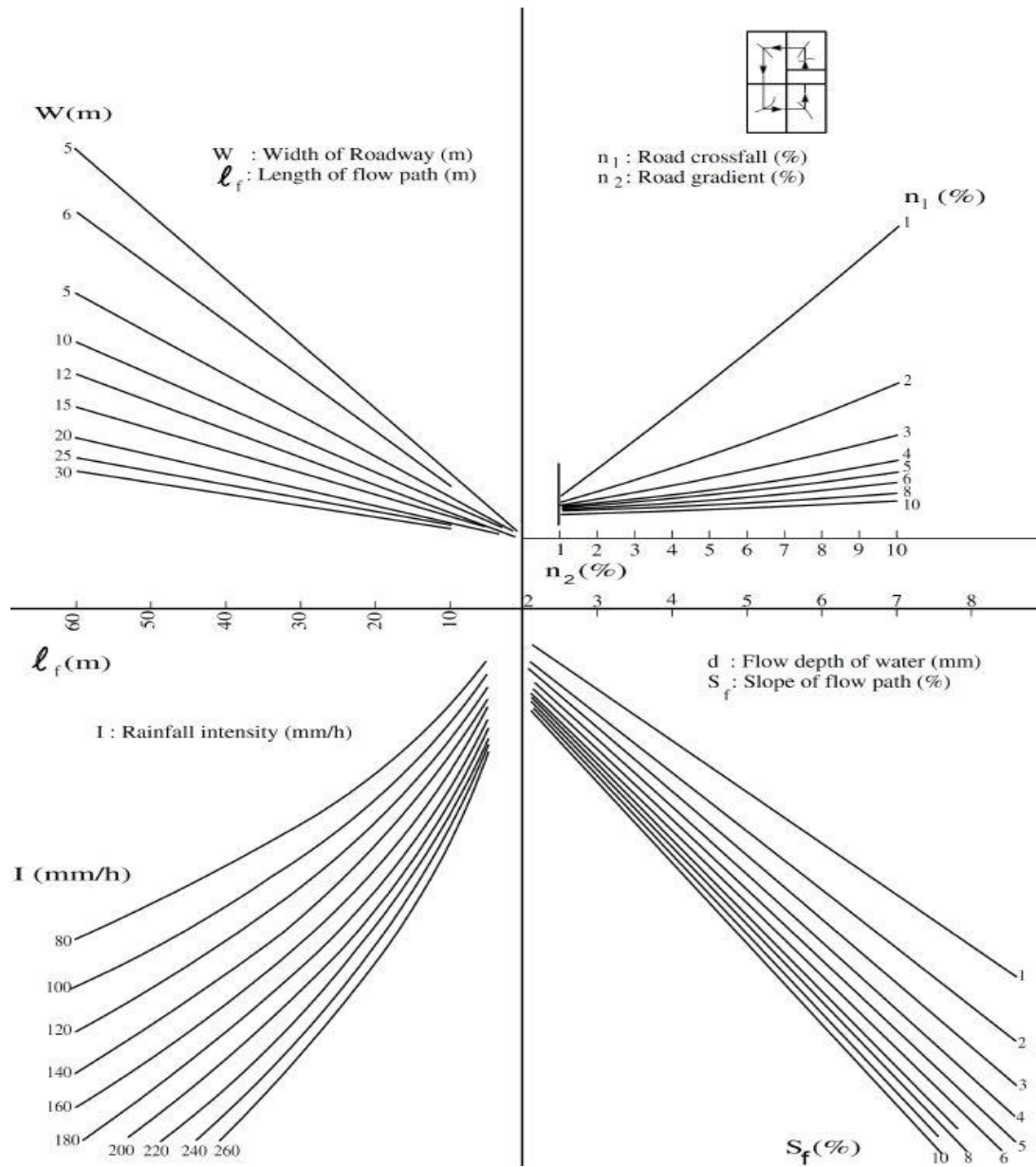


Chart 1: Depth of sheet flow on a road surface (SANRAL, 2013)

Chart 2 can be used to obtain the optimum slotted drain inlet length for a 100% flow interception. For any given combination of water flow (Q), longitudinal slope (S), cross slope (S<sub>x</sub>) and Manning's roughness coefficient (n), the optimum slotted inlet length (L<sub>T</sub>) can graphically be determined from the chart below. An example is provided on the chart to illustrate how the optimum slotted drain length can be obtained with different input parameters.

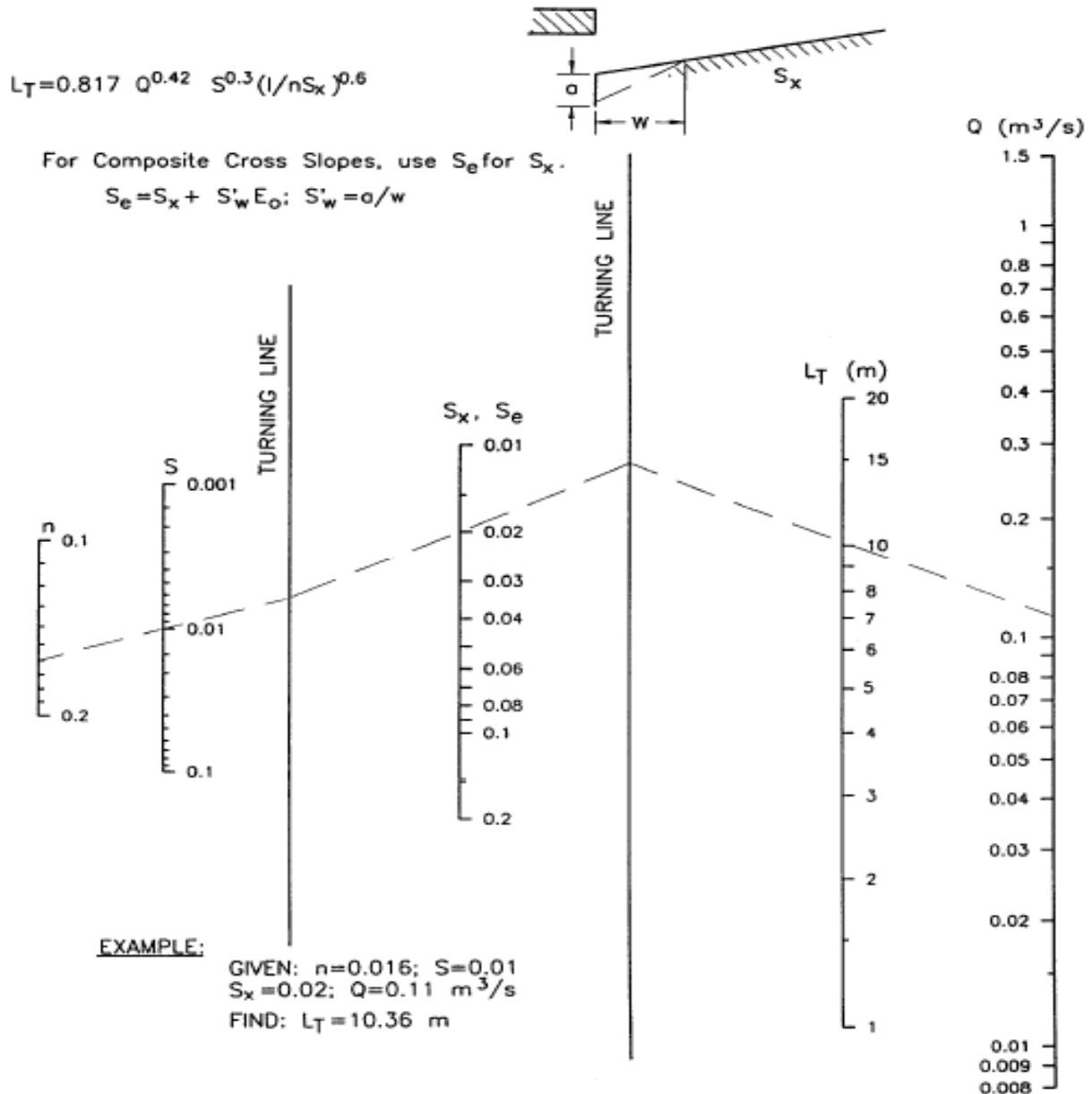


Chart 2: Slotted drain inlet length for total interception (Brown et al., 2009)

The interception efficiency of a slotted drain inlet can be determined with Equation 2-15 or graphically from Chart 3. For any relationship between the slotted inlet length to intercept 100% of the gutter flow ( $L_T$ ) and the slotted drain inlet length ( $L$ ), expressed as  $(L/L_T)$ , the efficiency of the slotted drain can be obtained from the chart.

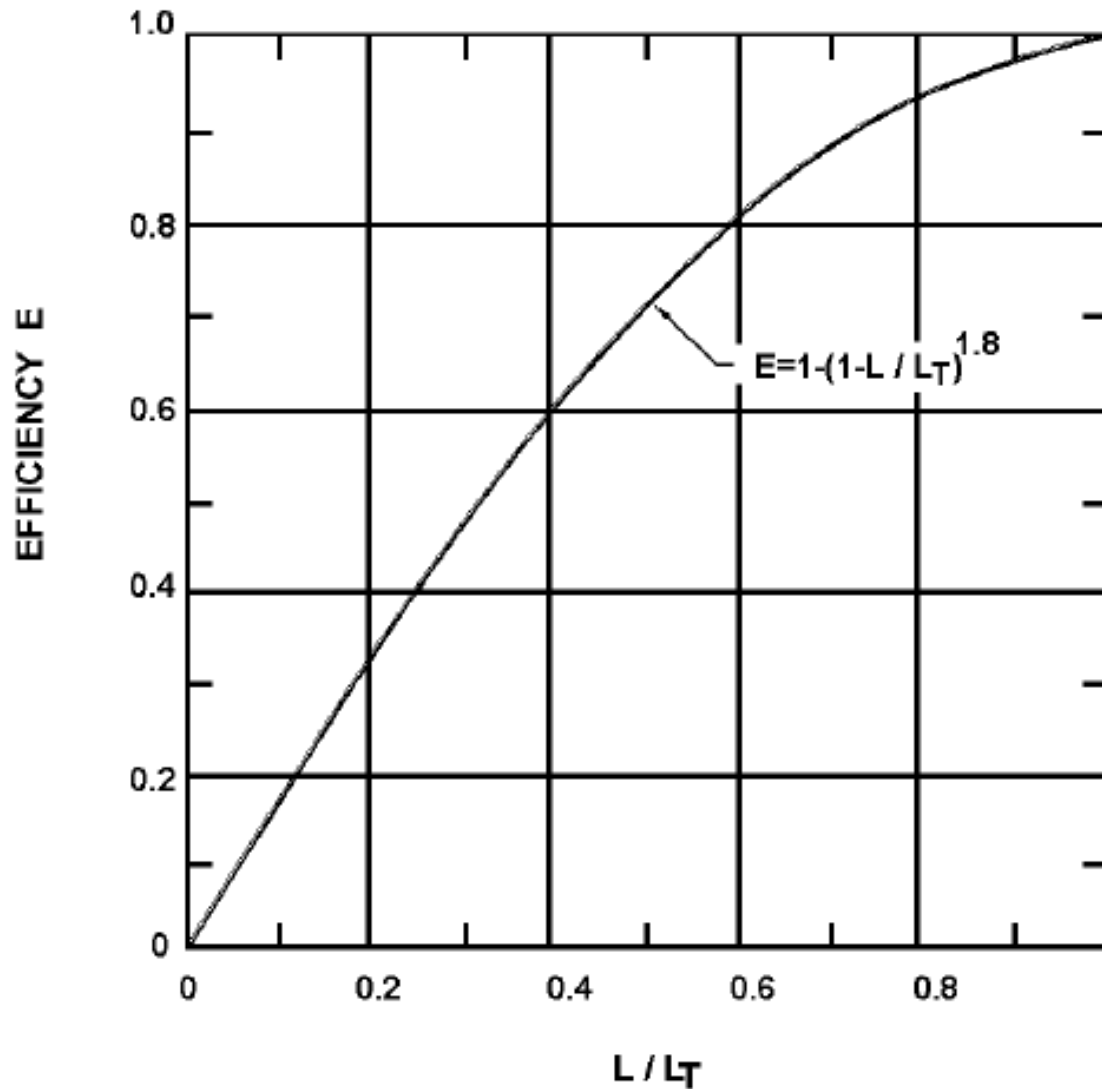


Chart 3: Slotted drain inlet interception efficiency (Brown et al., 2009)

The right quadrant of Chart 4 may be used to determine the discharge conveyance ( $\text{m}^3/\text{s}$ ) for any combination of cross fall, longitudinal slope and shoulder width. The left quadrant of Chart 4 may be used to determine the maximum capacity of the shoulder for any combination of discharge conveyance and longitudinal slope. The drain conveyance is constant and independent of the pavement cross fall, represented by line AB in the left quadrant below. Therefore, for any longitudinal slope, the maximum capacity of the drain can be determined. The minor between shoulder capacity and the drain capacity is the limiting flow. Subsequently, the grid length can be determined by using the limiting flow and interpolating between the dotted lines which represent the length of grids.

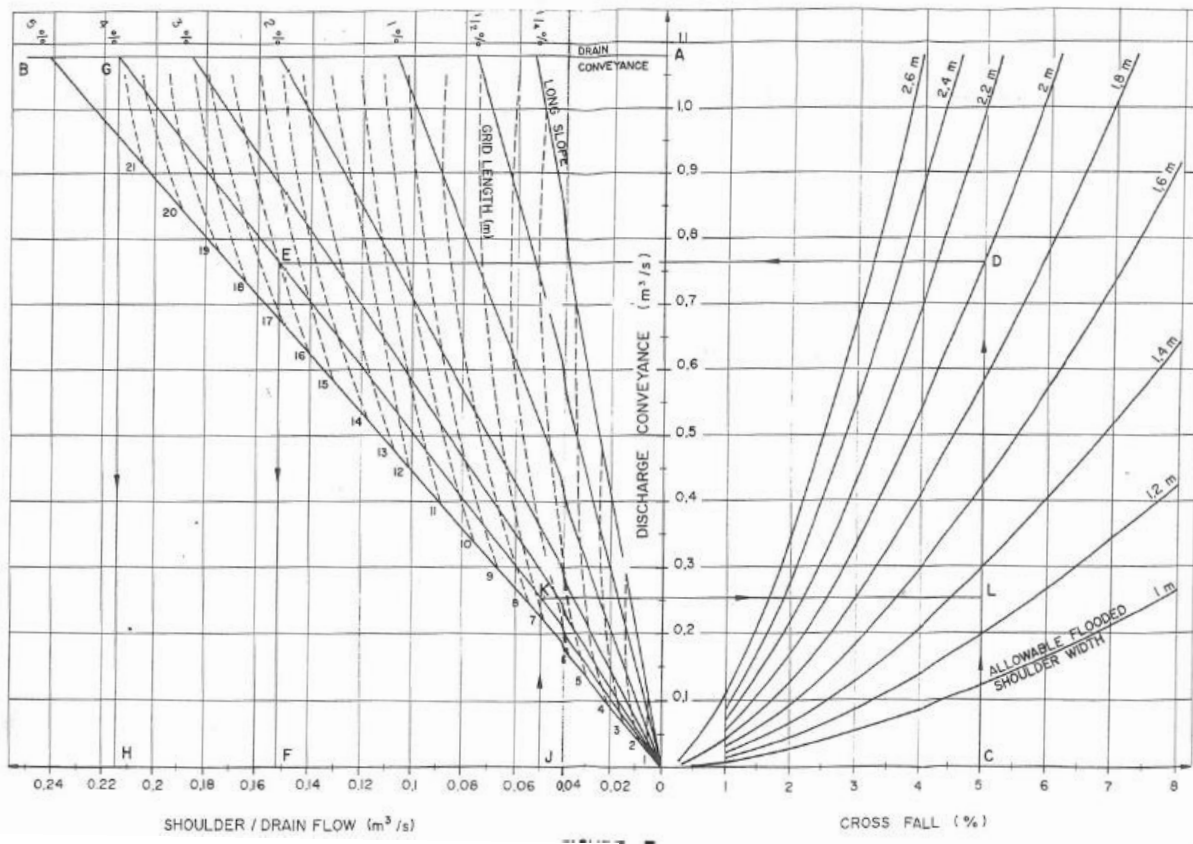


Chart 4: Design Chart (Gouws, 1993)



Chart 5 is developed from the results obtained from Equation 2-17 and Equation 2-18. The chart can be used to obtain graphical values of the interception capacities of slotted drains in sag locations. Thus, for any combination of water depth ( $d$ ), slot length ( $L$ ) and slot width ( $W$ ), the interception capacity of the slotted drain can graphically be determined accordingly.

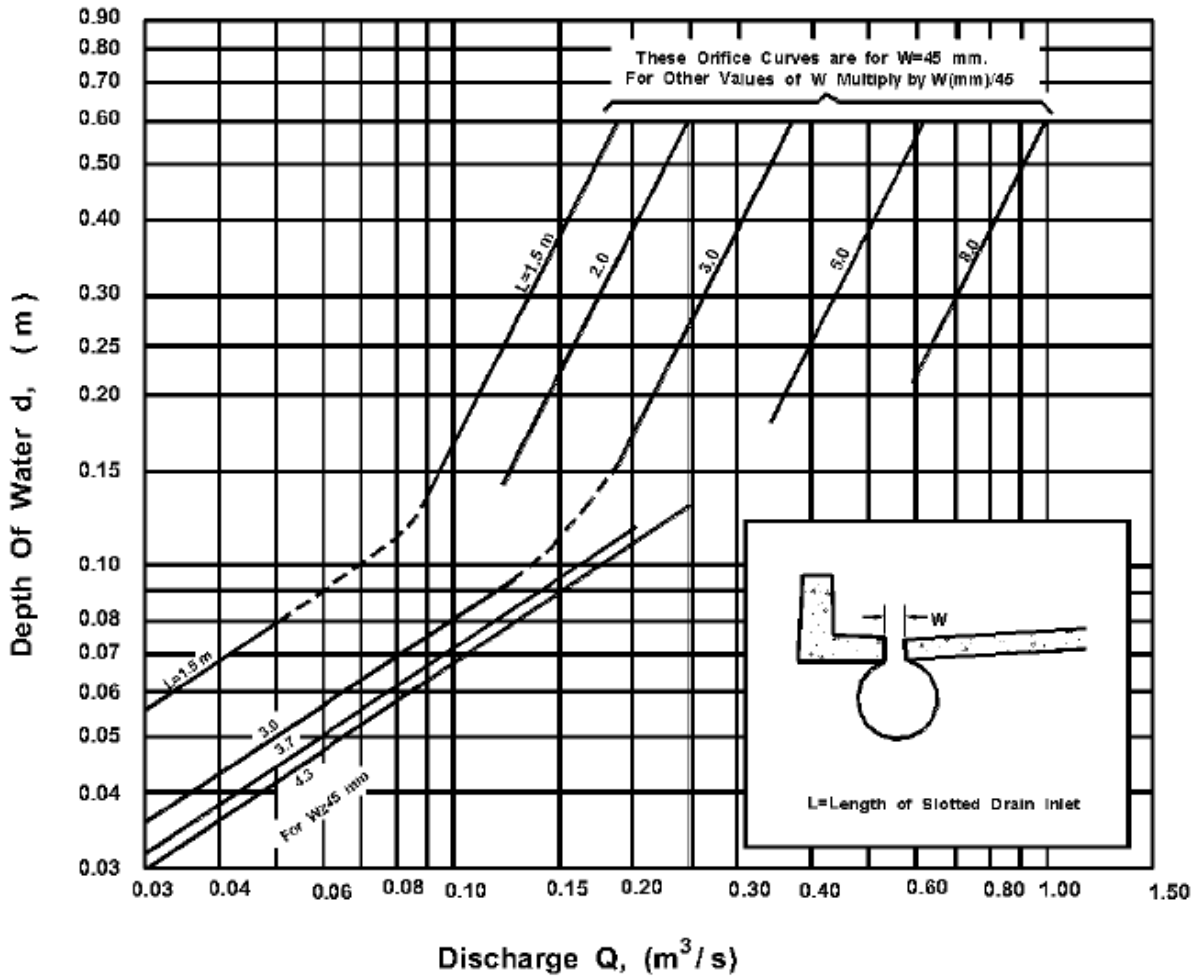


Chart 5: Slotted drain inlet capacity at sag location (Brown et al., 2009)

## B. APPENDIX B

Table B-1: Flow measurement verification data

Time interval	Measurement no	Flow meter reading 1 (m <sup>3</sup> )	Flow meter reading 2 (m <sup>3</sup> )	Running time (sec)	Flow rate 1 (l/s)	Flow rate 2 (l/s)	Manually measured flow rate (l/s)		
							1	2	3
1	1	6.579	2.635				1	2	3
	2	6.640	2.695	180	0.339	0.333	0.352	0.346	0.343
	3	6.702	2.757	180	0.344	0.344	0.342	0.347	0.342
	4	6.764	2.819	180	0.344	0.344	0.343	0.343	0.342
	<b>Averages</b>					<b>0.343</b>	<b>0.341</b>	<b>0.345</b>	
2	1	6.911	2.977				1	2	3
	2	7.010	3.075	180	0.550	0.544	0.536	0.558	0.544
	3	7.109	3.174	180	0.550	0.550	0.544	0.544	0.547
	4	7.207	3.272	180	0.544	0.544	0.542	0.541	0.539
	<b>Averages</b>					<b>0.548</b>	<b>0.546</b>	<b>0.544</b>	
3	1	7.721	3.824				1	2	3
	2	7.900	4.002	180	0.994	0.989	1.001	0.986	1.013
	3	8.077	4.178	180	0.983	0.978	0.996	1.003	0.995
	4	8.255	4.354	180	0.989	0.978	0.990	0.998	0.998
	<b>Averages</b>					<b>0.989</b>	<b>0.981</b>	<b>0.998</b>	
4	1	8.810	4.968				1	2	3
	2	9.105	5.256	180	1.639	1.600	1.607	1.629	1.573
	3	9.399	5.551	180	1.633	1.639	1.595	1.649	1.640
	4	9.686	5.832	180	1.594	1.561	1.577	1.593	1.583
	<b>Averages</b>					<b>1.622</b>	<b>1.600</b>	<b>1.605</b>	
5	1	10.817	7.048				1	2	3
	2	11.205	7.433	180	2.156	2.139	2.152	2.166	2.091
	3	11.590	7.817	180	2.139	2.133	2.071	2.135	2.160
	4	11.984	8.203	180	2.189	2.144	2.176	2.124	2.135
	<b>Averages</b>					<b>2.161</b>	<b>2.139</b>	<b>2.134</b>	

Table B-2: Test Data-Type I model, 20mm slot width, 0% longitudinal slope & 2% cross slope

Test no	Longitudinal slope	Cross slope	Measurement no	Flow meter reading 1 (m <sup>3</sup> )	Flow meter reading 2 (m <sup>3</sup> )	Running time (sec)	Flow rate 1 (l/s)	Flow rate 2 (l/s)	Interception efficiency (%)
1	0	2	1	6.479	4.776				
			2	6.596	4.892	180	0.650	0.644	99.145
			3	6.714	5.009	180	0.656	0.650	99.153
			4	6.830	5.124	180	0.644	0.639	99.138
			<b>Averages</b>				<b>0.650</b>	<b>0.644</b>	<b>99.145</b>
2	0	2	1	8.152	6.555				
			2	8.363	6.763	180	1.172	1.156	98.578
			3	8.571	6.970	180	1.156	1.150	99.519
			4	8.778	7.175	180	1.150	1.139	99.034
			<b>Averages</b>				<b>1.159</b>	<b>1.148</b>	<b>99.042</b>
3	0	2	1	0.244	8.652				
			2	0.584	8.986	180	1.889	1.856	98.235
			3	0.921	9.319	180	1.872	1.850	98.813
			4	1.260	9.654	180	1.883	1.861	98.820
			<b>Averages</b>				<b>1.881</b>	<b>1.856</b>	<b>98.622</b>
4	0	2	1	3.214	1.701				
			2	3.631	2.111	180	2.317	2.278	98.321
			3	4.044	2.519	180	2.294	2.267	98.789
			4	4.456	2.923	180	2.289	2.244	98.058
			<b>Averages</b>				<b>2.300</b>	<b>2.263</b>	<b>98.390</b>
5	0	2	1	6.076	4.532				
			2	6.607	5.053	180	2.950	2.894	98.117
			3	7.128	5.567	180	2.894	2.856	98.656
			4	7.654	6.083	180	2.922	2.867	98.099
			<b>Averages</b>				<b>2.922</b>	<b>2.872</b>	<b>98.289</b>

Table B-3: Test Data-Type I model, 20mm slot width, 0% longitudinal slope & 4% cross slope

Test no	Longitudinal slope	Cross slope	Measurement no	Flow meter reading 1 (m <sup>3</sup> )	Flow meter reading 2 (m <sup>3</sup> )	Running time (Sec)	Flow rate 1 (l/s)	Flow rate 2 (l/s)	Interception efficiency (%)
1	0	4	1	1.614	0.860				
			2	1.690	0.936	180	0.422	0.422	100.000
			3	1.765	1.011	180	0.417	0.417	100.000
			4	1.841	1.086	180	0.422	0.417	98.684
			<b>Averages</b>				<b>0.420</b>	<b>0.419</b>	<b>99.559</b>
2	0	4	1	9.131	8.377				
			2	9.330	8.574	180	1.106	1.094	98.995
			3	9.531	8.773	180	1.117	1.106	99.005
			4	9.731	8.971	180	1.111	1.100	99.000
			<b>Averages</b>				<b>1.111</b>	<b>1.100</b>	<b>99.000</b>
3	0	4	1	0.637	9.905				
			2	0.920	10.185	180	1.572	1.556	98.940
			3	1.198	10.462	180	1.544	1.539	99.640
			4	1.479	10.740	180	1.561	1.544	98.932
			<b>Averages</b>				<b>1.559</b>	<b>1.546</b>	<b>99.169</b>
4	0	4	1	2.083	1.314				
			2	2.471	1.697	180	2.156	2.128	98.711
			3	2.864	2.087	180	2.183	2.167	99.237
			4	3.256	2.474	180	2.178	2.150	98.724
			<b>Averages</b>				<b>2.172</b>	<b>2.148</b>	<b>98.892</b>
5	0	4	1	4.521	3.985				
			2	5.062	4.520	180	3.006	2.972	98.891
			3	5.596	5.046	180	2.967	2.922	98.502
			4	6.134	5.579	180	2.989	2.961	99.071
			<b>Averages</b>				<b>2.987</b>	<b>2.952</b>	<b>98.822</b>

Table B-4: Test Data-Type I model, 20mm slot width, 0% longitudinal slope & 6% cross slope

Test no	Longitudinal slope	Cross slope	Measurement no	Flow meter reading 1 (m <sup>3</sup> )	Flow meter reading 2 (m <sup>3</sup> )	Running time (Sec)	Flow rate 1 (l/s)	Flow rate 2 (l/s)	Interception efficiency (%)
1	0	6	1	6.761	4.274				
			2	6.872	4.384	180	0.617	0.611	99.099
			3	6.982	4.494	180	0.611	0.611	100.000
			4	7.094	4.605	180	0.622	0.617	99.107
			<b>Averages</b>				<b>0.617</b>	<b>0.613</b>	<b>99.399</b>
2	0	6	1	8.251	5.779				
			2	8.472	5.997	180	1.228	1.211	98.643
			3	8.694	6.216	180	1.233	1.217	98.649
			4	8.912	6.433	180	1.211	1.206	99.541
			<b>Averages</b>				<b>1.224</b>	<b>1.211</b>	<b>98.941</b>
3	0	6	1	0.164	8.699				
			2	0.452	8.984	180	1.600	1.583	98.958
			3	0.745	9.274	180	1.628	1.611	98.976
			4	1.034	9.560	180	1.606	1.589	98.962
			<b>Averages</b>				<b>1.611</b>	<b>1.594</b>	<b>98.966</b>
4	0	6	1	2.399	1.864				
			2	2.840	2.300	180	2.450	2.422	98.866
			3	3.278	2.731	180	2.433	2.394	98.402
			4	3.715	3.164	180	2.428	2.406	99.085
			<b>Averages</b>				<b>2.437</b>	<b>2.407</b>	<b>98.784</b>
5	0	6	1	5.208	4.688				
			2	5.744	5.216	180	2.978	2.933	98.507
			3	6.286	5.749	180	3.011	2.961	98.339
			4	6.824	6.281	180	2.989	2.956	98.885
			<b>Averages</b>				<b>2.993</b>	<b>2.950</b>	<b>98.577</b>

Table B-5: Test Data-Type I model, 20mm slot width, 2% longitudinal slope & 6% cross slope

Test no	Longitudinal slope	Cross slope	Measurement no	Flow meter reading 1 (m <sup>3</sup> )	Flow meter reading 2 (m <sup>3</sup> )	Running time (Sec)	Flow rate 1 (l/s)	Flow rate 2 (l/s)	Interception efficiency (%)
1	2	6	1	5.711	3.265				
			2	5.814	3.368	180	0.572	0.572	100.000
			3	5.916	3.469	180	0.567	0.561	99.020
			4	6.019	3.571	180	0.572	0.567	99.029
			<b>Averages</b>				<b>0.570</b>	<b>0.567</b>	<b>99.351</b>
2	2	6	1	7.948	5.467				
			2	8.183	5.701	180	1.306	1.300	99.574
			3	8.417	5.934	180	1.300	1.294	99.573
			4	8.654	6.169	180	1.317	1.306	99.156
			<b>Averages</b>				<b>1.307</b>	<b>1.300</b>	<b>99.433</b>
3	2	6	1	0.285	7.881				
			2	0.631	8.223	180	1.922	1.900	98.844
			3	0.971	8.561	180	1.889	1.878	99.412
			4	1.315	8.900	180	1.911	1.883	98.547
			<b>Averages</b>				<b>1.907</b>	<b>1.887</b>	<b>98.932</b>
4	2	6	1	3.262	0.444				
			2	3.711	0.891	180	2.494	2.483	99.555
			3	4.163	1.335	180	2.511	2.467	98.230
			4	4.609	1.774	180	2.478	2.439	98.430
			<b>Averages</b>				<b>2.494</b>	<b>2.463</b>	<b>98.738</b>
5	2	6	1	6.734	3.904				
			2	7.271	4.431	180	2.983	2.928	98.138
			3	7.803	4.953	180	2.956	2.900	98.120
			4	8.338	5.479	180	2.972	2.922	98.318
			<b>Averages</b>				<b>2.970</b>	<b>2.917</b>	<b>98.192</b>

Table B-6: Test Data-Type I model, 20mm slot width, 4% longitudinal slope & 6% cross slope

Test no	Longitudinal slope	Cross slope	Measurement no	Flow meter reading 1 (m <sup>3</sup> )	Flow meter reading 2 (m <sup>3</sup> )	Running time (Sec)	Flow rate 1 (l/s)	Flow rate 2 (l/s)	Interception efficiency (%)
1	4	6	1	3.404	9.610				
			2	3.527	9.733	180	0.683	0.683	100.000
			3	3.652	9.856	180	0.694	0.683	98.400
			4	3.777	9.980	180	0.694	0.689	99.200
			<b>Averages</b>				<b>0.691</b>	<b>0.685</b>	<b>99.196</b>
2	4	6	1	4.883	1.084				
			2	5.087	1.286	180	1.133	1.122	99.020
			3	5.293	1.490	180	1.144	1.133	99.029
			4	5.497	1.693	180	1.133	1.128	99.510
			<b>Averages</b>				<b>1.137</b>	<b>1.128</b>	<b>99.186</b>
3	4	6	1	6.699	2.906				
			2	6.992	3.196	180	1.628	1.611	98.976
			3	7.289	3.490	180	1.650	1.633	98.990
			4	7.581	3.779	180	1.622	1.606	98.973
			<b>Averages</b>				<b>1.633</b>	<b>1.617</b>	<b>98.980</b>
4	4	6	1	8.923	5.098				
			2	9.409	5.579	180	2.700	2.672	98.971
			3	9.898	6.063	180	2.717	2.689	98.978
			4	10.382	6.539	180	2.689	2.644	98.347
			<b>Averages</b>				<b>2.702</b>	<b>2.669</b>	<b>98.766</b>
5	4	6	1	7.901	3.441				
			2	8.443	3.976	180	3.011	2.972	98.708
			3	8.981	4.503	180	2.989	2.928	97.955
			4	9.522	5.040	180	3.006	2.983	99.261
			<b>Averages</b>				<b>3.002</b>	<b>2.961</b>	<b>98.643</b>

Table B-7: Test Data-Type I model, 20mm slot width, 6% longitudinal slope & 6% cross slope

Test no	Longitudinal slope	Cross slope	Measurement no	Flow meter reading 1 (m <sup>3</sup> )	Flow meter reading 2 (m <sup>3</sup> )	Running time (Sec)	Flow rate 1 (l/s)	Flow rate 2 (l/s)	Interception efficiency (%)
1	6	6	1	9.885	4.624				
			2	10.010	4.748	180	0.694	0.689	99.200
			3	10.135	4.872	180	0.694	0.689	99.200
			4	10.262	4.998	180	0.706	0.700	99.213
			<b>Averages</b>				<b>0.698</b>	<b>0.693</b>	<b>99.204</b>
2	6	6	1	1.446	6.191				
			2	1.646	6.390	180	1.111	1.106	99.500
			3	1.847	6.591	180	1.117	1.117	100.000
			4	2.049	6.791	180	1.122	1.111	99.010
			<b>Averages</b>				<b>1.117</b>	<b>1.111</b>	<b>99.502</b>
3	6	6	1	3.261	7.986				
			2	3.585	8.306	180	1.800	1.778	98.765
			3	3.911	8.630	180	1.811	1.800	99.387
			4	4.234	8.952	180	1.794	1.789	99.690
			<b>Averages</b>				<b>1.802</b>	<b>1.789</b>	<b>99.281</b>
4	6	6	1	5.443	0.157				
			2	5.860	0.569	180	2.317	2.289	98.801
			3	6.270	0.975	180	2.278	2.256	99.024
			4	6.687	1.388	180	2.317	2.294	99.041
			<b>Averages</b>				<b>2.304</b>	<b>2.280</b>	<b>98.955</b>
5	6	6	1	4.181	8.466				
			2	4.729	9.005	180	3.044	2.994	98.358
			3	5.268	9.534	180	2.994	2.939	98.145
			4	5.807	10.065	180	2.994	2.950	98.516
			<b>Averages</b>				<b>3.011</b>	<b>2.961</b>	<b>98.339</b>



Table B-8: Test Data-Type I model, 40mm slot width, 0% longitudinal slope & 2% cross slope

Test no	Longitudinal slope	Cross slope	Measurement no	Flow meter reading 1 (m <sup>3</sup> )	Flow meter reading 2 (m <sup>3</sup> )	Running time (Sec)	Flow rate 1 (l/s)	Flow rate 2 (l/s)	Interception efficiency (%)
1	0	2	1	7.458	2.538				
			2	7.610	2.689	180	0.844	0.839	99.342
			3	7.761	2.840	180	0.839	0.839	100.000
			4	7.912	2.990	180	0.839	0.833	99.338
						<b>Averages</b>	<b>0.841</b>	<b>0.837</b>	<b>99.559</b>
2	0	2	1	8.624	3.765				
			2	8.837	3.977	180	1.183	1.178	99.531
			3	9.053	4.190	180	1.200	1.183	98.611
			4	9.267	4.403	180	1.189	1.183	99.533
						<b>Averages</b>	<b>1.191</b>	<b>1.181</b>	<b>99.222</b>
3	0	2	1	0.047	5.268				
			2	0.380	5.597	180	1.850	1.828	98.799
			3	0.718	5.931	180	1.878	1.856	98.817
			4	1.052	6.261	180	1.856	1.833	98.802
						<b>Averages</b>	<b>1.861</b>	<b>1.839</b>	<b>98.806</b>
4	0	2	1	2.354	7.583				
			2	2.759	7.982	180	2.250	2.217	98.519
			3	3.158	8.383	180	2.217	2.228	100.501
			4	3.559	8.776	180	2.228	2.183	98.005
						<b>Averages</b>	<b>2.231</b>	<b>2.209</b>	<b>99.004</b>
5	0	2	1	4.970	10.113				
			2	5.506	10.645	180	2.978	2.957	99.310
			3	6.033	11.167	180	2.928	2.898	98.994
			4	6.568	11.695	180	2.972	2.933	98.692
						<b>Averages</b>	<b>2.959</b>	<b>2.930</b>	<b>98.999</b>

**Table B-9: Test Data-Type I model, 40mm slot width, 0% longitudinal slope & 4% cross slope**

Test no	Longitudinal slope	Cross slope	Measurement no	Flow meter reading 1 (m <sup>3</sup> )	Flow meter reading 2 (m <sup>3</sup> )	Running time (Sec)	Flow rate 1 (l/s)	Flow rate 2 (l/s)	Interception efficiency (%)
1	0	4	1	1.208	8.446				
			2	1.335	8.572	180	0.706	0.700	99.213
			3	1.460	8.696	180	0.694	0.689	99.200
			4	1.586	8.821	180	0.700	0.694	99.206
						<b>Averages</b>			<b>0.700</b>
2	0	4	1	3.699	0.058				
			2	3.882	0.240	180	1.017	1.011	99.454
			3	4.067	0.425	180	1.028	1.028	100.000
			4	4.251	0.608	180	1.022	1.017	99.457
						<b>Averages</b>			<b>1.022</b>
3	0	4	1	4.720	1.103				
			2	4.962	1.342	180	1.344	1.329	98.884
			3	5.200	1.579	180	1.322	1.315	99.454
			4	5.438	1.814	180	1.322	1.306	98.739
						<b>Averages</b>			<b>1.330</b>
4	0	4	1	5.832	2.198				
			2	6.262	2.624	180	2.389	2.367	99.070
			3	6.691	3.048	180	2.383	2.356	98.834
			4	7.119	3.470	180	2.378	2.344	98.598
						<b>Averages</b>			<b>2.383</b>
5	0	4	1	7.567	3.855				
			2	8.115	4.393	180	3.044	2.989	98.175
			3	8.654	4.927	180	2.994	2.967	99.072
			4	9.192	5.469	180	2.989	3.011	100.743
						<b>Averages</b>			<b>3.009</b>

Table B-10: Test Data-Type I model, 40mm slot width, 0% longitudinal slope &amp; 6% cross slope

Test no	Longitudinal slope	Cross slope	Measurement no	Flow meter reading 1 (m <sup>3</sup> )	Flow meter reading 2 (m <sup>3</sup> )	Running time (Sec)	Flow rate 1 (l/s)	Flow rate 2 (l/s)	Interception efficiency (%)
1	0	6	1	2.879	7.907				
			2	3.040	8.067	180	0.894	0.889	99.379
			3	3.204	8.229	180	0.911	0.900	98.780
			4	3.365	8.389	180	0.894	0.889	99.379
			<b>Averages</b>				<b>0.900</b>	<b>0.893</b>	<b>99.177</b>
2	0	6	1	3.651	8.694				
			2	3.855	8.898	180	1.133	1.133	100.000
			3	4.061	9.103	180	1.144	1.139	99.515
			4	4.268	9.309	180	1.150	1.144	99.517
			<b>Averages</b>				<b>1.143</b>	<b>1.139</b>	<b>99.676</b>
3	0	6	1	5.691	9.748				
			2	5.993	10.048	180	1.678	1.667	99.338
			3	6.298	10.353	180	1.694	1.694	100.000
			4	6.602	10.656	180	1.689	1.683	99.671
			<b>Averages</b>				<b>1.687</b>	<b>1.681</b>	<b>99.671</b>
4	0	6	1	7.165	1.256				
			2	7.617	1.703	180	2.511	2.483	98.894
			3	8.077	2.154	180	2.556	2.506	98.043
			4	8.535	2.604	180	2.544	2.500	98.253
			<b>Averages</b>				<b>2.537</b>	<b>2.496</b>	<b>98.394</b>
5	0	6	1	9.465	3.638				
			2	10.016	4.178	180	3.061	3.000	98.004
			3	10.571	4.724	180	3.083	3.033	98.378
			4	11.119	5.261	180	3.044	2.983	97.993
			<b>Averages</b>				<b>3.063</b>	<b>3.006</b>	<b>98.126</b>

**Table B-11: Test Data-Type I model, 40mm slot width, 2% longitudinal slope & 6% cross slope**

Test no	Longitudinal slope	Cross slope	Measurement no	Flow meter reading 1 (m <sup>3</sup> )	Flow meter reading 2 (m <sup>3</sup> )	Running time (Sec)	Flow rate 1 (l/s)	Flow rate 2 (l/s)	Interception efficiency (%)
1	2	6	1	7.263	0.797				
			2	7.406	0.939	180	0.794	0.789	99.301
			3	7.548	1.080	180	0.789	0.783	99.296
			4	7.691	1.223	180	0.794	0.794	100.000
						<b>Averages</b>	<b>0.793</b>	<b>0.789</b>	<b>99.533</b>
2	2	6	1	7.907	1.470				
			2	8.156	1.717	180	1.383	1.372	99.197
			3	8.404	1.963	180	1.378	1.367	99.194
			4	8.651	2.210	180	1.372	1.372	100.000
						<b>Averages</b>	<b>1.378</b>	<b>1.370</b>	<b>99.462</b>
3	2	6	1	9.052	2.633				
			2	9.397	2.974	180	1.917	1.894	98.841
			3	9.744	3.316	180	1.928	1.900	98.559
			4	10.086	3.655	180	1.900	1.883	99.123
						<b>Averages</b>	<b>1.915</b>	<b>1.893</b>	<b>98.839</b>
4	2	6	1	0.563	4.092				
			2	1.044	4.568	180	2.672	2.644	98.960
			3	1.516	5.035	180	2.622	2.594	98.941
			4	1.994	5.504	180	2.656	2.606	98.117
						<b>Averages</b>	<b>2.650</b>	<b>2.615</b>	<b>98.672</b>
5	2	6	1	3.095	6.658				
			2	3.652	7.208	180	3.094	3.056	98.743
			3	4.206	7.747	180	3.078	2.994	97.292
			4	4.758	8.289	180	3.067	3.011	98.188
						<b>Averages</b>	<b>3.080</b>	<b>3.020</b>	<b>98.076</b>

**Table B-12: Test Data-Type I model, 40mm slot width, 4% longitudinal slope & 6% cross slope**

Test no	Longitudinal slope	Cross slope	Measurement no	Flow meter reading 1 (m <sup>3</sup> )	Flow meter reading 2 (m <sup>3</sup> )	Running time (Sec)	Flow rate 1 (l/s)	Flow rate 2 (l/s)	Interception efficiency (%)
1	4	6	1	5.609	9.181				
			2	5.759	9.330	180	0.833	0.828	99.333
			3	5.908	9.479	180	0.828	0.828	100.000
			4	6.057	9.626	180	0.828	0.817	98.658
			<b>Averages</b>				<b>0.830</b>	<b>0.824</b>	<b>99.330</b>
2	4	6	1	6.353	7.948				
			2	6.616	8.210	180	1.461	1.456	99.620
			3	6.881	8.473	180	1.472	1.461	99.245
			4	7.147	8.737	180	1.478	1.467	99.248
			<b>Averages</b>				<b>1.470</b>	<b>1.461</b>	<b>99.370</b>
3	4	6	1	7.600	9.256				
			2	7.960	9.613	180	2.000	1.983	99.167
			3	8.324	9.972	180	2.022	1.994	98.626
			4	8.683	10.328	180	1.994	1.978	99.164
			<b>Averages</b>				<b>2.006</b>	<b>1.985</b>	<b>98.984</b>
4	4	6	1	9.204	1.024				
			2	9.678	1.495	180	2.633	2.617	99.367
			3	10.161	1.973	180	2.683	2.656	98.965
			4	10.638	2.445	180	2.650	2.622	98.952
			<b>Averages</b>				<b>2.656</b>	<b>2.631</b>	<b>99.093</b>
5	4	6	1	1.296	3.186				
			2	1.839	3.722	180	3.017	2.978	98.711
			3	2.372	4.250	180	2.961	2.933	99.062
			4	2.909	4.784	180	2.983	2.967	99.441
			<b>Averages</b>				<b>2.987</b>	<b>2.959</b>	<b>99.070</b>

**Table B-13: Test Data-Type I model, 40mm slot width, 6% longitudinal slope & 6% cross slope**

Test no	Longitudinal slope	Cross slope	Measurement no	Flow meter reading 1 (m <sup>3</sup> )	Flow meter reading 2 (m <sup>3</sup> )	Running time (Sec)	Flow rate 1 (l/s)	Flow rate 2 (l/s)	Interception efficiency (%)
1	6	6	1	4.064	6.441				
			2	4.194	6.570	180	0.722	0.717	99.231
			3	4.322	6.698	180	0.711	0.711	100.000
			4	4.452	6.827	180	0.722	0.717	99.231
			<b>Averages</b>				<b>0.719</b>	<b>0.715</b>	<b>99.485</b>
2	6	6	1	6.714	8.186				
			2	6.968	8.438	180	1.411	1.400	99.213
			3	7.221	8.689	180	1.406	1.394	99.209
			4	7.474	8.939	180	1.406	1.389	98.814
			<b>Averages</b>				<b>1.407</b>	<b>1.394</b>	<b>99.079</b>
3	6	6	1	8.081	9.444				
			2	8.440	9.798	180	1.994	1.967	98.607
			3	8.800	10.151	180	2.000	1.961	98.056
			4	9.153	10.499	180	1.961	1.933	98.584
			<b>Averages</b>				<b>1.985</b>	<b>1.954</b>	<b>98.414</b>
4	6	6	1	9.688	1.062				
			2	10.138	1.507	180	2.500	2.472	98.889
			3	10.593	1.956	180	2.528	2.494	98.681
			4	11.052	2.409	180	2.550	2.517	98.693
			<b>Averages</b>				<b>2.526</b>	<b>2.494</b>	<b>98.754</b>
5	6	6	1	3.689	5.077				
			2	4.229	5.611	180	3.000	2.967	98.889
			3	4.759	6.135	180	2.944	2.911	98.868
			4	5.295	6.661	180	2.978	2.922	98.134
			<b>Averages</b>				<b>2.974</b>	<b>2.933</b>	<b>98.630</b>

**Table B-14: Test Data-Type I model, 60mm slot width, 0% longitudinal slope & 2% cross slope**

Test no	Longitudinal slope	Cross slope	Measurement no	Flow meter reading 1 (m <sup>3</sup> )	Flow meter reading 2 (m <sup>3</sup> )	Running time (Sec)	Flow rate 1 (l/s)	Flow rate 2 (l/s)	Interception efficiency (%)
1	0	2	1	4.972	7.148				
			2	5.116	7.291	180	0.800	0.794	99.306
			3	5.262	7.435	180	0.811	0.800	98.630
			4	5.407	7.58	180	0.806	0.806	100.000
			<b>Averages</b>				<b>0.806</b>	<b>0.800</b>	<b>99.310</b>
2	0	2	1	3.644	5.862				
			2	3.875	6.091	180	1.283	1.272	99.134
			3	4.11	6.322	180	1.306	1.283	98.298
			4	4.341	6.549	180	1.283	1.261	98.268
			<b>Averages</b>				<b>1.291</b>	<b>1.272</b>	<b>98.565</b>
3	0	2	1	2.387	4.594				
			2	2.666	4.869	180	1.550	1.528	98.566
			3	2.941	5.142	180	1.528	1.517	99.273
			4	3.215	5.414	180	1.522	1.511	99.270
			<b>Averages</b>				<b>1.533</b>	<b>1.519</b>	<b>99.034</b>
4	0	2	1	5.778	7.943				
			2	6.133	8.292	180	1.972	1.939	98.310
			3	6.494	8.648	180	2.006	1.978	98.615
			4	6.848	8.998	180	1.967	1.944	98.870
			<b>Averages</b>				<b>1.981</b>	<b>1.954</b>	<b>98.598</b>
5	0	2	1	7.592	9.527				
			2	8.121	10.045	180	2.939	2.878	97.921
			3	8.653	10.565	180	2.956	2.889	97.744
			4	9.183	11.088	180	2.944	2.906	98.679
			<b>Averages</b>				<b>2.946</b>	<b>2.891</b>	<b>98.114</b>

**Table B-15: Test Data-Type I model, 60mm slot width, 0% longitudinal slope & 4% cross slope**

Test no	Longitudinal slope	Cross slope	Measurement no	Flow meter reading 1 (m <sup>3</sup> )	Flow meter reading 2 (m <sup>3</sup> )	Running time (Sec)	Flow rate 1 (l/s)	Flow rate 2 (l/s)	Interception efficiency (%)
1	0	4	1	4.066	6.536				
			2	4.207	6.676	180	0.783	0.778	99.291
			3	4.346	6.814	180	0.772	0.767	99.281
			4	4.486	6.953	180	0.778	0.772	99.286
						<b>Averages</b>	<b>0.778</b>	<b>0.772</b>	<b>99.286</b>
2	0	4	1	5.011	7.486				
			2	5.253	7.726	180	1.344	1.333	99.174
			3	5.497	7.969	180	1.356	1.350	99.590
			4	5.739	8.209	180	1.344	1.333	99.174
						<b>Averages</b>	<b>1.348</b>	<b>1.339</b>	<b>99.313</b>
3	0	4	1	6.421	9.899				
			2	6.735	10.210	180	1.744	1.728	99.045
			3	7.045	10.516	180	1.722	1.700	98.710
			4	7.358	10.825	180	1.739	1.717	98.722
						<b>Averages</b>	<b>1.735</b>	<b>1.715</b>	<b>98.826</b>
4	0	4	1	0.558	1.488				
			2	0.963	1.888	180	2.250	2.222	98.765
			3	1.371	2.291	180	2.267	2.239	98.775
			4	1.78	2.693	180	2.272	2.233	98.289
						<b>Averages</b>	<b>2.263</b>	<b>2.231</b>	<b>98.609</b>
5	0	4	1	3.539	4.596				
			2	4.097	5.145	180	3.100	3.050	98.387
			3	4.645	5.683	180	3.044	2.989	98.175
			4	5.201	6.229	180	3.089	3.033	98.201
						<b>Averages</b>	<b>3.078</b>	<b>3.024</b>	<b>98.255</b>



**Table B-16: Test Data-Type I model, 60mm slot width, 0% longitudinal slope & 6% cross slope**

Test no	Longitudinal slope	Cross slope	Measurement no	Flow meter reading 1 (m <sup>3</sup> )	Flow meter reading 2 (m <sup>3</sup> )	Running time (Sec)	Flow rate 1 (l/s)	Flow rate 2 (l/s)	Interception efficiency (%)
1	0	6	1	3.294	4.507				
			2	3.467	4.68	180	0.961	0.961	100.000
			3	3.639	4.851	180	0.956	0.950	99.419
			4	3.814	5.025	180	0.972	0.967	99.429
			<b>Averages</b>				<b>0.963</b>	<b>0.959</b>	<b>99.615</b>
2	0	6	1	4.487	5.671				
			2	4.697	5.879	180	1.167	1.156	99.048
			3	4.911	6.091	180	1.189	1.178	99.065
			4	5.122	6.3	180	1.172	1.161	99.052
			<b>Averages</b>				<b>1.176</b>	<b>1.165</b>	<b>99.055</b>
3	0	6	1	1.895	3.14				
			2	2.189	3.431	180	1.633	1.617	98.980
			3	2.482	3.721	180	1.628	1.611	98.976
			4	2.779	4.012	180	1.650	1.617	97.980
			<b>Averages</b>				<b>1.637</b>	<b>1.615</b>	<b>98.643</b>
4	0	6	1	5.699	6.901				
			2	6.056	7.253	180	1.983	1.956	98.599
			3	6.409	7.598	180	1.961	1.917	97.734
			4	6.763	7.947	180	1.967	1.939	98.588
			<b>Averages</b>				<b>1.970</b>	<b>1.937</b>	<b>98.308</b>
5	0	6	1	7.579	8.554				
			2	8.106	9.071	180	2.928	2.872	98.102
			3	8.624	9.582	180	2.878	2.839	98.649
			4	9.141	10.089	180	2.872	2.817	98.066
			<b>Averages</b>				<b>2.893</b>	<b>2.843</b>	<b>98.271</b>

**Table B-17: Test Data-Type I model, 60mm slot width, 2% longitudinal slope & 6% cross slope**

Test no	Longitudinal slope	Cross slope	Measurement no	Flow meter reading 1 (m <sup>3</sup> )	Flow meter reading 2 (m <sup>3</sup> )	Running time (Sec)	Flow rate 1 (l/s)	Flow rate 2 (l/s)	Interception efficiency (%)
1	2	6	1	1.248	1.031				
			2	1.394	1.176	180	0.811	0.806	99.315
			3	1.539	1.319	180	0.806	0.794	98.621
			4	1.684	1.464	180	0.806	0.806	100.000
			<b>Averages</b>				<b>0.807</b>	<b>0.802</b>	<b>99.312</b>
2	2	6	1	1.832	1.617				
			2	2.052	1.836	180	1.222	1.217	99.545
			3	2.270	2.053	180	1.211	1.206	99.541
			4	2.491	2.271	180	1.228	1.211	98.643
			<b>Averages</b>				<b>1.220</b>	<b>1.211</b>	<b>99.241</b>
3	2	6	1	3.059	2.859				
			2	3.340	3.136	180	1.561	1.539	98.577
			3	3.616	3.411	180	1.533	1.528	99.638
			4	3.894	3.684	180	1.544	1.517	98.201
			<b>Averages</b>				<b>1.546</b>	<b>1.528</b>	<b>98.802</b>
4	2	6	1	4.183	3.993				
			2	4.590	4.395	180	2.261	2.233	98.771
			3	4.993	4.79	180	2.239	2.194	98.015
			4	5.403	5.192	180	2.278	2.233	98.049
			<b>Averages</b>				<b>2.259</b>	<b>2.220</b>	<b>98.279</b>
5	2	6	1	6.154	5.954				
			2	6.689	6.486	180	2.972	2.956	99.439
			3	7.227	7.019	180	2.989	2.961	99.071
			4	7.756	7.542	180	2.939	2.906	98.866
			<b>Averages</b>				<b>2.967</b>	<b>2.941</b>	<b>99.126</b>

**Table B-18: Test Data-Type I model, 60mm slot width, 4% longitudinal slope & 6% cross slope**

Test no	Longitudinal slope	Cross slope	Measurement no	Flow meter reading 1 (m <sup>3</sup> )	Flow meter reading 2 (m <sup>3</sup> )	Running time (Sec)	Flow rate 1 (l/s)	Flow rate 2 (l/s)	Interception efficiency (%)
1	4	6	1	1.193	7.612				
			2	1.308	7.727	180	0.639	0.639	100.000
			3	1.424	7.841	180	0.644	0.633	98.276
			4	1.538	7.954	180	0.633	0.628	99.123
			<b>Averages</b>				<b>0.639</b>	<b>0.633</b>	<b>99.130</b>
2	4	6	1	1.966	8.389				
			2	2.192	8.612	180	1.256	1.239	98.673
			3	2.415	8.833	180	1.239	1.228	99.103
			4	2.637	9.052	180	1.233	1.217	98.649
			<b>Averages</b>				<b>1.243</b>	<b>1.228</b>	<b>98.808</b>
3	4	6	1	2.534	1.843				
			2	2.786	2.091	180	1.400	1.378	98.413
			3	3.035	2.338	180	1.383	1.372	99.197
			4	3.284	2.584	180	1.383	1.367	98.795
			<b>Averages</b>				<b>1.389</b>	<b>1.372</b>	<b>98.800</b>
4	4	6	1	3.039	9.459				
			2	3.393	9.807	180	1.967	1.933	98.305
			3	3.746	10.156	180	1.961	1.939	98.867
			4	4.098	10.502	180	1.956	1.922	98.295
			<b>Averages</b>				<b>1.961</b>	<b>1.931</b>	<b>98.489</b>
5	4	6	1	3.632	2.952				
			2	4.185	3.494	180	3.072	3.011	98.011
			3	4.734	4.033	180	3.050	2.994	98.179
			4	5.29	4.579	180	3.089	3.033	98.201
			<b>Averages</b>				<b>3.070</b>	<b>3.013</b>	<b>98.130</b>

**Table B-19: Test Data-Type I model, 60mm slot width, 6% longitudinal slope & 6% cross slope**

Test no	Longitudinal slope	Cross slope	Measurement no	Flow meter reading 1 (m <sup>3</sup> )	Flow meter reading 2 (m <sup>3</sup> )	Running time (Sec)	Flow rate 1 (l/s)	Flow rate 2 (l/s)	Interception efficiency (%)
1	6	6	1	6.341	3.729				
			2	6.456	3.843	180	0.639	0.633	99.130
			3	6.570	3.957	180	0.633	0.633	100.000
			4	6.685	4.07	180	0.639	0.628	98.261
			<b>Averages</b>				<b>0.637</b>	<b>0.631</b>	<b>99.128</b>
2	6	6	1	6.862	4.261				
			2	7.091	4.488	180	1.272	1.261	99.127
			3	7.319	4.714	180	1.267	1.256	99.123
			4	7.545	4.937	180	1.256	1.239	98.673
			<b>Averages</b>				<b>1.265</b>	<b>1.252</b>	<b>98.975</b>
3	6	6	1	2.038	9.299				
			2	2.310	9.57	180	1.511	1.506	99.632
			3	2.585	9.841	180	1.528	1.506	98.545
			4	2.857	10.111	180	1.511	1.500	99.265
			<b>Averages</b>				<b>1.517</b>	<b>1.504</b>	<b>99.145</b>
4	6	6	1	8.014	5.383				
			2	8.359	5.726	180	1.917	1.906	99.420
			3	8.710	6.073	180	1.950	1.928	98.860
			4	9.062	6.421	180	1.956	1.933	98.864
			<b>Averages</b>				<b>1.941</b>	<b>1.922</b>	<b>99.046</b>
5	6	6	1	9.469	6.877				
			2	10.021	7.418	180	3.067	3.006	98.007
			3	10.566	7.953	180	3.028	2.972	98.165
			4	11.114	8.491	180	3.044	2.989	98.175
			<b>Averages</b>				<b>3.046</b>	<b>2.989</b>	<b>98.116</b>

Table B-20: Test Data-Type II model, 20mm slot width, 0% longitudinal slope &amp; 2% cross slope

Test no	Longitudinal slope	Cross slope	Measurement no	Flow meter reading 1 (m <sup>3</sup> )	Flow meter reading 2 (m <sup>3</sup> )	Running time (Sec)	Flow rate 1 (l/s)	Flow rate 2 (l/s)	Interception efficiency (%)
1	0	2	1	3.249	7.838				
			2	3.368	7.956	180	0.661	0.656	99.160
			3	3.486	8.073	180	0.656	0.650	99.153
			4	3.603	8.190	180	0.650	0.650	100.000
			<b>Averages</b>				<b>0.656</b>	<b>0.652</b>	<b>99.435</b>
2	0	2	1	5.101	9.786				
			2	5.337	10.019	180	1.311	1.294	98.729
			3	5.570	10.250	180	1.294	1.283	99.142
			4	5.802	10.479	180	1.289	1.272	98.707
			<b>Averages</b>				<b>1.298</b>	<b>1.283</b>	<b>98.859</b>
3	0	2	1	7.563	2.266				
			2	7.876	2.575	180	1.739	1.717	98.722
			3	8.186	2.881	180	1.722	1.700	98.710
			4	8.502	3.192	180	1.756	1.728	98.418
			<b>Averages</b>				<b>1.739</b>	<b>1.715</b>	<b>98.616</b>
4	0	2	1	0.643	5.313				
			2	1.036	5.701	180	2.183	2.156	98.728
			3	1.424	6.084	180	2.156	2.128	98.711
			4	1.814	6.467	180	2.167	2.128	98.205
			<b>Averages</b>				<b>2.169</b>	<b>2.137</b>	<b>98.548</b>
5	0	2	1	3.986	7.607				
			2	4.534	8.146	180	3.044	2.994	98.358
			3	5.085	8.689	180	3.061	3.019	98.621
			4	5.626	9.223	180	3.006	2.964	98.632
			<b>Averages</b>				<b>3.037</b>	<b>2.993</b>	<b>98.537</b>

**Table B-21: Test Data-Type II model, 20mm slot width, 0% longitudinal slope & 4% cross slope**

Test no	Longitudinal slope	Cross slope	Measurement no	Flow meter reading 1 (m <sup>3</sup> )	Flow meter reading 2 (m <sup>3</sup> )	Running time (Sec)	Flow rate 1 (l/s)	Flow rate 2 (l/s)	Interception efficiency (%)
1	0	4	1	6.707	0.215				
			2	6.803	0.310	180	0.533	0.528	98.958
			3	6.898	0.404	180	0.528	0.522	98.947
			4	6.994	0.499	180	0.533	0.528	98.958
						<b>Averages</b>			<b>0.531</b>
2	0	4	1	8.119	1.632				
			2	8.325	1.837	180	1.144	1.139	99.515
			3	8.529	2.040	180	1.133	1.128	99.510
			4	8.734	2.242	180	1.139	1.122	98.537
						<b>Averages</b>			<b>1.139</b>
3	0	4	1	9.897	3.434				
			2	10.212	3.744	180	1.750	1.722	98.413
			3	10.524	4.053	180	1.733	1.717	99.038
			4	10.838	4.365	180	1.744	1.733	99.363
						<b>Averages</b>			<b>1.743</b>
4	0	4	1	2.262	5.954				
			2	2.699	6.384	180	2.428	2.389	98.398
			3	3.135	6.813	180	2.422	2.383	98.394
			4	3.573	7.245	180	2.433	2.400	98.630
						<b>Averages</b>			<b>2.428</b>
5	0	4	1	5.026	9.005				
			2	5.565	9.536	180	2.994	2.950	98.516
			3	6.114	10.075	180	3.050	2.994	98.179
			4	6.659	10.61	180	3.028	2.972	98.165
						<b>Averages</b>			<b>3.024</b>

Table B-22: Test Data-Type II model, 20mm slot width, 0% longitudinal slope & 6% cross slope

Test no	Longitudinal slope	Cross slope	Measurement no	Flow meter reading 1 (m <sup>3</sup> )	Flow meter reading 2 (m <sup>3</sup> )	Running time (Sec)	Flow rate 1 (l/s)	Flow rate 2 (l/s)	Interception efficiency (%)
1	0	6	1	8.404	0.221				
			2	8.508	0.325	180	0.578	0.578	100.000
			3	8.611	0.428	180	0.572	0.572	100.000
			4	8.716	0.532	180	0.583	0.578	99.048
			<b>Averages</b>				<b>0.578</b>	<b>0.576</b>	<b>99.679</b>
2	0	6	1	3.163	5.406				
			2	3.337	5.578	180	0.967	0.956	98.851
			3	3.510	5.749	180	0.961	0.950	98.844
			4	3.684	5.921	180	0.967	0.956	98.851
			<b>Averages</b>				<b>0.965</b>	<b>0.954</b>	<b>98.848</b>
3	0	6	1	4.826	7.090				
			2	5.131	7.391	180	1.694	1.672	98.689
			3	5.431	7.687	180	1.667	1.644	98.667
			4	5.730	7.982	180	1.661	1.639	98.662
			<b>Averages</b>				<b>1.674</b>	<b>1.652</b>	<b>98.673</b>
4	0	6	1	7.128	9.503				
			2	7.581	9.947	180	2.517	2.467	98.013
			3	8.025	10.388	180	2.467	2.450	99.324
			4	8.471	10.828	180	2.478	2.444	98.655
			<b>Averages</b>				<b>2.487</b>	<b>2.454</b>	<b>98.660</b>
5	0	6	1	0.668	3.363				
			2	1.207	3.892	180	2.994	2.939	98.145
			3	1.736	4.415	180	2.939	2.906	98.866
			4	2.269	4.940	180	2.961	2.917	98.499
			<b>Averages</b>				<b>2.965</b>	<b>2.920</b>	<b>98.501</b>

**Table B-23: Test Data-Type II model, 20mm slot width, 2% longitudinal slope & 6% cross slope**

Test no	Longitudinal slope	Cross slope	Measurement no	Flow meter reading 1 (m <sup>3</sup> )	Flow meter reading 2 (m <sup>3</sup> )	Running time (Sec)	Flow rate 1 (l/s)	Flow rate 2 (l/s)	Interception efficiency (%)
1	2	6	1	3.209	5.264				
			2	3.339	5.392	180	0.722	0.711	98.462
			3	3.467	5.519	180	0.711	0.706	99.219
			4	3.595	5.647	180	0.711	0.711	100.000
			<b>Averages</b>				<b>0.715</b>	<b>0.709</b>	<b>99.223</b>
2	2	6	1	4.805	7.020				
			2	5.053	7.266	180	1.378	1.367	99.194
			3	5.300	7.509	180	1.372	1.350	98.381
			4	5.544	7.751	180	1.356	1.344	99.180
			<b>Averages</b>				<b>1.369</b>	<b>1.354</b>	<b>98.917</b>
3	2	6	1	6.936	9.231				
			2	7.283	9.573	180	1.928	1.900	98.559
			3	7.633	9.916	180	1.944	1.906	98.000
			4	7.978	10.255	180	1.917	1.883	98.261
			<b>Averages</b>				<b>1.930</b>	<b>1.896</b>	<b>98.273</b>
4	2	6	1	0.047	2.333				
			2	0.462	2.742	180	2.306	2.272	98.554
			3	0.873	3.150	180	2.283	2.267	99.270
			4	1.292	3.563	180	2.328	2.294	98.568
			<b>Averages</b>				<b>2.306</b>	<b>2.278</b>	<b>98.795</b>
5	2	6	1	3.427	5.896				
			2	3.968	6.427	180	3.006	2.950	98.152
			3	4.505	6.959	180	2.983	2.956	99.069
			4	5.048	7.498	180	3.017	2.994	99.263
			<b>Averages</b>				<b>3.002</b>	<b>2.967</b>	<b>98.828</b>



**Table B-24: Test Data-Type II model, 20mm slot width, 4% longitudinal slope & 6% cross slope**

Test no	Longitudinal slope	Cross slope	Measurement no	Flow meter reading 1 (m <sup>3</sup> )	Flow meter reading 2 (m <sup>3</sup> )	Running time (Sec)	Flow rate 1 (l/s)	Flow rate 2 (l/s)	Interception efficiency (%)
1	4	6	1	8.896	0.750				
			2	9.033	0.886	180	0.761	0.756	99.270
			3	9.169	1.021	180	0.756	0.750	99.265
			4	9.304	1.155	180	0.750	0.744	99.259
						<b>Averages</b>	<b>0.756</b>	<b>0.750</b>	<b>99.265</b>
2	4	6	1	1.721	2.569				
			2	1.981	2.825	180	1.444	1.422	98.462
			3	2.237	3.079	180	1.422	1.411	99.219
			4	2.497	3.335	180	1.444	1.422	98.462
						<b>Averages</b>	<b>1.437</b>	<b>1.419</b>	<b>98.711</b>
3	4	6	1	4.232	5.096				
			2	4.564	5.424	180	1.844	1.822	98.795
			3	4.891	5.747	180	1.817	1.794	98.777
			4	5.220	6.071	180	1.828	1.800	98.480
						<b>Averages</b>	<b>1.830</b>	<b>1.806</b>	<b>98.684</b>
4	4	6	1	7.718	8.787				
			2	8.156	9.219	180	2.433	2.400	98.630
			3	8.586	9.644	180	2.389	2.361	98.837
			4	9.022	10.075	180	2.422	2.394	98.853
						<b>Averages</b>	<b>2.415</b>	<b>2.385</b>	<b>98.773</b>
5	4	6	1	4.982	6.869				
			2	5.532	7.411	180	3.056	3.011	98.545
			3	6.073	7.947	180	3.006	2.978	99.076
			4	6.616	8.482	180	3.017	2.972	98.527
						<b>Averages</b>	<b>3.026</b>	<b>2.987</b>	<b>98.715</b>

Table B-25: Test Data-Type II model, 20mm slot width, 6% longitudinal slope &amp; 6% cross slope

Test no	Longitudinal slope	Cross slope	Measurement no	Flow meter reading 1 (m <sup>3</sup> )	Flow meter reading 2 (m <sup>3</sup> )	Running time (Sec)	Flow rate 1 (l/s)	Flow rate 2 (l/s)	Interception efficiency (%)
1	6	6	1	9.441	1.586				
			2	9.554	1.698	180	0.628	0.622	99.115
			3	9.666	1.809	180	0.622	0.617	99.107
			4	9.778	1.920	180	0.622	0.617	99.107
			<b>Averages</b>				<b>0.624</b>	<b>0.619</b>	<b>99.110</b>
2	6	6	1	1.636	3.874				
			2	1.917	4.154	180	1.561	1.556	99.644
			3	2.195	4.431	180	1.544	1.539	99.640
			4	2.478	4.711	180	1.572	1.556	98.940
			<b>Averages</b>				<b>1.559</b>	<b>1.550</b>	<b>99.406</b>
3	6	6	1	3.932	6.312				
			2	4.277	6.655	180	1.917	1.906	99.420
			3	4.616	6.990	180	1.883	1.861	98.820
			4	4.957	7.329	180	1.894	1.883	99.413
			<b>Averages</b>				<b>1.898</b>	<b>1.883</b>	<b>99.220</b>
4	6	6	1	7.848	9.584				
			2	8.305	10.038	180	2.539	2.522	99.344
			3	8.758	10.484	180	2.517	2.478	98.455
			4	9.208	10.931	180	2.500	2.483	99.333
			<b>Averages</b>				<b>2.519</b>	<b>2.494</b>	<b>99.044</b>
5	6	6	1	2.313	14.050				
			2	2.844	14.575	180	2.950	2.917	98.870
			3	3.379	15.103	180	2.972	2.933	98.692
			4	3.918	15.634	180	2.994	2.950	98.516
			<b>Averages</b>				<b>2.972</b>	<b>2.933</b>	<b>98.692</b>

**Table B-26: Rainfall intensity and flow depth data-0.5l/s applied test sheet flow**

Road width (m)	Road cross fall (%)	Road gradient (%)	Flow path slope (%)	Flow path length (m)	Area (km <sup>2</sup> )	Run-off coefficient	Time of concentration (hr)	Test applied sheet flow (l/s)	Rainfall intensity (mm/hr)	Flow depth calculations (mm)			
										w	n <sub>1</sub>	n <sub>2</sub>	s <sub>f</sub>
3.6	2	0	2.00	3.60	0.000004	1.0	0.01750	0.5	500	8.8	4.3	4.3	2.3
	2	6	6.32	11.38	0.000011	1.0	0.02290		158	3.6	3.4	1.9	1.6
	4	0	4.00	3.60	0.000004	1.0	0.01489		500	7.4	3.7	3.1	1.8
	4	6	7.21	6.49	0.000006	1.0	0.01708		277	4.7	3.3	2.0	1.5
	6	0	6.00	3.60	0.000004	1.0	0.01354		500	6.8	3.4	2.5	1.6
	6	6	8.49	5.09	0.000005	1.0	0.01468		354	5.2	3.2	1.9	1.5
7.2	2	0	2.00	7.20	0.000007	1.0	0.02419		250	6.0	4.3	3.8	2.3
	2	6	6.32	22.77	0.000023	1.0	0.03166		79	2.5	3.4	1.6	1.6
	4	0	4.00	7.20	0.000007	1.0	0.02058		250	5.1	3.7	2.7	1.8
	4	6	7.21	12.98	0.000013	1.0	0.02361		139	3.3	3.3	1.7	1.5
	6	0	6.00	7.20	0.000007	1.0	0.01872		250	4.7	3.4	2.2	1.6
	6	6	8.49	10.18	0.000010	1.0	0.02030		177	3.6	3.2	1.7	1.5
10.8	2	0	2.00	10.80	0.000011	1.0	0.02924		167	4.9	4.3	3.5	2.3
	2	6	6.32	34.15	0.000034	1.0	0.03825		53	2.0	3.4	1.5	1.6
	4	0	4.00	10.80	0.000011	1.0	0.02487		167	4.1	3.7	2.5	1.8
	4	6	7.21	19.47	0.000019	1.0	0.02854		92	2.6	3.3	1.6	1.5
	6	0	6.00	10.80	0.000011	1.0	0.02262		167	3.8	3.4	2.0	1.6
	6	6	8.49	15.27	0.000015	1.0	0.02453		118	2.9	3.2	1.5	1.5
14.4	2	0	2.00	14.40	0.000014	1.0	0.03344		125	4.2	4.3	3.3	2.3
	2	6	6.32	45.54	0.000046	1.0	0.04376		40	1.7	3.4	1.4	1.6
	4	0	4.00	14.40	0.000014	1.0	0.02844		125	3.6	3.7	2.3	1.8
	4	6	7.21	25.96	0.000026	1.0	0.03264		69	2.3	3.3	1.5	1.5
	6	0	6.00	14.40	0.000014	1.0	0.02587		125	3.2	3.4	1.9	1.6
	6	6	8.49	20.36	0.000020	1.0	0.02806		88	2.5	3.2	1.4	1.5

**Table B-27: Rainfall intensity and flow depth data-1.0l/s applied test sheet flow**

Road width (m)	Road cross fall (%)	Road gradient (%)	Flow path slope (%)	Flow path length (m)	Area (km <sup>2</sup> )	Run-off coefficient	Time of concentration (hr)	Test applied sheet flow (l/s)	Rainfall intensity (mm/hr)	Flow depth calculations (mm)			
										d= I*Tc	d, using RRL equation	d, using Gallaway equation	d, using Manning's n equation
w	n <sub>1</sub>	n <sub>2</sub>	s <sub>f</sub>	l <sub>f</sub>	A	C	T <sub>c</sub>	Test Q	I (mm/hr)	d= I*Tc	d, using RRL equation	d, using Gallaway equation	d, using Manning's n equation
3.6	2	0	2.00	3.60	0.000004	1.0	0.01750	1.0	1000	17.5	6.0	6.8	3.4
	2	6	6.32	11.38	0.000011	1.0	0.02290		316	7.2	4.8	3.2	2.4
	4	0	4.00	3.60	0.000004	1.0	0.01489		1000	14.9	5.3	4.9	2.8
	4	6	7.21	6.49	0.000006	1.0	0.01708		555	9.5	4.7	3.3	2.3
	6	0	6.00	3.60	0.000004	1.0	0.01354		1000	13.5	4.8	4.1	2.5
	6	6	8.49	5.09	0.000005	1.0	0.01468		707	10.4	4.5	3.2	2.2
7.2	2	0	2.00	7.20	0.000007	1.0	0.02419		500	12.1	6.0	6.0	3.4
	2	6	6.32	22.77	0.000023	1.0	0.03166		158	5.0	4.8	2.8	2.4
	4	0	4.00	7.20	0.000007	1.0	0.02058		500	10.3	5.3	4.4	2.8
	4	6	7.21	12.98	0.000013	1.0	0.02361		277	6.5	4.7	2.9	2.3
	6	0	6.00	7.20	0.000007	1.0	0.01872		500	9.4	4.8	3.6	2.5
	6	6	8.49	10.18	0.000010	1.0	0.02030		354	7.2	4.5	2.8	2.2
10.8	2	0	2.00	10.80	0.000011	1.0	0.02924		333	9.7	6.0	5.6	3.4
	2	6	6.32	34.15	0.000034	1.0	0.03825		105	4.0	4.8	2.6	2.4
	4	0	4.00	10.80	0.000011	1.0	0.02487		333	8.3	5.3	4.0	2.8
	4	6	7.21	19.47	0.000019	1.0	0.02854		185	5.3	4.7	2.7	2.3
	6	0	6.00	10.80	0.000011	1.0	0.02262		333	7.5	4.8	3.3	2.5
	6	6	8.49	15.27	0.000015	1.0	0.02453		236	5.8	4.5	2.6	2.2
14.4	2	0	2.00	14.40	0.000014	1.0	0.03344		250	8.4	6.0	5.3	3.4
	2	6	6.32	45.54	0.000046	1.0	0.04376		79	3.5	4.8	2.4	2.4
	4	0	4.00	14.40	0.000014	1.0	0.02844		250	7.1	5.3	3.8	2.8
	4	6	7.21	25.96	0.000026	1.0	0.03264		139	4.5	4.7	2.5	2.3
	6	0	6.00	14.40	0.000014	1.0	0.02587		250	6.5	4.8	3.1	2.5
	6	6	8.49	20.36	0.000020	1.0	0.02806		177	5.0	4.5	2.4	2.2

**Table B-28: Rainfall intensity and flow depth data-1.5l/s applied test sheet flow**

Road width (m)	Road cross fall (%)	Road gradient (%)	Flow path slope (%)	Flow path length (m)	Area (km <sup>2</sup> )	Run-off coefficient	Time of concentration (hr)	Test applied sheet flow (l/s)	Rainfall intensity (mm/hr)	Flow depth calculations (mm)			
										d= I*Tc	d, using RRL equation	d, using Gallaway equation	d, using Manning's n equation
w	n <sub>1</sub>	n <sub>2</sub>	s <sub>f</sub>	l <sub>f</sub>	A	C	T <sub>c</sub>	Test Q	I (mm/hr)	d= I*Tc	d, using RRL equation	d, using Gallaway equation	d, using Manning's n equation
3.6	2	0	2.00	3.60	0.000004	1.0	0.01750	1.5	1500	26.3	7.4	8.8	4.4
	2	6	6.32	11.38	0.000011	1.0	0.02290		474	10.9	5.9	4.2	3.1
	4	0	4.00	3.60	0.000004	1.0	0.01489		1500	22.3	6.4	6.4	3.6
	4	6	7.21	6.49	0.000006	1.0	0.01708		832	14.2	5.7	4.4	3.0
	6	0	6.00	3.60	0.000004	1.0	0.01354		1500	20.3	5.9	5.3	3.1
	6	6	8.49	5.09	0.000005	1.0	0.01468		1061	15.6	5.5	4.3	2.8
7.2	2	0	2.00	7.20	0.000007	1.0	0.02419		750	18.1	7.4	7.8	4.4
	2	6	6.32	22.77	0.000023	1.0	0.03166		237	7.5	5.9	3.7	3.1
	4	0	4.00	7.20	0.000007	1.0	0.02058		750	15.4	6.4	5.7	3.6
	4	6	7.21	12.98	0.000013	1.0	0.02361		416	9.8	5.7	3.9	3.0
	6	0	6.00	7.20	0.000007	1.0	0.01872		750	14.0	5.9	4.7	3.1
	6	6	8.49	10.18	0.000010	1.0	0.02030		530	10.8	5.5	3.7	2.8
10.8	2	0	2.00	10.80	0.000011	1.0	0.02924		500	14.6	7.4	7.3	4.4
	2	6	6.32	34.15	0.000034	1.0	0.03825		158	6.0	5.9	3.4	3.1
	4	0	4.00	10.80	0.000011	1.0	0.02487		500	12.4	6.4	5.3	3.6
	4	6	7.21	19.47	0.000019	1.0	0.02854		277	7.9	5.7	3.6	3.0
	6	0	6.00	10.80	0.000011	1.0	0.02262		500	11.3	5.9	4.4	3.1
	6	6	8.49	15.27	0.000015	1.0	0.02453		354	8.7	5.5	3.5	2.8
14.4	2	0	2.00	14.40	0.000014	1.0	0.03344		375	12.5	7.4	7.0	4.4
	2	6	6.32	45.54	0.000046	1.0	0.04376		119	5.2	5.9	3.3	3.1
	4	0	4.00	14.40	0.000014	1.0	0.02844		375	10.7	6.4	5.0	3.6
	4	6	7.21	25.96	0.000026	1.0	0.03264		208	6.8	5.7	3.4	3.0
	6	0	6.00	14.40	0.000014	1.0	0.02587		375	9.7	5.9	4.2	3.1
	6	6	8.49	20.36	0.000020	1.0	0.02806		265	7.4	5.5	3.3	2.8

**Table B-29: Rainfall intensity and flow depth data-2.0l/s applied test sheet flow**

Road width (m)	Road cross fall (%)	Road gradient (%)	Flow path slope (%)	Flow path length (m)	Area (km <sup>2</sup> )	Run-off coefficient	Time of concentration (hr)	Test applied sheet flow (l/s)	Rainfall intensity (mm/hr)	Flow depth calculations (mm)			
										d= I*T <sub>c</sub>	d, using RRL equation	d, using Gallaway equation	d, using Manning's n equation
w	n <sub>1</sub>	n <sub>2</sub>	s <sub>f</sub>	l <sub>f</sub>	A	C	T <sub>c</sub>	Test Q	I (mm/hr)	d= I*T <sub>c</sub>	d, using RRL equation	d, using Gallaway equation	d, using Manning's n equation
3.6	2	0	2.00	3.60	0.000004	1.0	0.01750	2.0	2000	35.0	8.5	10.6	5.2
	2	6	6.32	11.38	0.000011	1.0	0.02290		632	14.5	6.8	5.1	3.7
	4	0	4.00	3.60	0.000004	1.0	0.01489		2000	29.8	7.4	7.8	4.2
	4	6	7.21	6.49	0.000006	1.0	0.01708		1109	19.0	6.6	5.3	3.5
	6	0	6.00	3.60	0.000004	1.0	0.01354		2000	27.1	6.9	6.4	3.7
	6	6	8.49	5.09	0.000005	1.0	0.01468		1414	20.8	6.4	5.2	3.4
7.2	2	0	2.00	7.20	0.000007	1.0	0.02419		1000	24.2	8.5	9.4	5.2
	2	6	6.32	22.77	0.000023	1.0	0.03166		316	10.0	6.8	4.5	3.7
	4	0	4.00	7.20	0.000007	1.0	0.02058		1000	20.6	7.4	6.9	4.2
	4	6	7.21	12.98	0.000013	1.0	0.02361		555	13.1	6.6	4.7	3.5
	6	0	6.00	7.20	0.000007	1.0	0.01872		1000	18.7	6.9	5.7	3.7
	6	6	8.49	10.18	0.000010	1.0	0.02030		707	14.4	6.4	4.5	3.4
10.8	2	0	2.00	10.80	0.000011	1.0	0.02924		667	19.5	8.5	8.8	5.2
	2	6	6.32	34.15	0.000034	1.0	0.03825		211	8.1	6.8	4.2	3.7
	4	0	4.00	10.80	0.000011	1.0	0.02487		667	16.6	7.4	6.4	4.2
	4	6	7.21	19.47	0.000019	1.0	0.02854		370	10.6	6.6	4.4	3.5
	6	0	6.00	10.80	0.000011	1.0	0.02262		667	15.1	6.9	5.3	3.7
	6	6	8.49	15.27	0.000015	1.0	0.02453		471	11.6	6.4	4.2	3.4
14.4	2	0	2.00	14.40	0.000014	1.0	0.03344		500	16.7	8.5	8.4	5.2
	2	6	6.32	45.54	0.000046	1.0	0.04376		158	6.9	6.8	4.0	3.7
	4	0	4.00	14.40	0.000014	1.0	0.02844		500	14.2	7.4	6.1	4.2
	4	6	7.21	25.96	0.000026	1.0	0.03264		277	9.1	6.6	4.1	3.5
	6	0	6.00	14.40	0.000014	1.0	0.02587		500	12.9	6.9	5.0	3.7
	6	6	8.49	20.36	0.000020	1.0	0.02806		354	9.9	6.4	4.0	3.4

**Table B-30: Rainfall intensity and flow depth data-2.5l/s applied test sheet flow**

Road width (m)	Road cross fall (%)	Road gradient (%)	Flow path slope (%)	Flow path length (m)	Area (km <sup>2</sup> )	Run-off coefficient	Time of concentration (hr)	Test applied sheet flow (l/s)	Rainfall intensity (mm/hr)	Flow depth calculations (mm)			
										w	n <sub>1</sub>	n <sub>2</sub>	s <sub>f</sub>
3.6	2	0	2.00	3.60	0.000004	1.0	0.01750	2.5	2500	43.8	9.5	12.2	6.0
	2	6	6.32	11.38	0.000011	1.0	0.02290		791	18.1	7.6	5.9	4.2
	4	0	4.00	3.60	0.000004	1.0	0.01489		2500	37.2	8.3	8.9	4.8
	4	6	7.21	6.49	0.000006	1.0	0.01708		1387	23.7	7.4	6.2	4.1
	6	0	6.00	3.60	0.000004	1.0	0.01354		2500	33.9	7.7	7.4	4.3
	6	6	8.49	5.09	0.000005	1.0	0.01468		1768	26.0	7.1	6.0	3.9
7.2	2	0	2.00	7.20	0.000007	1.0	0.02419		1250	30.2	9.5	10.8	6.0
	2	6	6.32	22.77	0.000023	1.0	0.03166		395	12.5	7.6	5.2	4.2
	4	0	4.00	7.20	0.000007	1.0	0.02058		1250	25.7	8.3	7.9	4.8
	4	6	7.21	12.98	0.000013	1.0	0.02361		693	16.4	7.4	5.5	4.1
	6	0	6.00	7.20	0.000007	1.0	0.01872		1250	23.4	7.7	6.6	4.3
	6	6	8.49	10.18	0.000010	1.0	0.02030		884	17.9	7.1	5.3	3.9
10.8	2	0	2.00	10.80	0.000011	1.0	0.02924		833	24.4	9.5	10.1	6.0
	2	6	6.32	34.15	0.000034	1.0	0.03825		264	10.1	7.6	4.9	4.2
	4	0	4.00	10.80	0.000011	1.0	0.02487		833	20.7	8.3	7.4	4.8
	4	6	7.21	19.47	0.000019	1.0	0.02854		462	13.2	7.4	5.1	4.1
	6	0	6.00	10.80	0.000011	1.0	0.02262		833	18.9	7.7	6.1	4.3
	6	6	8.49	15.27	0.000015	1.0	0.02453		589	14.5	7.1	4.9	3.9
14.4	2	0	2.00	14.40	0.000014	1.0	0.03344		625	20.9	9.5	9.6	6.0
	2	6	6.32	45.54	0.000046	1.0	0.04376		198	8.6	7.6	4.6	4.2
	4	0	4.00	14.40	0.000014	1.0	0.02844		625	17.8	8.3	7.0	4.8
	4	6	7.21	25.96	0.000026	1.0	0.03264		347	11.3	7.4	4.8	4.1
	6	0	6.00	14.40	0.000014	1.0	0.02587		625	16.2	7.7	5.8	4.3
	6	6	8.49	20.36	0.000020	1.0	0.02806		442	12.4	7.1	4.7	3.9

**Table B-31: Rainfall intensity and flow depth data-3.0l/s applied test sheet flow**

Road width (m)	Road cross fall (%)	Road gradient (%)	Flow path slope (%)	Flow path length (m)	Area (km <sup>2</sup> )	Run-off coefficient	Time of concentration (hr)	Test applied sheet flow (l/s)	Rainfall intensity (mm/hr)	Flow depth calculations (mm)			
										d= I*Tc	d, using RRL equation	d, using Gallaway equation	d, using Manning's n equation
w	n <sub>1</sub>	n <sub>2</sub>	s <sub>f</sub>	l <sub>f</sub>	A	C	T <sub>c</sub>	Test Q	I (mm/hr)	d= I*Tc	d, using RRL equation	d, using Gallaway equation	d, using Manning's n equation
3.6	2	0	2.00	3.60	0.000004	1.0	0.01750	3.0	3000	52.5	10.5	13.6	6.7
	2	6	6.32	11.38	0.000011	1.0	0.02290		949	21.7	8.3	6.7	4.7
	4	0	4.00	3.60	0.000004	1.0	0.01489		3000	44.7	9.1	10.0	5.4
	4	6	7.21	6.49	0.000006	1.0	0.01708		1664	28.4	8.1	6.9	4.5
	6	0	6.00	3.60	0.000004	1.0	0.01354		3000	40.6	8.4	8.4	4.8
	6	6	8.49	5.09	0.000005	1.0	0.01468		2121	31.2	7.8	6.7	4.3
7.2	2	0	2.00	7.20	0.000007	1.0	0.02419		1500	36.3	10.5	12.1	6.7
	2	6	6.32	22.77	0.000023	1.0	0.03166		474	15.0	8.3	5.9	4.7
	4	0	4.00	7.20	0.000007	1.0	0.02058		1500	30.9	9.1	8.9	5.4
	4	6	7.21	12.98	0.000013	1.0	0.02361		832	19.6	8.1	6.1	4.5
	6	0	6.00	7.20	0.000007	1.0	0.01872		1500	28.1	8.4	7.4	4.8
	6	6	8.49	10.18	0.000010	1.0	0.02030		1061	21.5	7.8	5.9	4.3
10.8	2	0	2.00	10.80	0.000011	1.0	0.02924		1000	29.2	10.5	11.3	6.7
	2	6	6.32	34.15	0.000034	1.0	0.03825		316	12.1	8.3	5.5	4.7
	4	0	4.00	10.80	0.000011	1.0	0.02487		1000	24.9	9.1	8.3	5.4
	4	6	7.21	19.47	0.000019	1.0	0.02854		555	15.8	8.1	5.7	4.5
	6	0	6.00	10.80	0.000011	1.0	0.02262		1000	22.6	8.4	6.9	4.8
	6	6	8.49	15.27	0.000015	1.0	0.02453		707	17.3	7.8	5.5	4.3
14.4	2	0	2.00	14.40	0.000014	1.0	0.03344		750	25.1	10.5	10.8	6.7
	2	6	6.32	45.54	0.000046	1.0	0.04376		237	10.4	8.3	5.2	4.7
	4	0	4.00	14.40	0.000014	1.0	0.02844		750	21.3	9.1	7.9	5.4
	4	6	7.21	25.96	0.000026	1.0	0.03264		416	13.6	8.1	5.4	4.5
	6	0	6.00	14.40	0.000014	1.0	0.02587		750	19.4	8.4	6.6	4.8
	6	6	8.49	20.36	0.000020	1.0	0.02806		530	14.9	7.8	5.3	4.3